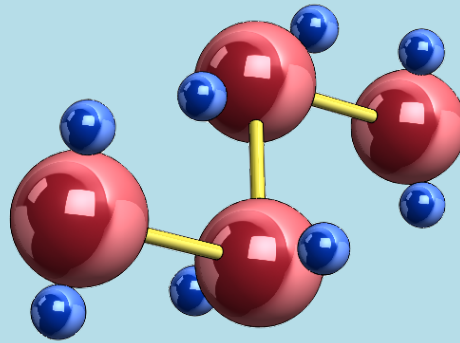


QUEEN'S UNIVERSITY

POLYMERS RESEARCH GROUP

19 Division Street, Kingston, ON, K7L 3N6 Canada



**EXACT ANALYTICAL SOLUTION
FOR LARGE-AMPLITUDE OSCILLATORY SHEAR FLOW**

C. Saengow (ชัยมงคล แซ่โจ้ว)^{1,2}, A.J. Giacomin^{2,*},
and C. Kolutawong (ชาญยุทธ โกสิทธิ์วงษ์)¹

¹Mechanical and Aerospace Engineering Department
Polymer Research Center
King Mongkut's University of Technology North Bangkok
Bangkok, THAILAND 10800

²Chemical Engineering Department
Polymers Research Group
Queen's University
Kingston, Ontario, CANADA K7L 3N6

This report is circulated to persons believed to have an active interest in the subject matter; it is intended to furnish rapid communication and to stimulate comment, including corrections of possible errors.

*Corresponding author (giacomin@queensu.ca)

EXACT ANALYTICAL SOLUTION FOR LARGE-AMPLITUDE OSCILLATORY SHEAR FLOW

C. Saengow^{1,2}, A.J. Giacomin^{2,*}, and C. Kolitawong¹

¹Mechanical and Aerospace Engineering Department
Polymer Research Center
King Mongkut's University of Technology North Bangkok
Bangkok, THAILAND 10800

²Chemical Engineering Department
Polymers Research Group
Queen's University
Kingston, Ontario, CANADA K7L 3N6

ABSTRACT

When polymeric liquids undergo large-amplitude shearing oscillations, the shear stress responds as a Fourier series, the higher harmonics of which are caused by fluid nonlinearity. Previous work on large-amplitude oscillatory shear flow has produced analytical solutions for the first few harmonics of a Fourier series for the shear stress response (none beyond the fifth) or for the normal stress difference responses (none beyond the fourth) [*JNNFM*, **166**, 1081 (2011)], but this growing subdiscipline of mathematical physics has yet to produce an exact solution. Here, we derive what we believe to be the first exact analytical solution for the response of the extra stress tensor in large-amplitude oscillatory shear flow. Our solution, unique and in closed form, includes both the normal stress differences and the shear stress for both startup and alternance. We solve the corotational Maxwell model as a pair of nonlinear coupled ordinary differential equations, simultaneously. We choose the corotational Maxwell model because this two-parameter model (η_0 and λ) is the simplest constitutive model relevant to large-amplitude oscillatory shear flow, and because it has previously been found to be accurate for molten plastics. By *relevant* we mean that the model predicts higher harmonics. We find good agreement between the first few harmonics of our exact solution, and of our previous approximate expressions (obtained using the Goddard integral transform). Our exact solution agrees closely with the measured behavior for molten plastics, not only at alternance, but also in startup.

Keywords: Large-amplitude oscillatory shear flow, LAOS, higher harmonics, Fourier-transform rheology, FT-rheology, corotational Maxwell fluid, Kovacic method

* Corresponding author (giacomin@queensu.ca).

CONTENTS

| | |
|---|----|
| I. INTRODUCTION | 7 |
| II. MECHANICS OF LARGE-AMPLITUDE OSCILLATORY SHEAR..... | 10 |
| III. THE COROTATIONAL MAXWELL MODEL | 10 |
| a. Simple Shear Flow | 13 |
| b. Oscillatory Shear Flow | 13 |
| IV. ANALYSIS | 14 |
| V. RESULTS..... | 15 |
| a. Normal Stress Difference Responses | 16 |
| b. Shear Stress Response | 20 |
| c. Generalized Corotational Maxwell Model..... | 27 |
| VI. CONSISTENCY CHECKS..... | 29 |
| VII. COMPARISONS WITH EXPERIMENTAL DATA..... | 31 |
| a. Shear Stress Versus Shear Rate Loops..... | 31 |
| i. Startup | 31 |
| ii. Alternance..... | 31 |
| b. Shear Stress Amplitude | 31 |
| VIII. CONCLUSION..... | 32 |
| IX. ACKNOWLEDGMENT | 32 |
| X. APPENDIX: FUNDAMENTAL MATRIX | 33 |
| XI. APPENDIX: I_1, I_2 AND THEIR LIMITS | 35 |
| XII. APPENDIX: FOURIER ANALYSIS OF COMPACT FORMS | 38 |
| a. Normal Stress Differences | 39 |
| i. Transient parts of Eq. (147) | 39 |
| ii. First alternant part of Eq. (147) | 39 |
| iii. Second alternant part of Eq. (147)..... | 42 |
| b. Shear Stress | 45 |
| i. Transient parts of Eq. (187) | 45 |
| ii. First alternant part of Eq. (187) | 45 |
| iii. Second alternant part of Eq. (187)..... | 47 |
| XIII. REFERENCES | 83 |

TABLES

| | |
|--|----|
| Table I: Literature on Analytical Solution for Large-Amplitude Oscillatory Shear Flow..... | 51 |
| Table II: Dimensional Variables..... | 53 |
| Table III: Dimensionless Variables and Groups..... | 54 |
| Table IV: Intermediate Results for Kovacic Method (Case 2)..... | 57 |

FIGURES

| | |
|--|----|
| Figure 1: Orthomorphic isometric sketch of alternating velocity profile in oscillatory shear flow [Eq. (1)]. Cartesian coordinates with origin on the stationary plate. The linear velocity profile results from the assumption that inertial effects can be neglected..... | 58 |
| Figure 2. Exact solution [Eq. (54) with Eqs. (55) and (56)] using 40 even harmonics, 0 through 78, and 40 odd ones, 1 through 79, for startup (first two cycles). Minus dimensionless first normal stress differences, $-\mathbb{N}_1 = 2\mathbb{N}_2$, versus dimensionless shear rate, $\lambda\dot{\gamma}$, calculated for the 2-constant corotational Maxwell model, for a Deborah number of $\lambda\omega = \frac{1}{10}$ | 59 |
| Figure 3. Exact solution [Eq. (54) with Eqs. (55) and (56)] using 40 even harmonics, 0 through 78, and 40 odd ones, 1 through 79, for startup (first two cycles). Minus dimensionless first normal stress differences, $-\mathbb{N}_1 = 2\mathbb{N}_2$, versus dimensionless shear rate, $\lambda\dot{\gamma}$, calculated for the 2-constant corotational Maxwell model, for a Deborah number of $\lambda\omega = 1$ | 60 |
| Figure 4. Exact solution [Eq. (54) with Eqs. (55) and (56)] using 40 even harmonics, 0 through 78, and 40 odd ones, 1 through 79, for startup (first two cycles). Minus dimensionless first normal stress differences, $-\mathbb{N}_1 = 2\mathbb{N}_2$, versus dimensionless shear rate, $\lambda\dot{\gamma}$, calculated for the 2-constant corotational Maxwell model, for a Deborah number of $\lambda\omega = 10$ | 61 |
| Figure 5. Exact solution [Eq. (56)] using 40 even harmonics, 0 through 78, for alternance. Minus dimensionless first normal stress differences, $-\mathbb{N}_1 = 2\mathbb{N}_2$, versus dimensionless shear rate, $\lambda\dot{\gamma}$, left-clockwise loops calculated for the 2-constant corotational Maxwell model, for a Deborah number of $\lambda\omega = \frac{1}{10}$ | 62 |
| Figure 6. Exact solution [Eq. (56)] using 40 even harmonics, 0 through 78, for alternance. Minus dimensionless first normal stress differences, $-\mathbb{N}_1 = 2\mathbb{N}_2$, versus dimensionless shear rate, $\lambda\dot{\gamma}$, left-clockwise loops calculated for the 2-constant corotational Maxwell model, for a Deborah number of $\lambda\omega = 1$ | 63 |
| Figure 7. Exact solution [Eq. (56)] using 40 even harmonics, 0 through 78, for alternance. Minus dimensionless first normal stress differences, $-\mathbb{N}_1 = 2\mathbb{N}_2$, versus dimensionless shear rate, $\lambda\dot{\gamma}$, left-clockwise loops calculated for the 2-constant corotational Maxwell model, for a Deborah number of $\lambda\omega = 10$... | 64 |

Figure 8. Exact solution [Eq. (64) with Eqs. (65) and (66)] using 40 even harmonics, 0 through 78, and 40 odd ones, 1 through 79, for startup (first two cycles). Minus dimensionless shear stress, $-\mathbb{S}$, versus dimensionless shear rate, $\lambda\dot{\gamma}$, calculated for the 2-constant corotational Maxwell model with a Deborah number of $\lambda\omega = \frac{1}{10}$ 65

Figure 9. Exact solution [Eq. (64) with Eqs. (65) and (66)] using 40 even harmonics, 0 through 78, and 40 odd ones, 1 through 79, for startup (first two cycles). Minus dimensionless shear stress, $-\mathbb{S}$, versus dimensionless shear rate, $\lambda\dot{\gamma}$, calculated for the 2-constant corotational Maxwell model with a Deborah number of $\lambda\omega = 1$ 66

Figure 10. Exact solution [Eq. (64) with Eqs. (65) and (66)] using 40 even harmonics, 0 through 78, and 40 odd ones, 1 through 79, for startup (first two cycles). Minus dimensionless shear stress, $-\mathbb{S}$, versus dimensionless shear rate, $\lambda\dot{\gamma}$, calculated for the 2-constant corotational Maxwell model with a Deborah number of $\lambda\omega = 10$ 67

Figure 11. Exact solution [Eq. (66)] using 40 odd harmonics, 1 through 79, for alternance. Counterclockwise loops of minus dimensionless shear stress, $-\mathbb{S}$, versus dimensionless shear rate, $\lambda\dot{\gamma}$, calculated for the 2-constant corotational Maxwell model with a Deborah number of $\lambda\omega = \frac{1}{10}$ 68

Figure 12. Exact solution [Eq. (66)] using 40 odd harmonics, 1 through 79, for alternance. Counterclockwise loops of minus dimensionless shear stress, $-\mathbb{S}$, versus dimensionless shear rate, $\lambda\dot{\gamma}$, calculated for the 2-constant corotational Maxwell model with a Deborah number of $\lambda\omega = 1$ 69

Figure 13. Exact solution [Eq. (66)] using 40 odd harmonics, 1 through 79, for alternance. Counterclockwise loops of minus dimensionless shear stress, $-\mathbb{S}$, versus dimensionless shear rate, $\lambda\dot{\gamma}$, calculated for the 2-constant corotational Maxwell model with a Deborah number of $\lambda\omega = 10$ 70

Figure 14. Comparison of exact solution (black) [Eq. (56) with 40 harmonics, 0 through 78] with approximate solution (red) [Eq. (20)] for loops of minus dimensionless first normal stress differences, $-\mathbb{N}_1 = 2\mathbb{N}_2$, versus normalized shear rate, $\dot{\gamma}/\dot{\gamma}^0 = \cos\tau$, left-clockwise loops calculated for the 2-constant corotational Maxwell model with a Deborah number of $\lambda\omega = 10$ for $Wi/De = 5/4$ and $\lambda\omega = \frac{1}{10}, 1, 10$. For the normal stress differences, the exact solution is an improvement over the approximate solution. 71

Figure 15. Comparison of exact solution (black) [Eq. (66) using 40 harmonics, 1 through 79] with approximate solution (red) [Eq. (21)] for counterclockwise loops of minus dimensionless shear stress, $-\mathbb{S}$, versus dimensionless shear rate, $\lambda\dot{\gamma}$, calculated for the 2-constant corotational Maxwell model with a Deborah number of $\lambda\omega = 10$ for $Wi/De = 5/4$ and $\lambda\omega = \frac{1}{10}, 1, 10$. For the shear stress, the exact and approximate solutions nearly match. 72

Figure 16. Comparison of exact solution (black) [Eq. (66) using 40 harmonics, 1 through 79] with approximate solution (red) [Eq. (21)] for counterclockwise loops of minus dimensionless shear stress, $-\mathbb{S}$, versus dimensionless shear

rate, $\lambda\dot{\gamma}$, calculated for the 2-constant corotational Maxwell model with a Deborah number of $\lambda\omega = 10$ for $Wi/De = 2$ and $\lambda\omega = 1$. **Pink** curve shows corresponding linear viscoelastic behavior [alternant part of Eq. (83)]. The exact solution is a significant improvement over the approximate one, and specifically, is much further from the corresponding linear response..... 73

Figure 17. Exact solution (black) [Eq. (56) with 40 harmonics, 0 through 78] with approximate solution (**red**) [Eq. (20)], with $\lambda\omega = \frac{1}{10}$ and $\lambda\dot{\gamma}^0 = \frac{1}{2}$, compared with exact solution for steady shear flow (**red**) (Eq. (84) of [5]). Left-clockwise loops of minus dimensionless first normal stress differences, $-\mathbb{N}_1 = 2\mathbb{N}_2$, versus dimensionless shear rate, $\lambda\dot{\gamma}$, calculated for the 2-constant corotational Maxwell model. Curves nearly overlap, as they should..... 74

Figure 18. Comparison of exact solution (black) [Eq. (66) using 40 harmonics, 1 through 79] with approximate solution (**red**) [Eq. (21)] with $\lambda\omega = \frac{1}{10}$ and $\lambda\dot{\gamma}^0 = \frac{1}{2}$, with exact solution for steady shear flow (**red**) (Eq. (84) of [5]). Counterclockwise loops of minus dimensionless shear stress, $-\mathbb{S}$, versus dimensionless shear rate, $\lambda\dot{\gamma}$, calculated for the 2-constant corotational Maxwell model. Curves nearly overlap, as they should..... 75

Figure 19. Exact solution (**blue** response is Eq. (71) using 40 even harmonics, 0 through 78, and 40 odd ones, 1 through 79, for startup and evaluated for multiple relaxation times, taken from Table 4 of [5]) for counterclockwise response of minus dimensionless shear stress, $-\mathbb{S}$, versus dimensionless shear rate, $\lambda\dot{\gamma}$, calculated for the generalized corotational Maxwell model and compared with measured behavior of molten HDPE (**red** dots).

$Wi = \bar{\lambda}\dot{\gamma}^0 = 1.25$ and $De = \bar{\lambda}\omega = 1.0$ 76

Figure 20. Exact solution (**black** loop is Eq. (73) with 40 harmonics, 1 through 79 and evaluated for multiple relaxation times, taken from Table 4 of [5]) for counterclockwise loops of minus dimensionless shear stress, $-\mathbb{S}$, versus dimensionless shear rate, $\lambda\dot{\gamma}$, calculated for the generalized corotational Maxwell model and compared with measured behavior of molten HDPE (**red** dots). $Wi = \bar{\lambda}\dot{\gamma}^0 = 0.486$ and $De = \bar{\lambda}\omega = 1.0$. **Pink** curve shows corresponding linear viscoelastic behavior [alternant part of Eq. (83)]...... 77

Figure 21. Exact solution (**black** loop is Eq. (73) with 40 harmonics, 1 through 79 and evaluated for multiple relaxation times, taken from Table 4 of [5]) for counterclockwise loops of minus dimensionless shear stress, $-\mathbb{S}$, versus dimensionless shear rate, $\lambda\dot{\gamma}$, calculated for the generalized corotational Maxwell model and compared with measured behavior of molten HDPE (**red** dots). $Wi = \bar{\lambda}\dot{\gamma}^0 = 0.983$ and $De = \bar{\lambda}\omega = 1.0$. **Pink** curve shows corresponding linear viscoelastic behavior [alternant part of Eq. (83)]...... 78

Figure 22. Exact solution (**black** loop is Eq. (73) with 40 harmonics, 1 through 79 and evaluated for multiple relaxation times, taken from Table 4 of [5]) for counterclockwise loops of minus dimensionless shear stress, $-\mathbb{S}$, versus dimensionless shear rate, $\lambda\dot{\gamma}$, calculated for the generalized corotational Maxwell model and compared with measured behavior of molten HDPE

(red dots). $Wi = \bar{\lambda}\dot{\gamma}^0 = 1.388$ and $De = \bar{\lambda}\omega = 1.0$. Pink curve shows corresponding linear viscoelastic behavior [alternant part of Eq. (83)]..... 79

Figure 23. Exact solution (black loop is Eq. (73) with 40 harmonics, 1 through 79 and evaluated for multiple relaxation times, taken from Table 4 of [5]) for counterclockwise alternance loops of minus dimensionless shear stress, $-\mathbb{S}$, versus dimensionless shear rate, $\lambda\dot{\gamma}$, calculated for the generalized corotational Maxwell model and compared with measured behavior of molten HDPE (red dots). $Wi = \bar{\lambda}\dot{\gamma}^0 = 2.183$ and $De = \bar{\lambda}\omega = 1.0$. Pink curve shows corresponding linear viscoelastic behavior [alternant part of Eq. (83)]. 80

Figure 24. Comparison of exact solution [Eq. (71) with Eqs. (72) and (73) using 40 odd harmonics, 1 through 79] with experimental measurements of the maximum value of the shear stress response in large-amplitude oscillatory shear flow at $\omega = 10\pi$ rad/s (from Fig. 1 of [36] or *Puc. 1.* of [37]). Black line is polyisoprene ($\eta_0 = 1.0 \times 10^7$ Pa·s, $\lambda = 33.12$ s) with $De = 1040$. Red line is polyisoprene ($\eta_0 = 2.87 \times 10^6$ Pa·s, $\lambda = 5.89$ s) with $De = 902$. Blue line is polybutadiene ($\eta_0 = 3.0 \times 10^6$ Pa·s, $\lambda = 4.34$ s) $De = 139$. Pink line is polybutadiene ($\eta_0 = 3.0 \times 10^4$ Pa·s, $\lambda = 0.04$ s) with $De = 1.26$ 81

Figure 25. Comparison of exact solution [Eq. (71) with Eqs. (72) and (73) using 40 odd harmonics, 1 through 79] with experimental measurements of the maximum value of the shear stress response in large-amplitude oscillatory shear flow at $\omega = 200\pi$ rad/s (from Fig. 1 of [36] or *Puc. 1.* of [37]). Black line is polyisoprene ($\eta_0 = 1.0 \times 10^7$ Pa·s, $\lambda = 33.12$ s) with $De = 20,810$. Red line is polyisoprene ($\eta_0 = 2.87 \times 10^6$ Pa·s, $\lambda = 5.89$ s) with $De = 18,033$). Blue line is polybutadiene ($\eta_0 = 3.0 \times 10^6$ Pa·s, $\lambda = 4.34$ s) with $De = 2,727$. Pink line is polybutadiene ($\eta_0 = 3.0 \times 10^4$ Pa·s, $\lambda = 0.04$ s) with $De = 25$ 82

I. INTRODUCTION

The rheology of polymeric liquids presents many challenges in mathematical physics, not the least of which is the pursuit of analytical solutions for transient flow problems. Though exact solutions to rheological problems give us the deepest physical insight, exact solutions to nonlinear problems are elusive. Instead, rheologists must often settle for truncated expansions (see column 11 of Table I), obtained only with great mathematical effort. Consider, for instance, the truncated expansions for the corotational Maxwell model (Eqs. (20) and (21) from [5]). In no subdiscipline of mathematical physics have exact solutions been more elusive than in the physics of viscoelastic liquids subject to oscillatory deformations.

In this paper, we apply the Kovacic method [1], pioneered in the mid-eighties, to arrive at our exact solution. The usefulness of this method appears to have been overlooked by the rheological community. We write this paper not only to benefit the professional mathematical physicist, but with sufficient detail to help graduate students arrive at their own exact solutions for oscillatory shear flow at least some constitutive equations other than the corotational Maxwell model treated here. Specifically, we would expect educators to use our work in both their research and teaching, and for their graduate students to train themselves from our analysis (Section IV) and detailed appendices (Sections X, XI and XII).

Since its conception in 1935 [2,3,4] oscillatory shear flow has become by far the most popular laboratory method for exploring the physics of polymeric liquids. We generate oscillatory shear flow by confining the fluid to a simple shear apparatus, and then subject one solid-liquid boundary to a coplanar sinusoidal displacement, and thus, the fluid to the following velocity profile (see the coordinate system defined and the flow field illustrated in Figure 1):

$$v_x = \dot{\gamma}^0 \cos \omega t y; v_y = v_z = 0 \quad (1)$$

and hence, to a corresponding cosinusoidal shear rate:

$$\dot{\gamma}(t) = \dot{\gamma}^0 \cos \omega t \quad (2)$$

Using the characteristic relaxation time of the viscoelastic fluid, λ , we can nondimensionalize Eq. (2):

$$\begin{aligned} \lambda \dot{\gamma}(t) &= \lambda \dot{\gamma}^0 \cos \lambda \omega (t / \lambda) \\ &\equiv Wi \cos De(t / \lambda) \end{aligned} \quad (3)$$

where:

$$De \equiv \lambda \omega \quad (4)$$

and:

$$Wi \equiv \lambda \dot{\gamma}^0 \quad (5)$$

The dimensionless Eq. (3) suggests that dimensionless solutions to large-amplitude oscillatory shear flow problems shall be written in terms of Wi or De only, and we follow this throughout this work.

Increasing either the Weissenberg number or the Deborah number in Eq. (3) causes the fluid response to depart from Newtonian behavior. We can construct a complex dimensionless number from the ordered pair (De, Wi) thus (see this illustrated in Fig. 1 of [5]):

$$G_n \equiv De + iWi \quad (6)$$

which defines a vector with magnitude:

$$|G_n| \equiv \sqrt{De^2 + Wi^2} \quad (7)$$

and with angle:

$$\phi \equiv \arctan \frac{Wi}{De}. \quad (8)$$

The magnitude of G_n reflects how far the fluid behavior departs from Newtonian behavior. We call such departures *non-Newtonian*. We can associate behavior in steady shear flow with $De = 0$, where $G_n = iWi$. We further associate *linear viscoelastic* behavior with $Wi = 0$, where $G_n \equiv De$. The angle ϕ thus reflects the type of departure from Newtonian behavior. The value $\phi = 0$ corresponds to linear viscoelastic behavior, and $\phi = \pi/2$, to steady shear flow. We use these last two concepts below when performing consistency checks of our exact solution for large-amplitude oscillatory shear flow (in Section VI).

When higher harmonics are observed in the shear stress response, we call the oscillatory experiment *large-amplitude*. For polymeric liquids, these higher harmonics are commonly observed when:

$$\frac{Wi}{De} > 1 \quad (9)$$

Eq. (9) is thus our working definition of large-amplitude oscillatory shear flow [6,7], and with recent advances in rheometry, conducting experiments satisfying Eq. (9) is now commonplace for exploring the physics of polymeric liquids [8]. The material functions in this flow are most commonly defined as coefficients of the Fourier series:

$$\frac{\tau_{yx}(\tau, \gamma_0)}{\gamma_0} = - \sum_{\substack{n=1 \\ \text{odd}}}^{\infty} G'_n(\omega, \gamma_0) \sin n\tau + G''_n(\omega, \gamma_0) \cos n\tau \quad (10)$$

where $\tau \equiv \omega t$. We call this set of coefficients, $G'_n(\omega, \gamma_0)$ and $G''_n(\omega, \gamma_0)$, the *Fourier moduli*. These Fourier moduli are readily obtained from a measured time series $\tau_{yx}(\tau, \gamma_0)$ using the discrete Fourier transform [7]. The Fourier moduli in (10) are occasionally expanded in odd powers of γ_0 defining a matrix of frequency dependent nonlinear moduli [9,10,11]:

$$\frac{\tau_{yx}(\tau)}{\gamma_0} = - \sum_{\substack{m=1 \\ \text{odd}}}^{\infty} \sum_{\substack{n=1 \\ \text{odd}}}^m \gamma_0^{m-1} [G'_{mn}(\omega) \sin n\tau + G''_{mn}(\omega) \cos n\tau] \quad (11)$$

where $\tau \equiv \omega t$.

The shear stress response in LAOS has also been expanded in odd powers of $\dot{\gamma}^0$, defining a matrix of frequency dependent nonlinear viscosities [12]:

$$\frac{\tau_{yx}(\tau)}{\dot{\gamma}_0} = - \sum_{\substack{n=1 \\ \text{odd}}}^{\infty} \sum_{\substack{m=1 \\ \text{odd}}}^n \dot{\gamma}_0^{n-1} [\eta'_{mn}(\omega) \cos m\tau + \eta''_{mn}(\omega) \sin m\tau] \quad (12)$$

where $(\eta'_{mn}, \eta''_{mn})$ are named the *storage and loss viscosities of mnth order*, where $(\eta'_{11}, \eta''_{11}) = (\eta', \eta'')$. The “ m ” in the “ $mnth$ order” corresponds to the number of the harmonic in the shear stress response. The “ n ” in the “ $mnth$ order” corresponds to *one plus* the power of the expansion in Eq. (12).

Table I summarizes the developing literature on analytical solutions for large-amplitude oscillatory shear flow. From column 11 of Table I we glean that no constitutive equation has heretofore been solved exactly for large-amplitude oscillatory shear flow. In fact, previous work provides only approximate solutions for large-amplitude oscillatory shear flow for, at best, just a few harmonics of the shear stress, or of the normal stress differences. Our ability to measure higher harmonics far surpasses our ability to predict them from theory. For instance, of the shear stress response for beer foam in large-amplitude oscillatory shear flow, higher harmonics up to and including the 289th have been measured precisely [13].

From the literature summarized in Table I, we learn that previous analytical solutions normally take the form of a truncated expansion in $\lambda\dot{\gamma}^0$ [given by Eq. (11)], but that a few of these take the form of a truncated expansion in $\dot{\gamma}^0/\omega$ [given by Eq. (12)]. At large values of the expansion variable, these expansions eventually break down. Thus, for rheologists, one main advantage of an exact solution is that it allows exploration of nonlinear physics that cannot be probed with truncated expansions. Now, one of the great advantages of any analytical solution for oscillatory shear is that, when integrable, it can be used to explore temperature rise in a viscoelastic fluid subjected to large-amplitude oscillatory shear flow [14,15]. The exact solution can also be used to evaluate the accuracy of the truncated expansions. Further, if the exact solution can be written as a Fourier series, it can even be used to assess if or when a constitutive model will predict self-intersecting loops of shear stress versus shear rate, for example [16].

Inasmuch as large-amplitude oscillatory shear flow of a polymeric liquid is used for viscous dampers in many kinds of machinery, exact solutions can be used for more accurate viscous damper design, especially where large vibrations are to be damped ([17,18,19, 20]; Section 3.3 of [21]; Section 8.7 of [22]; Problem 5.5 of [23,24]). If the shear stress is measured in the viscous damper fluid, then an exact solution can be used to estimate the temperature rise in the damper fluid accurately. This information can then be used to project the thermal degradation of the viscoelastic damping fluid, for example, and to establish a replacement cycle for this damping fluid.

When seeking exact solutions, we prefer outcomes in closed form. By closed form, we mean, roughly, one that can be written down by a first-year calculus student (see Section 1.1. of [1]). In general, for teaching, scholars thus prefer examples with solutions in closed form.

When a differential equation satisfies an existence theorem, we can know that the solution exists before we have it. When a differential equation satisfies a uniqueness theorem, we know that once found, the exact solution provides one unique way to look at the answer. In this paper, we first adimensionalize the corotational Maxwell model for large-amplitude oscillatory shear flow. We then rewrite it into a particular matrix form. This particular form then satisfies a

theorem for both the existence and the uniqueness of the exact solution. We then follow the method of Kovacic (Section 4.1 of [1]) to arrive at an exact, unique solution in closed form, which we believe to be the first exact solution to a large-amplitude oscillatory shear flow problem for which higher harmonics in the shear stress are predicted.

We chose the corotational Maxwell model because this two-parameter model (η_0 and λ) is the simplest constitutive model that is relevant to large-amplitude oscillatory shear flow, and because it has previously been found to be accurate for molten plastics. By *relevant* we mean that the model predicts higher harmonics for the shear stress, and for the normal stress differences. We compare our exact solution with an approximate truncated expansion solution to the same problem, and we then compare our exact solution with experimental data for molten high-density polyethylene, a pair of polyisoprenes, and another pair of polybutylenes.

We find that our exact solution takes neither of the forms of an expansion in $\lambda\dot{\gamma}^0$ [given by Eq. (11)], nor of an expansion in $\dot{\gamma}^0/\omega$ [given by Eq. (12)]. Instead, the exact solution takes a form that we find to be surprising and intrinsically beautiful.

II. MECHANICS OF LARGE-AMPLITUDE OSCILLATORY SHEAR

For oscillatory shear flow, the rate of deformation tensor is given by:

$$\dot{\boldsymbol{\gamma}} = \begin{bmatrix} 0 & \dot{\gamma}^0 \cos \omega t & 0 \\ \dot{\gamma}^0 \cos \omega t & 0 & 0 \\ 0 & 0 & 0 \end{bmatrix} \quad (13)$$

which, with a characteristic time for the fluid λ , can be nondimensionalized as

$$\lambda \dot{\boldsymbol{\gamma}} = \begin{bmatrix} 0 & \lambda \dot{\gamma}^0 \cos \tau & 0 \\ \lambda \dot{\gamma}^0 \cos \tau & 0 & 0 \\ 0 & 0 & 0 \end{bmatrix} \quad (14)$$

in which τ is not to be confused with the **bold face** Greek $\boldsymbol{\tau}$, which we use below for the extra stress tensor. Further, the **bold face** Greek $\dot{\boldsymbol{\gamma}}$ is not to be confused with the italicized symbol for its yx -component, $\dot{\gamma}$. We will need these expressions for $\dot{\boldsymbol{\gamma}}$ [Eqs. (13) through (14)] for our analysis of oscillatory shear flow below.

III. THE COROTATIONAL MAXWELL MODEL

For a single-relaxation time, the corotational Maxwell model is:

$$\boldsymbol{\tau} + \lambda \frac{\mathcal{D}\boldsymbol{\tau}}{\mathcal{D}t} = -\eta_0 \dot{\boldsymbol{\gamma}} \quad (15)$$

in which:

$$\frac{\mathcal{D}\boldsymbol{\tau}}{\mathcal{D}t} \equiv \frac{D\boldsymbol{\tau}}{Dt} + \frac{1}{2}\{\boldsymbol{\omega} \cdot \boldsymbol{\tau} - \boldsymbol{\tau} \cdot \boldsymbol{\omega}\} \quad (16)$$

defines the Jaumann derivative; here $D\boldsymbol{\tau}/Dt$ is the substantial derivative and:

$$\dot{\boldsymbol{\gamma}} \equiv \nabla\mathbf{v} + (\nabla\mathbf{v})^\dagger \quad (17)$$

is the rate-of-strain tensor, given by Eq. (14), and:

$$\boldsymbol{\omega} \equiv \nabla\mathbf{v} - (\nabla\mathbf{v})^\dagger \quad (18)$$

is the vorticity tensor. We call the derivative given by Eq. (16) *corotational* because it measures rates of changes of the extra stress tensor with respect to a coordinate frame that both translates and rotates with the fluid. For an extensive discussion of corotational models and their applications, see Chapters 7 and 8 of [25], and also [26,27,28,29,30]. If Eq. (16) is replaced with a codeformational derivative, though this leads to an exact solution for oscillatory shear flow, the interesting nonlinear physics disappears (mindful of the errata in Ref. 31, see Eqs. 6.40 and 6.41 of [31]; [32]). By *codeformational* we mean a derivative that measures rates of changes of the extra stress tensor with respect to a coordinate frame that translates, rotates and deforms with the fluid. With a codeformational derivative, the higher harmonics in the extra stress responses disappear (see Table I below). This is why, for exploring the mathematical physics of fluid continua, we prefer the corotational framework over the codeformational.

Eq. (15) can be nondimensionalized as:

$$\frac{\lambda}{\eta_0}\boldsymbol{\tau} + \text{De} \frac{\partial}{\partial\tau} \left(\frac{\lambda}{\eta_0}\boldsymbol{\tau} \right) + \frac{\lambda\text{De}}{2\eta_0\omega} \{\boldsymbol{\omega} \cdot \boldsymbol{\tau} - \boldsymbol{\tau} \cdot \boldsymbol{\omega}\} = -\lambda\dot{\boldsymbol{\gamma}} \quad (19)$$

Goddard and Miller [33] have shown how to convert any corotational model into an integral form, for any simple shear flow, and previous work on large-amplitude oscillatory shear flow attacks this integral form [5,34]. Approximate analytical solutions have thus been produced for the first few harmonics of both the shear stress (up to the fifth) and the normal stress differences (up to the fourth). Specifically, for the zeroth, second and fourth harmonics of the normal stress differences (Eq. (66) of [5]):

$$\begin{aligned} \mathbb{N}_1(\boldsymbol{\tau}) &= -2\mathbb{N}_2(\boldsymbol{\tau}) \\ &= -\text{Wi} \left[\frac{1}{1+\text{De}^2} + \frac{(1-2\text{De}^2)\cos 2\tau + 3\text{De}\sin 2\tau}{(1+\text{De}^2)(1+4\text{De}^2)} \right] \\ &\quad + \frac{\text{Wi}^3}{4} \left[\frac{3}{(1+\text{De}^2)(1+4\text{De}^2)} + \frac{(4-24\text{De}^2)\cos 2\tau + 20\text{De}\sin 2\tau}{(1+\text{De}^2)(1+4\text{De}^2)(1+9\text{De}^2)} \right. \\ &\quad \left. + \frac{(1-35\text{De}^2+24\text{De}^4)\cos 4\tau + (10-50\text{De}^2)\text{De}\sin 4\tau}{(1+\text{De}^2)(1+4\text{De}^2)(1+9\text{De}^2)(1+16\text{De}^2)} \right] \end{aligned} \quad (20)$$

and the approximate expressions for the first, third and fifth harmonics of the shear stress are (Eq. (58) of [5]):

$$\begin{aligned}
\mathbb{S}(\tau) = & -\frac{\cos \tau + De \sin \tau}{1+De^2} \\
& + \frac{Wi^2}{4} \left[\frac{3 \cos \tau + 6De \sin \tau}{(1+De^2)(1+4De^2)} \right. \\
& \left. + \frac{(1-11De^2) \cos 3\tau + 6(1-De^2) De \sin 3\tau}{(1+De^2)(1+4De^2)(1+9De^2)} \right] \\
& - \frac{Wi^4}{8} \left[\frac{5 \cos \tau + 15De \sin \tau}{(1+De^2)(1+4De^2)(1+9De^2)} \right. \\
& \left. + \frac{(5-130De^2) \cos 3\tau + (45-120De^2) De \sin 3\tau}{2(1+De^2)(1+4De^2)(1+9De^2)(1+16De^2)} \right] \\
& \left. + \frac{(1-85De^2 + 274De^4) \cos 5\tau + (15-225De^2 + 120De^4) De \sin 5\tau}{2(1+De^2)(1+4De^2)(1+9De^2)(1+16De^2)(1+25De^2)} \right]
\end{aligned} \tag{21}$$

The shear stress measurements for these approximate solutions compare well with experimental measurements on molten plastics (see Figs. 8, 9 and 10 of [5]), so long as the Weissenberg number is not too high (see Fig. 11 of [5]).

Eqs. (21) and (20) reduce to the well-known result for the corotational Maxwell fluid in steady shear flow (Eq. (84) of [5]):

$$\frac{\eta}{\eta_0} = \frac{\Psi_1}{2\eta_0\lambda} = -\frac{\Psi_2}{\eta_0\lambda} = 1 - Wi^2 + Wi^4 - \dots = \frac{1}{1+(\lambda\dot{\gamma})^2} \tag{22}$$

that is, for vanishingly small values of De . The material functions for steady shear flow, η , Ψ_1 and Ψ_2 in Eq. (22) are defined in Table II. Further, Eqs. (21) and (20) reduce to the well-known results for linear viscoelasticity (for any Maxwell fluid):

$$\mathbb{S}(\tau) = -\frac{\cos \tau + De \sin \tau}{1+De^2} \tag{23}$$

and:

$$\mathbb{N}_1(\tau) = \mathbb{N}_2(\tau) = 0 \tag{24}$$

that is, for vanishingly small values of Wi .

In this paper, we obtain exact analytical solutions for both the shear stress and the normal stress differences by attacking the corotational Maxwell model, Eq. (15), in its differential form. We then compare our exact solutions with its corresponding approximations, Eqs. (21) and (20). We further test the exact solution by comparing it with experimental measurements. For this comparison we must extend Eq. (15) to (see Section 8 of [5]):

$$\tau_{yx} = \sum_{j=1}^{\infty} \tau_j \tag{25}$$

and:

$$\tau_j + \lambda_j \frac{\mathcal{D}\tau_j}{\mathcal{D}t} = -\eta_j \dot{\gamma} \quad (26)$$

for multiple relaxation times, where τ_j is the contribution to the extra stress tensor from the j th relaxation time.

a. Simple Shear Flow

For simple shear flows (see Eq. (19) of [35]) the rightmost term in Eq. (16) is given by:

$$\frac{1}{2\omega} \{ \boldsymbol{\omega} \cdot \boldsymbol{\tau} - \boldsymbol{\tau} \cdot \boldsymbol{\omega} \} = \frac{1}{2\omega} \begin{bmatrix} -2\tau_{yx} & \tau_{xx} - \tau_{yy} & 0 \\ \tau_{xx} - \tau_{yy} & 2\tau_{yx} & 0 \\ 0 & 0 & 0 \end{bmatrix} \dot{\gamma}_{yx}(t) \quad (27)$$

b. Oscillatory Shear Flow

For oscillatory shear flow, the xx and yy components of Eq. (19) are given by:

$$\frac{\lambda}{\eta_0} \tau_{xx} + \text{De} \frac{d}{d\tau} \left(\frac{\lambda}{\eta_0} \tau_{xx} \right) - \frac{\lambda \dot{\gamma}^0}{\eta_0 \omega} \cos \tau \text{De} \tau_{yx} = 0 \quad (28)$$

and:

$$\frac{\lambda}{\eta_0} \tau_{yy} + \text{De} \frac{d}{d\tau} \left(\frac{\lambda}{\eta_0} \tau_{yy} \right) + \frac{\text{Wi}}{\eta_0 \omega} \cos \tau \text{De} \tau_{yx} = 0 \quad (29)$$

Subtracting Eq. (28) from Eq. (29) and then using Table III:

$$\frac{dN_1}{d\tau} = -\frac{1}{\text{De}} N_1 + 2 \frac{\text{Wi}}{\text{De}} S \cos \tau \quad (30)$$

The yx -component of Eq. (19) is given by:

$$\frac{\lambda}{\eta_0} \tau_{yx} + \text{De} \frac{d}{d\tau} \left(\frac{\lambda}{\eta_0} \tau_{yx} \right) + \frac{\lambda}{2\eta_0 \omega} \text{De} N_1 = -\text{Wi} \cos \tau \quad (31)$$

or, in terms of dimensionless groups and variables:

$$\frac{dS}{d\tau} = -\frac{1}{2} \frac{\text{Wi}}{\text{De}} N_1 \cos \tau - \frac{1}{\text{De}} S - \frac{1}{\text{De}} \cos \tau \quad (32)$$

We can write Eqs. (30) and (32) in matrix form:

$$\frac{d}{d\tau} \begin{bmatrix} N_1(\tau) \\ S(\tau) \end{bmatrix} = \begin{bmatrix} -\frac{1}{\text{De}} & 2 \frac{\text{Wi}}{\text{De}} \cos \tau \\ -\frac{1}{2} \frac{\text{Wi}}{\text{De}} \cos \tau & -\frac{1}{\text{De}} \end{bmatrix} \begin{bmatrix} N_1(\tau) \\ S(\tau) \end{bmatrix} - \begin{bmatrix} 0 \\ \frac{1}{\text{De}} \cos \tau \end{bmatrix} \quad (33)$$

For startup from a quiescent melt, Eqs. (33) are subject to the initial conditions:

$$\begin{bmatrix} N_1(0) \\ S(0) \end{bmatrix} = \begin{bmatrix} 0 \\ 0 \end{bmatrix} \quad (34)$$

We will next solve Eqs. (33) simultaneously, subject to Eq. (34). Although a partial solution to this problem has been suggested (see Eqs. (3) and (4) of [36,37], this suggestion contains integrals that have not been evaluated analytically. Instead, these integrals were evaluated numerically (see solid curves in Fig. 1 of [36] or *Puc. 1.* of [37]).

IV. ANALYSIS

From Eq. (33), we get the homogeneous system:

$$\frac{d}{d\tau} \begin{bmatrix} \mathbb{N}_1(\tau) \\ \mathbb{S}(\tau) \end{bmatrix} = \begin{bmatrix} -\frac{1}{De} & 2\frac{Wi}{De}\cos\tau \\ -\frac{1}{2}\frac{Wi}{De}\cos\tau & -\frac{1}{De} \end{bmatrix} \begin{bmatrix} \mathbb{N}_1(\tau) \\ \mathbb{S}(\tau) \end{bmatrix} \quad (35)$$

which matches the general form to which Theorem 10 on pp. 710-711 of [38] applies, and which guarantees the *existence* of a *unique* solution to Eq. (35) of the form:

$$\begin{bmatrix} \mathbb{N}_1(\tau) \\ \mathbb{S}(\tau) \end{bmatrix} = \Phi(\tau)\Phi^{-1}(0) \begin{bmatrix} \mathbb{N}_1(0) \\ \mathbb{S}(0) \end{bmatrix} + \Phi(\tau) \int_0^\tau \Phi^{-1}(\tau') \begin{bmatrix} 0 \\ -\frac{1}{De}\cos\tau' \end{bmatrix} d\tau' \quad (36)$$

To solve Eqs. (35), subject to the initial conditions Eqs. (34), we follow the general method of Kovacic (Section 4.1 of [1]) benefitting from the corresponding textbook treatment for nonhomogeneous linear systems of Adkins and Davidson (Section 9.7 of [38]). Thusly, in Section X below, we derive the following closed form for the *fundamental matrix*:

$$\Phi(\tau) = e^{-\tau/De} \begin{bmatrix} \cos(\frac{Wi}{De}\sin\tau) & \sin(\frac{Wi}{De}\sin\tau) \\ -\frac{1}{2}\sin(\frac{Wi}{De}\sin\tau) & \frac{1}{2}\cos(\frac{Wi}{De}\sin\tau) \end{bmatrix} \quad (37)$$

which we will then use to get the homogeneous startup solution:

$$\begin{bmatrix} \mathbb{N}_{1,h}(\tau) \\ \mathbb{S}_h(\tau) \end{bmatrix} = \Phi(\tau) \begin{bmatrix} C_1 \\ C_2 \end{bmatrix} \quad (38)$$

in which the subscript *h* denotes *homogeneous*. Substituting Eq. (37) into Eq. (38) yields:

$$\begin{bmatrix} \mathbb{N}_{1,h}(\tau) \\ \mathbb{S}_h(\tau) \end{bmatrix} = \begin{bmatrix} C_1 e^{-\tau/De} \cos(\frac{Wi}{De}\sin\tau) + C_2 e^{-\tau/De} \sin(\frac{Wi}{De}\sin\tau) \\ -\frac{1}{2}C_1 e^{-\tau/De} \sin(\frac{Wi}{De}\sin\tau) + \frac{1}{2}C_2 e^{-\tau/De} \cos(\frac{Wi}{De}\sin\tau) \end{bmatrix} \quad (39)$$

Next we investigate the particular alternance solution (following Eq. (10), p. 711 of [38]):

$$\begin{bmatrix} \mathbb{N}_{1,p}(\tau) \\ \mathbb{S}_p(\tau) \end{bmatrix} = \Phi(\tau) \int_0^\tau \Phi^{-1}(\tau') \begin{bmatrix} 0 \\ -\frac{1}{De}\cos\tau' \end{bmatrix} d\tau' \quad (40)$$

where *p* denotes *particular*. Substituting Eq. (37) into Eq. (40) yields:

$$\begin{bmatrix} \mathbb{N}_{1,p}(\tau) \\ \mathbb{S}_p(\tau) \end{bmatrix} = e^{-\tau/\text{De}} \begin{bmatrix} \cos(\frac{Wi}{\text{De}} \sin \tau) & \sin(\frac{Wi}{\text{De}} \sin \tau) \\ -\frac{1}{2} \sin(\frac{Wi}{\text{De}} \sin \tau) & \frac{1}{2} \cos(\frac{Wi}{\text{De}} \sin \tau) \end{bmatrix} \begin{bmatrix} \frac{2}{\text{De}} I_1 \\ -\frac{2}{\text{De}} I_2 \end{bmatrix} \quad (41)$$

$$\begin{bmatrix} \mathbb{N}_{1,p}(\tau) \\ \mathbb{S}_p(\tau) \end{bmatrix} = \begin{bmatrix} \frac{2}{\text{De}} e^{-\tau/\text{De}} \cos(\frac{Wi}{\text{De}} \sin \tau) I_1 - \frac{2}{\text{De}} e^{-\tau/\text{De}} \sin(\frac{Wi}{\text{De}} \sin \tau) I_2 \\ -\frac{1}{\text{De}} e^{-\tau/\text{De}} \sin(\frac{Wi}{\text{De}} \sin \tau) I_1 - \frac{1}{\text{De}} e^{-\tau/\text{De}} \cos(\frac{Wi}{\text{De}} \sin \tau) I_2 \end{bmatrix} \quad (42)$$

where:

$$I_1 \equiv \int_0^\tau e^{\tau'/\text{De}} \cos \tau' \sin(\frac{Wi}{\text{De}} \sin \tau') d\tau' \quad (43)$$

$$I_2 \equiv \int_0^\tau e^{\tau'/\text{De}} \cos \tau' \cos(\frac{Wi}{\text{De}} \sin \tau') d\tau' \quad (44)$$

where the integrals I_1 and I_2 are derived in Section XI and are given by Eqs.

(132) [with Eqs. (133) and (134)] and (139) [with Eqs. (140) and (141)]. By *alternance* we mean the limit cycles (or standing waves) of the shear stress, and of the normal stress differences that are produced once the transients due to startup vanish (see Section 6 of [5]). Finally, we combine both the homogeneous startup, Eq. (39), and particular alternance responses, Eq. (42) to get:

$$\begin{aligned} \mathbb{N}_1(\tau) = & C_1 e^{-\tau/\text{De}} \cos(\frac{Wi}{\text{De}} \sin \tau) + C_2 e^{-\tau/\text{De}} \sin(\frac{Wi}{\text{De}} \sin \tau) \\ & + \frac{2}{\text{De}} e^{-\tau/\text{De}} \cos(\frac{Wi}{\text{De}} \sin \tau) I_1 - \frac{2}{\text{De}} e^{-\tau/\text{De}} \sin(\frac{Wi}{\text{De}} \sin \tau) I_2 \end{aligned} \quad (45)$$

$$\begin{aligned} \mathbb{S}(\tau) = & -\frac{1}{2} C_1 e^{-\tau/\text{De}} \sin(\frac{Wi}{\text{De}} \sin \tau) + \frac{1}{2} C_2 e^{-\tau/\text{De}} \cos(\frac{Wi}{\text{De}} \sin \tau) \\ & - \frac{1}{\text{De}} e^{-\tau/\text{De}} \sin(\frac{Wi}{\text{De}} \sin \tau) I_1 - \frac{1}{\text{De}} e^{-\tau/\text{De}} \cos(\frac{Wi}{\text{De}} \sin \tau) I_2 \end{aligned} \quad (46)$$

since, for the corotational Maxwell model in any simple shearing flow (Eq. (30) of [35]):

$$\tau_{33}(\tau) = 0 \quad (47)$$

Applying the initial conditions, Eqs. (34), to Eqs. (45) and (46), we get:

$$C_1 = -\frac{2}{\text{De}} \lim_{\tau \rightarrow 0} I_1 \quad (48)$$

and:

$$C_2 = \frac{2}{\text{De}} \lim_{\tau \rightarrow 0} I_2 \quad (49)$$

Further, in any simple shearing flow, for the corotational Maxwell model (evaluating Eq. (48) of [34] for $\lambda_0 = 0$; see also Eq. (62) of [5]):

$$\mathbb{N}_1(\tau) = -2\mathbb{N}_2(\tau) \quad (50)$$

Hence, by using Eq. (50), we can get the second normal stress difference, $\mathbb{N}_2(\tau)$, by dividing $\mathbb{N}_1(\tau)$ by minus two.

V. RESULTS

Here, we present the results of our analysis, the exact solution for the corotational Maxwell model in large-amplitude oscillatory shear flow. We first cover the normal stress differences in Section V.a and then, the shear stress response in Section V.b.

When comparing this exact solution with approximate solutions, or with experimental data, one must decide on the number of terms to keep in the many Bessel functions, and also on how many harmonics to keep in the stress calculations. For the Bessel functions, we find 40 terms to be more than sufficient for our results to be at least invariant to within a line width for all of the figures reported in this paper, and so we kept 40 terms throughout. When the evaluation of the exact solution involves even harmonics, we used 40 (0 through 78), when involving odd harmonics we used 40 (1 through 79), and when involving both even and odd we used 80 (0 through 79).

In the following Sections V.a and V.b, we will arrive respectively at Eqs. (53) and (63), the main results of this work. We believe these equations to be the first exact solution for large-amplitude oscillatory shear flow for any constitutive equation from which higher harmonics of the shear stress are predicted.

a. Normal Stress Difference Responses

Substituting Eqs. (48) and (49) into Eq. (45) and then rearranging yields:

$$\mathbb{N}_1(\tau) = -2\mathbb{N}_2(\tau) = \frac{2e^{-\tau/De}}{De} \left\{ \cos\left(\frac{Wi}{De} \sin \tau\right) \left(I_1 - \lim_{\tau \rightarrow 0} I_1\right) - \sin\left(\frac{Wi}{De} \sin \tau\right) \left(I_2 - \lim_{\tau \rightarrow 0} I_2\right) \right\} \quad (51)$$

which we call the *compact form* of the exact solution. When alternance is reached, this compact form reduces to:

$$\mathbb{N}_1(\tau) = -2\mathbb{N}_2(\tau) = \frac{2}{De} e^{-\tau/De} \cos\left(\frac{Wi}{De} \sin \tau\right) I_1 - \frac{2}{De} e^{-\tau/De} \sin\left(\frac{Wi}{De} \sin \tau\right) I_2 \quad (52)$$

Substituting Eqs. (121), (124), (132) [with Eqs. (133) and (134)], (135),(139) [with Eqs. (140) and (141)] and (142) into Eqs. (51) yields the exact explicit analytical solution for the first and second normal stress difference responses, for the corotational Maxwell model, in startup of large-amplitude oscillatory shear flow:

$$\begin{aligned}
\mathbb{N}_1(\tau) = -2\mathbb{N}_2(\tau) = 2 \left[J_0 + 2 \sum_{k=1}^{\infty} J_{2k} \cos 2k\tau \right] & \left(- \left[\sum_{k=1}^{\infty} J_{2k-1} \left(\frac{2De k \cos 2k\tau - \sin 2k\tau}{4De^2 k^2 + 1} \right) \right. \right. \\
& \left. \left. + \frac{2De(k-1) \cos 2(1-k)\tau + \sin 2(1-k)\tau}{4De^2(k-1)^2 + 1} \right] \right) \\
& + e^{-\tau/De} \sum_{k=1}^{\infty} J_{2k-1} \left(\frac{2De k}{4De^2 k^2 + 1} \right) \\
& \left. - \frac{2De(k-1)}{4De^2(k-1)^2 + 1} \right) \quad (53) \\
-4 \sum_{k=1}^{\infty} J_{2k-1} \sin(2k-1)\tau & \left(\left[\frac{J_0}{1+De^2} (\cos \tau + De \sin \tau) \right. \right. \\
& \left. \left. + \sum_{k=1}^{\infty} J_{2k} \left[\frac{\cos(2k-1)\tau + (2k-1)De \sin(2k-1)\tau}{De^2(2k-1)^2 + 1} \right] \right. \right. \\
& \left. \left. + \sum_{k=1}^{\infty} J_{2k} \left[\frac{\cos(2k+1)\tau + (2k+1)De \sin(2k+1)\tau}{De^2(2k+1)^2 + 1} \right] \right] \right) \\
& - e^{-\tau/De} \left\{ \frac{J_0}{1+De^2} + \sum_{k=1}^{\infty} J_{2k} \left[\frac{1}{De^2(2k-1)^2 + 1} \right. \right. \\
& \left. \left. + \frac{1}{De^2(2k+1)^2 + 1} \right] \right\}
\end{aligned}$$

and in which the alternant part is in blue. In this paper, all Bessel functions are of Wi/De , so for brevity, we just write J_m and J_0 to mean $J_m(Wi/De)$ and $J_0(Wi/De)$. We call Eqs. (53) the *substituted compact form*.

To transform the substituted compact form to a Fourier series, we begin by rewriting Eq. (53) as:

$$\mathbb{N}_1(\tau) = -2\mathbb{N}_2(\tau) = \mathbb{N}_{1,\text{tr}}(\tau) + \mathbb{N}_{1,\text{al}}(\tau) \quad (54)$$

where:

$$\begin{aligned}
\mathbb{N}_{1,\text{tr}}(\tau) = & -2 \sum_{n=1}^{\infty} \alpha_n^{(1)} e^{-\tau/De} A_0 + e^{-\tau/De} \sum_{n=1}^{\infty} \left[\left(- \sum_{k=1}^{\infty} \alpha_k^{(1)} A_k \right) \cos(2n\tau) \right] \\
& + 2e^{-\tau/De} \sum_{k=0}^{\infty} \alpha_k^{(2)} \sum_{n=1}^{\infty} B_n \sin(2n\tau - \tau)
\end{aligned} \quad (55)$$

which we derive in Section XII.a.i and in which the coefficients of Eq. (55) are defined [in order of occurrence in Eq. (55)] in Eqs. (133), (123), (140) and (126), and where $\mathbb{N}_{1,\text{al}}(\tau)$ in Eq. (54) is given by:

$$\begin{aligned}
\mathbb{N}_{1,\text{al}}(\tau) = & -\sum_{q=1}^{\infty} \frac{16q^2 \text{De}^2 J_{2q}^2}{\text{Wi}(4\text{De}^2 q^2 + 1)} - \sum_{q=1}^{\infty} \frac{2\text{De} J_{2q-1} (2q-1) (J_{2q} + J_{2q-2})}{\text{De}^2 (2q-1)^2 + 1} \\
& + \sum_{n=1}^{\infty} \left[\begin{aligned}
& \left(\frac{-16n^2 \text{De}^2 J_0 J_{2n}}{\text{Wi}(4\text{De}^2 n^2 + 1)} + \sum_{p=1}^{n-1} \frac{-16(n-p)^2 \text{De}^2 J_{2p} J_{2(n-p)}}{\text{Wi}(4\text{De}^2 (n-p)^2 + 1)} \right. \\
& + \sum_{q=1}^{\infty} \frac{-16(q+n)^2 \text{De}^2 J_{2q} J_{2(q+n)}}{\text{Wi}(4\text{De}^2 (q+n)^2 + 1)} + \sum_{q=1}^{\infty} \frac{-16q^2 \text{De}^2 J_{2(q+n)} J_{2q}}{\text{Wi}(4\text{De}^2 q^2 + 1)} \\
& + \sum_{p=1}^n \frac{2\text{De} J_{2p-1} (2n-2p+1) (J_{2n-2p+2} + J_{2n-2p})}{\text{De}^2 (2n-2p+1)^2 + 1} \\
& - \sum_{q=1}^{\infty} \frac{2\text{De} J_{2q-1} (2n+2q-1) (J_{2n+2q} + J_{2n+2q-2})}{\text{De}^2 (2n+2q-1)^2 + 1} \\
& \left. - \sum_{q=1}^{\infty} \frac{2\text{De} J_{2n+2q-1} (2q-1) (J_{2q} + J_{2q-2})}{\text{De}^2 (2q-1)^2 + 1} \right) \cos 2n\tau \\
& + \left(\frac{8n \text{De} J_0 J_{2n}}{\text{Wi}(4\text{De}^2 n^2 + 1)} + \sum_{p=1}^{n-1} \frac{8(n-p) \text{De} J_{2p} J_{2(n-p)}}{\text{Wi}(4\text{De}^2 (n-p)^2 + 1)} \right. \\
& + \sum_{q=1}^{\infty} \frac{8(n+q) \text{De} J_{2q} J_{2(n+q)}}{\text{Wi}(4\text{De}^2 (n+q)^2 + 1)} + \sum_{q=1}^{\infty} \frac{8q \text{De} J_{2q} J_{2(q+n)}}{\text{Wi}(4\text{De}^2 q^2 + 1)} \\
& - \sum_{p=1}^n \frac{2J_{2p-1} (J_{2n-2p+2} + J_{2n-2p})}{\text{De}^2 (2n-2p+1)^2 + 1} - \sum_{q=1}^{\infty} \frac{2J_{2n+2q-1} (J_{2q} + J_{2q-2})}{\text{De}^2 (2q-1)^2 + 1} \\
& \left. + \sum_{q=1}^{\infty} \frac{2J_{2q-1} (J_{2(q+n)} + J_{2(q+n)-2})}{\text{De}^2 (2n+2q-1)^2 + 1} \right) \sin 2n\tau
\end{aligned} \right] \quad (56)
\end{aligned}$$

which we derive in Sections XII.a.ii and XII.a.iii. We can thus extract exact expressions for individual harmonics of the alternant parts of the normal stress difference responses from Eq. (56).

Evaluating Eq. (56) for $n=0$ gives the exact expression for the zeroth harmonics of the alternant parts of the normal stress difference responses:

$$\mathbb{N}_{1,0}(\tau) = -2\mathbb{N}_{2,0}(\tau) = -\sum_{q=1}^{\infty} \frac{16q^2 \text{De}^2 J_{2q}^2}{\text{Wi}(4\text{De}^2 q^2 + 1)} - \sum_{q=1}^{\infty} \frac{2\text{De} J_{2q-1} (2q-1) (J_{2q} + J_{2q-2})}{\text{De}^2 (2q-1)^2 + 1} \quad (57)$$

and for $n=1$, we get the second harmonics:

$$\begin{aligned}
\mathbb{N}_{1,2}(\tau) &= -2\mathbb{N}_{2,2}(\tau) \\
&= \left(\begin{aligned} &\frac{-16\text{De}^2 J_0 J_2}{\text{Wi}(4\text{De}^2+1)} + \frac{2\text{De} J_1 (J_2 + J_0)}{\text{De}^2+1} \\ &-\sum_{q=1}^{\infty} \frac{16(q+1)^2 \text{De}^2 J_{2q} J_{2q+2}}{\text{Wi}(4\text{De}^2(q+1)^2+1)} - \sum_{q=1}^{\infty} \frac{16q^2 \text{De}^2 J_{2q+2} J_{2q}}{\text{Wi}(4\text{De}^2 q^2+1)} \\ &-\sum_{q=1}^{\infty} \frac{2\text{De} J_{2q-1} (1+2q)(J_{2+2q} + J_{2q})}{\text{De}^2(1+2q)^2+1} - \sum_{q=1}^{\infty} \frac{2\text{De} J_{1+2q} (2q-1)(J_{2q} + J_{2q-2})}{\text{De}^2(2q-1)^2+1} \end{aligned} \right) \cos 2\tau \\
&+ \left(\begin{aligned} &\frac{8\text{De} J_0 J_2}{\text{Wi}(4\text{De}^2+1)} - \frac{2J_1 (J_2 + J_0)}{\text{De}^2+1} + \sum_{q=1}^{\infty} \frac{8(1+q)\text{De} J_{2q} J_{2+2q}}{\text{Wi}(4\text{De}^2(2+q)^2+1)} \\ &+ \sum_{q=1}^{\infty} \frac{8q \text{De} J_{2q} J_{2q+2}}{\text{Wi}(4\text{De}^2 q^2+1)} - \sum_{q=1}^{\infty} \frac{2J_{1+2q} (J_{2q} + J_{2q-2})}{\text{De}^2(2q-1)^2+1} \\ &+ \sum_{q=1}^{\infty} \frac{2J_{2q-1} (J_{2q+2} + J_{2q})}{\text{De}^2(1+2q)^2+1} \end{aligned} \right) \sin 2\tau
\end{aligned} \tag{58}$$

and for $n = 2$, the fourths:

$$\begin{aligned}
\mathbb{N}_{1,4}(\tau) &= -2\mathbb{N}_{2,4}(\tau) \\
&= \left(\begin{aligned} &\frac{-64\text{De}^2 J_0 J_4}{\text{Wi}(16\text{De}^2+1)} - \frac{16\text{De}^2 J_2^2}{\text{Wi}(4\text{De}^2+1)} + \sum_{q=1}^{\infty} \frac{-16(q+2)^2 \text{De}^2 J_{2q} J_{2q+4}}{\text{Wi}(4\text{De}^2(q+2)^2+1)} \\ &+ \sum_{q=1}^{\infty} \frac{-16q^2 \text{De}^2 J_{2q+4} J_{2q}}{\text{Wi}(4\text{De}^2 q^2+1)} + \frac{6\text{De} J_1 (J_4 + J_2)}{9\text{De}^2+1} + \frac{2\text{De} J_3 (J_2 + J_0)}{\text{De}^2+1} \\ &-\sum_{q=1}^{\infty} \frac{2\text{De} J_{2q-1} (3+2q)(J_{4+2q} + J_{2+2q})}{\text{De}^2(3+2q)^2+1} - \sum_{q=1}^{\infty} \frac{2\text{De} J_{3+2q} (2q-1)(J_{2q} + J_{2q-2})}{\text{De}^2(2q-1)^2+1} \end{aligned} \right) \cos 4\tau \\
&+ \left(\begin{aligned} &\frac{16\text{De} J_0 J_4}{\text{Wi}(16\text{De}^2+1)} + \frac{8\text{De} J_2^2}{\text{Wi}(4\text{De}^2+1)} + \sum_{q=1}^{\infty} \frac{8(2+q)\text{De} J_{2q} J_{2q+4}}{\text{Wi}(4\text{De}^2(2+q)^2+1)} \\ &+ \sum_{q=1}^{\infty} \frac{8q \text{De} J_{2q} J_{2q+4}}{\text{Wi}(4\text{De}^2 q^2+1)} - \frac{2J_1 (J_4 + J_2)}{9\text{De}^2+1} - \frac{2J_3 (J_2 + J_0)}{\text{De}^2+1} \\ &-\sum_{q=1}^{\infty} \frac{2J_{3+2q} (J_{2q} + J_{2q-2})}{\text{De}^2(2q-1)^2+1} + \sum_{q=1}^{\infty} \frac{2J_{2q-1} (J_{2q+4} + J_{2q+2})}{\text{De}^2(3+2q)^2+1} \end{aligned} \right) \sin 4\tau
\end{aligned} \tag{59}$$

and for $n = 3$, the sixths:

$$\begin{aligned}
\mathbb{N}_{1,6}(\tau) &= -2\mathbb{N}_{2,6}(\tau) \\
&= \left(\begin{aligned}
&\frac{-144\text{De}^2 J_0 J_6}{\text{Wi}(36\text{De}^2+1)} - \frac{64\text{De}^2 J_2 J_4}{\text{Wi}(16\text{De}^2+1)} - \frac{16\text{De}^2 J_4 J_2}{\text{Wi}(4\text{De}^2+1)} \\
&- \sum_{q=1}^{\infty} \frac{16(q+3)^2 \text{De}^2 J_{2q} J_{2q+6}}{\text{Wi}(4\text{De}^2(q+3)^2+1)} - \sum_{q=1}^{\infty} \frac{16q^2 \text{De}^2 J_{2q+6} J_{2q}}{\text{Wi}(4\text{De}^2 q^2+1)} \\
&+ \frac{10\text{De} J_1 (J_6 + J_4)}{25\text{De}^2+1} + \frac{6\text{De} J_3 (J_4 + J_2)}{9\text{De}^2+1} + \frac{2\text{De} J_5 (J_2 + J_0)}{\text{De}^2+1} \\
&- \sum_{q=1}^{\infty} \frac{2\text{De} J_{2q-1} (5+2q)(J_{6+2q} + J_{4+2q})}{\text{De}^2 (5+2q)^2+1} - \sum_{q=1}^{\infty} \frac{2\text{De} J_{5+2q} (2q-1)(J_{2q} + J_{2q-2})}{\text{De}^2 (2q-1)^2+1}
\end{aligned} \right) \cos 6\tau \quad (60) \\
&+ \left(\begin{aligned}
&\frac{24\text{De} J_0 J_6}{\text{Wi}(36\text{De}^2+1)} + \frac{16\text{De} J_2 J_4}{\text{Wi}(16\text{De}^2+1)} + \frac{8\text{De} J_4 J_2}{\text{Wi}(4\text{De}^2+1)} + \sum_{q=1}^{\infty} \frac{8(3+q)\text{De} J_{2q} J_{6+2q}}{\text{Wi}(4\text{De}^2(3+q)^2+1)} \\
&+ \sum_{q=1}^{\infty} \frac{8q\text{De} J_{2q} J_{2q+6}}{\text{Wi}(4\text{De}^2 q^2+1)} - \frac{2J_1 (J_6 + J_4)}{25\text{De}^2+1} - \frac{2J_3 (J_4 + J_2)}{9\text{De}^2+1} - \frac{2J_5 (J_2 + J_0)}{\text{De}^2+1} \\
&- \sum_{q=1}^{\infty} \frac{2J_{5+2q} (J_{2q} + J_{2q-2})}{\text{De}^2 (2q-1)^2+1} + \sum_{q=1}^{\infty} \frac{2J_{2q-1} (J_{2q+6} + J_{2q+4})}{\text{De}^2 (5+2q)^2+1}
\end{aligned} \right) \sin 6\tau
\end{aligned}$$

We believe that Eqs. (60) are the first expressions for sixth harmonics for normal stress difference responses (be they exact or approximate) from any constitutive equation. We can, of course, follow this pattern to obtain exact expressions for the eighth, tenth, twelfth harmonics and so on.

Figure 2 through Figure 4 illustrate the predicted startup behaviors of the normal stress differences from the exact solution. We find these behaviors to be more reasonable than the prior approximate solution, Eq. (111) of [5]. Specifically, our exact solution eliminates the spurious spikes in the normal stress difference responses calculated from the integral expansion at startup. These spikes are believed to be artifacts of the truncation of the integral expansion.

Figure 5 through Figure 7 illustrate the alternant part of the normal stress difference responses given by the exact solution, Eq. (56). In Section VI, we will compare our exact solution, Eq. (56), with the approximation, Eq. (20).

b. Shear Stress Response

Substituting (48) and (49) into Eq. (46) and then rearranging yields:

$$\mathbb{S}(\tau) = \frac{1}{\text{De}} e^{-\tau/\text{De}} \left[\begin{aligned}
&\sin\left(\frac{\text{Wi}}{\text{De}} \sin \tau\right) \left(\lim_{\tau \rightarrow 0} I_1 - I_1 \right) \\
&+ \cos\left(\frac{\text{Wi}}{\text{De}} \sin \tau\right) \left(\lim_{\tau \rightarrow 0} I_2 - I_2 \right)
\end{aligned} \right] \quad (61)$$

which we call the *compact form* of the exact solution. When alternance is reached, this compact form reduces to:

$$\mathbb{S}(\tau) = -\frac{1}{\text{De}} e^{-\tau/\text{De}} \sin\left(\frac{\text{Wi}}{\text{De}} \sin \tau\right) I_1 - \frac{1}{\text{De}} e^{-\tau/\text{De}} \cos\left(\frac{\text{Wi}}{\text{De}} \sin \tau\right) I_2 \quad (62)$$

Substituting Eqs. (121), (124), (132) [with Eqs. (133) and (134)], (135), (139) [with Eqs. (140) and (141)] and (142) into Eq. (61) yields the exact explicit analytical solution for the shear stress response of the corotational Maxwell model, in startup of large-amplitude oscillatory shear flow:

$$\mathbb{S}(\tau) = e^{-\tau/De} \left[\begin{array}{l} 2 \left[\sum_{k=1}^{\infty} J_{2k-1} \sin(2k-1)\tau \right] \left(-2De \sum_{k=1}^{\infty} \left[J_{2k-1} \left(\frac{k}{4De^2 k^2 + 1} - \frac{(k-1)}{4De^2 (k-1)^2 + 1} \right) \right] \right) \\ + e^{\tau/De} \left[\sum_{k=1}^{\infty} J_{2k-1} \left(\frac{2De k \cos 2k\tau - \sin 2k\tau}{4De^2 k^2 + 1} + \frac{2De(k-1) \cos 2(1-k)\tau + \sin 2(1-k)\tau}{4De^2 (k-1)^2 + 1} \right) \right] \end{array} \right] \quad (63)$$

$$+ \left[J_0 + 2 \sum_{k=1}^{\infty} J_{2k} \cos 2k\tau \right] \left(\frac{J_0}{1+De^2} + \sum_{k=1}^{\infty} J_{2k} \left[\frac{1}{De^2 (2k-1)^2 + 1} + \frac{1}{De^2 (2k+1)^2 + 1} \right] \right)$$

$$- e^{\tau/De} \left\{ \begin{array}{l} \frac{J_0}{1+De^2} (\cos \tau + De \sin \tau) \\ + \sum_{k=1}^{\infty} J_{2k} \left[\frac{\cos(2k-1)\tau + (2k-1)De \sin(2k-1)\tau}{De^2 (2k-1)^2 + 1} \right] \\ + \sum_{k=1}^{\infty} J_{2k} \left[\frac{\cos(2k+1)\tau + (2k+1)De \sin(2k+1)\tau}{De^2 (2k+1)^2 + 1} \right] \end{array} \right\}$$

and in which the alternant part is in blue. We call Eqs. (63) the *substituted compact form*.

To transform the substituted compact form to a Fourier series, we begin by rewriting Eq. (63) as:

$$\mathbb{S}(\tau) = \mathbb{S}_{\text{tr}}(\tau) + \mathbb{S}_{\text{al}}(\tau) \quad (64)$$

where:

$$\mathbb{S}_{\text{tr}}(\tau) = e^{-\tau/De} \sum_{k=1}^{\infty} \alpha_k^{(1)} \sum_{k=0}^{\infty} B_k \sin(2k-1)\tau$$

$$+ e^{-\tau/De} \sum_{k=1}^{\infty} \alpha_k^{(2)} A_0 + e^{-\tau/De} \sum_{k=1}^{\infty} \alpha_k^{(2)} \sum_{k=1}^{\infty} A_k \cos 2k\tau \quad (65)$$

which we derive in Section XII.b.i and in which the coefficients of Eq. (65) are defined [in order of occurrence in Eq. (65)] in Eqs. (133), (126), (140) and (123), and where $\mathbb{S}_{\text{al}}(\tau)$ in Eq. (64) is given by:

$$\begin{aligned}
S_{\text{al}}(\tau) = & -\frac{1}{2} \sum_{n=1}^{\infty} \left[\begin{aligned}
& \left(-\sum_{p=1}^{n-1} \frac{16(n-p)^2 \text{De}^2 J_{2p-1} J_{2n-2p}}{\text{Wi}(4\text{De}^2(n-p)^2+1)} - \sum_{q=1}^{\infty} \left[\frac{16q^2 \text{De}^2 J_{2q+2n-1} J_{2q}}{\text{Wi}(4\text{De}^2 q^2+1)} \right] \right. \\
& + \sum_{q=1}^{\infty} \left[\frac{16(q+n-1)^2 \text{De}^2 J_{2q-1} J_{2q+2n-2}}{\text{Wi}(4\text{De}^2(q+n-1)^2+1)} \right] + \frac{2\text{De}(2n-1)J_0(J_{2n}+J_{2n-2})}{\text{De}^2(2n-1)^2+1} \\
& - \frac{2\text{De}J_{2n}(J_2+J_0)}{\text{De}^2+1} + \sum_{p=1}^{n-1} \frac{2\text{De}(2n-2p-1)J_{2p}(J_{2n-2p}+J_{2n-2p-2})}{\text{De}^2(2n-2p-1)^2+1} \\
& + \sum_{q=1}^{\infty} \left[\frac{2\text{De}(2q+2n-1)J_{2q}(J_{2q+2n}+J_{2q+2n-2})}{\text{De}^2(2q+2n-1)^2+1} \right] \\
& \left. - \sum_{q=1}^{\infty} \left[\frac{2\text{De}(2q+1)J_{2q+2n}(J_{2q+2}+J_{2q})}{\text{De}^2(2q+1)^2+1} \right] \right) \sin(2n-1)\tau \\
& + \left(-\sum_{p=1}^{n-1} \frac{8(n-p)\text{De}J_{2p-1}J_{2n-2p}}{\text{Wi}(4\text{De}^2(n-p)^2+1)} + \sum_{q=1}^{\infty} \left[\frac{8q\text{De}J_{2q-1}J_{2q+2n-2}}{\text{Wi}(4\text{De}^2 q^2+1)} \right] \right. \\
& + \sum_{q=1}^{\infty} \left[\frac{8(q+n-1)\text{De}J_{2q}J_{2q-1}}{\text{Wi}(4\text{De}^2(q+n-1)^2+1)} \right] + \frac{2J_0(J_{2n}+J_{2n-2})}{\text{De}^2(2n-1)^2+1} \\
& + \sum_{p=1}^{n-1} \frac{2J_{2p}(J_{2n-2p}+J_{2n-2p-2})}{\text{De}^2(2n-2p-1)^2+1} + \frac{2J_{2n}(J_2+J_0)}{\text{De}^2+1} \\
& \left. + \sum_{q=1}^{\infty} \left[\frac{2J_{2q+2n}(J_{2q+2}+J_{2q})}{\text{De}^2(2q+1)^2+1} \right] + \sum_{q=1}^{\infty} \left[\frac{2J_{2q}(J_{2q+2n}+J_{2q+2n-2})}{\text{De}^2(2q+2n-1)^2+1} \right] \right) \cos(2n-1)\tau
\end{aligned} \right] \quad (66)
\end{aligned}$$

which we derive in Sections XII.b.ii and XII.b.iii. We can thus extract exact expressions for individual harmonics of the alternant parts of the shear stress response from Eq. (66).

Evaluating Eq. (66) for $n=1$ gives the exact expression for the first harmonic of the alternant part of the shear stress response:

$$\mathbb{S}_1(\tau) = -\frac{1}{2} \left(\begin{aligned} & -\sum_{q=1}^{\infty} \left[\frac{16q^2 \text{De}^2 J_{2q+1} J_{2q}}{\text{Wi}(4\text{De}^2 q^2 + 1)} \right] + \sum_{q=1}^{\infty} \left[\frac{16q^2 \text{De}^2 J_{2q-1} J_{2q}}{\text{Wi}(4\text{De}^2 q^2 + 1)} \right] \\ & + \frac{2\text{De} J_0 (J_2 + J_0)}{\text{De}^2 + 1} - \frac{2\text{De} J_2 (J_2 + J_0)}{\text{De}^2 + 1} \\ & + \sum_{q=1}^{\infty} \left[\frac{2\text{De}(2q+1) J_{2q} (J_{2q+2} + J_{2q})}{\text{De}^2 (2q+1)^2 + 1} \right] \\ & - \sum_{q=1}^{\infty} \left[\frac{2\text{De}(2q+1) J_{2q+2} (J_{2q+2} + J_{2q})}{\text{De}^2 (2q+1)^2 + 1} \right] \end{aligned} \right) \sin \tau \quad (67)$$

$$-\frac{1}{2} \left(\begin{aligned} & + \sum_{q=1}^{\infty} \left[\frac{8q \text{De} J_{2q+1} J_{2q}}{\text{Wi}(4\text{De}^2 q^2 + 1)} \right] + \sum_{q=1}^{\infty} \left[\frac{8q \text{De} J_{2q} J_{2q-1}}{\text{Wi}(4\text{De}^2 q^2 + 1)} \right] \\ & + \frac{2J_0 (J_2 + J_0)}{\text{De}^2 + 1} + \frac{2J_2 (J_2 + J_0)}{\text{De}^2 + 1} + \sum_{q=1}^{\infty} \left[\frac{2J_{2q+2} (J_{2q+2} + J_{2q})}{\text{De}^2 (2q+1)^2 + 1} \right] \\ & + \sum_{q=1}^{\infty} \left[\frac{2J_{2q} (J_{2q+2} + J_{2q})}{\text{De}^2 (2q+1)^2 + 1} \right] \end{aligned} \right) \cos \tau$$

and for $n = 2$, we get the third harmonic:

$$\mathbb{S}_3(\tau) = -\frac{1}{2} \left(\begin{aligned} & -\frac{16\text{De}^2 J_1 J_2}{\text{Wi}(4\text{De}^2+1)} - \sum_{q=1}^{\infty} \frac{16q^2 \text{De}^2 J_{2q+3} J_{2q}}{\text{Wi}(4q^2 \text{De}^2+1)} \\ & + \sum_{q=1}^{\infty} \frac{16(q+1)^2 \text{De}^2 J_{2q-1} J_{2q+2}}{\text{Wi}(4(q+1)^2 \text{De}^2+1)} + \frac{6\text{De} J_0 (J_4 + J_2)}{9\text{De}^2+1} \\ & - \frac{2\text{De} J_4 (J_2 + J_0)}{\text{De}^2+1} + \frac{2\text{De} J_2 (J_2 + J_0)}{\text{De}^2+1} \\ & + \sum_{q=1}^{\infty} \frac{2\text{De}(2q+3) J_{2q} (J_{2q+4} + J_{2q+2})}{\text{De}^2 (2q+3)^2 + 1} \\ & - \sum_{q=1}^{\infty} \frac{2\text{De}(2q+1) J_{2q+4} (J_{2q+2} + J_{2q})}{\text{De}^2 (2q+1)^2 + 1} \end{aligned} \right) \sin 3\tau \quad (68)$$

$$-\frac{1}{2} \left(\begin{aligned} & -\frac{8\text{De} J_1 J_2}{\text{Wi}(4\text{De}^2+1)} + \sum_{q=1}^{\infty} \frac{8q \text{De} J_{2q} J_{2q+3}}{\text{Wi}(4\text{De}^2 q^2 + 1)} \\ & + \sum_{q=1}^{\infty} \frac{8(q+1) \text{De} J_{2q-1} J_{2q+2}}{\text{Wi}(4\text{De}^2 (q+1)^2 + 1)} + \frac{2J_0 (J_4 + J_2)}{9\text{De}^2+1} \\ & + \frac{2J_2 (J_2 + J_0)}{\text{De}^2+1} + \frac{2J_4 (J_2 + J_0)}{\text{De}^2+1} + \sum_{q=1}^{\infty} \frac{2J_{2q} (J_{2q+4} + J_{2q+2})}{\text{De}^2 (2q+3)^2 + 1} \\ & + \sum_{q=1}^{\infty} \frac{2J_{2q+4} (J_{2q+2} + J_{2q})}{\text{De}^2 (2q+1)^2 + 1} \end{aligned} \right) \cos 3\tau$$

and for $n = 3$, the fifth:

$$\begin{aligned}
\mathbb{S}_5(\tau) = & -\frac{1}{2} \left(\begin{aligned}
& -\frac{64\text{De}^2 J_1 J_4}{\text{Wi}(16\text{De}^2+1)} - \frac{16\text{De}^2 J_3 J_2}{\text{Wi}(4\text{De}^2+1)} - \sum_{q=1}^{\infty} \frac{16q^2 \text{De}^2 J_{2q+5} J_{2q}}{\text{Wi}(4q^2 \text{De}^2+1)} \\
& + \sum_{q=1}^{\infty} \frac{16(q+2)^2 \text{De}^2 J_{2q-1} J_{2q+4}}{\text{Wi}(4(q+2)^2 \text{De}^2+1)} + \frac{10\text{De} J_0 (J_6 + J_4)}{25\text{De}^2+1} \\
& - \frac{2\text{De} J_6 (J_2 + J_0)}{\text{De}^2+1} + \frac{6\text{De} J_2 (J_4 + J_2)}{9\text{De}^2+1} + \frac{2\text{De} J_4 (J_2 + J_0)}{\text{De}^2+1} \\
& + \sum_{q=1}^{\infty} \frac{2\text{De}(2q+5) J_{2q} (J_{2q+6} + J_{2q+4})}{\text{De}^2(2q+5)^2+1} \\
& - \sum_{q=1}^{\infty} \frac{2\text{De}(2q+1) J_{2q+6} (J_{2q+2} + J_{2q})}{\text{De}^2(2q+1)^2+1}
\end{aligned} \right) \sin 5\tau \\
& -\frac{1}{2} \left(\begin{aligned}
& -\frac{16\text{De} J_1 J_4}{\text{Wi}(16\text{De}^2+1)} - \frac{8\text{De} J_3 J_2}{\text{Wi}(4\text{De}^2+1)} + \sum_{q=1}^{\infty} \frac{8q \text{De} J_{2q} J_{2q+5}}{\text{Wi}(4\text{De}^2 q^2+1)} \\
& + \sum_{q=1}^{\infty} \frac{8(q+2)\text{De} J_{2q-1} J_{2q+4}}{\text{Wi}(4\text{De}^2(q+2)^2+1)} + \frac{2J_0 (J_6 + J_4)}{25\text{De}^2+1} + \frac{2J_2 (J_4 + J_2)}{9\text{De}^2+1} \\
& + \frac{2J_4 (J_2 + J_0)}{\text{De}^2+1} + \frac{2J_6 (J_2 + J_0)}{\text{De}^2+1} + \sum_{q=1}^{\infty} \frac{2J_{2q} (J_{2q+6} + J_{2q+4})}{\text{De}^2(2q+5)^2+1} \\
& + \sum_{q=1}^{\infty} \frac{2J_{2q+6} (J_{2q+2} + J_{2q})}{\text{De}^2(2q+1)^2+1}
\end{aligned} \right) \cos 5\tau
\end{aligned} \tag{69}$$

and for $n = 4$, the seventh:

$$\begin{aligned}
\mathbb{S}_7(\tau) = & -\frac{1}{2} \left(\begin{aligned}
& -\frac{144\text{De}^2 J_1 J_6}{\text{Wi}(36\text{De}^2+1)} - \frac{64\text{De}^2 J_3 J_4}{\text{Wi}(16\text{De}^2+1)} - \frac{16\text{De}^2 J_5 J_2}{\text{Wi}(4\text{De}^2+1)} \\
& - \sum_{q=1}^{\infty} \frac{16q^2 \text{De}^2 J_{2q+7} J_{2q}}{\text{Wi}(4q^2 \text{De}^2+1)} + \sum_{q=1}^{\infty} \frac{16(3+q)^2 \text{De}^2 J_{2q-1} J_{2q+6}}{\text{Wi}(4(3+q)^2 \text{De}^2+1)} \\
& + \frac{14\text{De} J_0 (J_8 + J_6)}{49\text{De}^2+1} - \frac{2\text{De} J_8 (J_2 + J_0)}{\text{De}^2+1} + \frac{10\text{De} J_2 (J_6 + J_4)}{25\text{De}^2+1} \\
& + \frac{6\text{De} J_4 (J_4 + J_2)}{9\text{De}^2+1} + \frac{2\text{De} J_6 (J_2 + J_0)}{\text{De}^2+1} \\
& + \sum_{q=1}^{\infty} \frac{2\text{De}(2q+7) J_{2q} (J_{2q+8} + J_{2q+6})}{\text{De}^2 (2q+7)^2 + 1} \\
& - \sum_{q=1}^{\infty} \frac{2\text{De}(2q+1) J_{2q+8} (J_{2q+2} + J_{2q})}{\text{De}^2 (2q+1)^2 + 1}
\end{aligned} \right) \sin 7\tau \\
& -\frac{1}{2} \left(\begin{aligned}
& -\frac{24\text{De} J_1 J_6}{\text{Wi}(36\text{De}^2+1)} - \frac{16\text{De} J_3 J_4}{\text{Wi}(16\text{De}^2+1)} - \frac{8\text{De} J_2 J_5}{\text{Wi}(4\text{De}^2+1)} \\
& + \sum_{q=1}^{\infty} \frac{8q \text{De} J_{2q} J_{2q+7}}{\text{Wi}(4\text{De}^2 q^2 + 1)} + \sum_{q=1}^{\infty} \frac{8(q+3) \text{De} J_{2q-1} J_{2q+6}}{\text{Wi}(4\text{De}^2 (q+3)^2 + 1)} \\
& + \frac{2J_0 (J_8 + J_6)}{49\text{De}^2+1} + \frac{2J_2 (J_6 + J_4)}{25\text{De}^2+1} + \frac{2J_4 (J_4 + J_2)}{9\text{De}^2+1} + \frac{2J_6 (J_2 + J_0)}{\text{De}^2+1} \\
& + \frac{2J_8 (J_2 + J_0)}{\text{De}^2+1} + \sum_{q=1}^{\infty} \frac{2J_{2q} (J_{2q+8} + J_{2q+6})}{\text{De}^2 (2q+7)^2 + 1} + \sum_{q=1}^{\infty} \frac{2J_{2q+8} (J_{2q+2} + J_{2q})}{\text{De}^2 (2q+1)^2 + 1}
\end{aligned} \right) \cos 7\tau
\end{aligned} \tag{70}$$

We believe that Eq. (70) is the first expression for the seventh harmonic for the shear stress response (be it exact or approximate) from any constitutive equation. We can, of course, follow this pattern to obtain exact expressions for the ninth, eleventh, thirteenth harmonics and so on.

Figure 8 through Figure 10 illustrate the predicted startup behaviors of the shear stress from the exact solution. We find these behaviors to be more reasonable than the prior approximate solution, Eq. (109) of [5]. Specifically, our exact solution eliminates the spurious spikes in the shear stress response calculated from the integral expansion at startup. These spikes are believed to be artifacts of the truncation of the integral expansion. In Section V.c below, we will generalize the corotational Maxwell model for multiple relaxation times, and then, in Section VII.a.i, we will compare experimental data for startup with the exact solution for the generalized model [Eq. (71) with Eqs. (72) and (73)].

Figure 11 through Figure 13 illustrate the alternant part of the shear stress response given by the exact solution. In Section VI, we will compare this exact solution, Eq. (66), with the approximation, Eq. (21).

c. Generalized Corotational Maxwell Model

When comparing with experimental data, we normally employ a set of relaxation times, and thus rewrite the corotational Maxwell model as (see Section 7. of [5]):

$$\tau = \sum_{j=1}^{\infty} \tau_{j,\text{tr}} + \tau_{j,\text{al}} \quad (71)$$

where the j th transient part of the shear stress response is given by:

$$\frac{\tau_{j,\text{tr}}}{\dot{\gamma}^0} = -\eta_{0,j} e^{-\tau/\lambda_j \omega} \left[\begin{aligned} & \sum_{k=1}^{\infty} \frac{-8k^2 \lambda_j^2 \omega^2 J_{2k}}{\text{Wi}(4\lambda_j^2 \omega^2 k^2 + 1)} \sum_{k=1}^{\infty} 2J_{2k-1} \sin(2k\tau - \tau) \\ & + \sum_{k=1}^{\infty} \frac{J_{2k} + J_{2k-2}}{\lambda_j^2 \omega^2 (2k-1)^2 + 1} \left[J_0 + \sum_{k=1}^{\infty} 2J_{2k} \cos(2k\tau) \right] \end{aligned} \right] \quad (72)$$

and, the j th alternant part, by:

$$\begin{aligned}
\frac{\tau_{j,\text{al}}}{\dot{\gamma}^0} = & -\eta_{0,j} \sum_{n=1}^{\infty} \left(\begin{aligned} & -\sum_{p=1}^{n-1} \left[\frac{8(n-p)^2 \lambda_j^2 \omega^2 J_{2p-1} J_{2n-2p}}{\lambda_j \dot{\gamma}^0 (4\lambda_j^2 \omega^2 (n-p)^2 + 1)} \right] \\ & -\sum_{q=1}^{\infty} \left[\frac{8q^2 \lambda_j^2 \omega^2 J_{2q} J_{2q+2n-1}}{\lambda_j \dot{\gamma}^0 (4\lambda_j^2 \omega^2 q^2 + 1)} \right] \\ & +\sum_{q=1}^{\infty} \left[\frac{8(q+n-1)^2 \lambda_j^2 \omega^2 J_{2q-1} J_{2q+2n-2}}{\lambda_j \dot{\gamma}^0 (4\lambda_j^2 \omega^2 (q+n-1)^2 + 1)} \right] \\ & +\frac{\lambda_j \omega (2n-1) J_0 (J_{2n} + J_{2n-2})}{\lambda_j^2 \omega^2 (2n-1)^2 + 1} - \frac{\lambda_j \omega J_{2n} (J_0 + J_2)}{\lambda_j^2 \omega^2 + 1} \sin(2n-1)\tau \\ & +\sum_{p=1}^{n-1} \left[\frac{\lambda_j \omega (2n-2p-1) J_{2p} (J_{2n-2p} + J_{2n-2p-2})}{\lambda_j^2 \omega^2 (2n-2p-1)^2 + 1} \right] \\ & +\sum_{q=1}^{\infty} \left[\frac{\lambda_j \omega (2q+2n-1) J_{2q} (J_{2q+2n} + J_{2q+2n-2})}{\lambda_j^2 \omega^2 (2q+2n-1)^2 + 1} \right] \\ & -\sum_{q=1}^{\infty} \left[\frac{\lambda_j \omega (2q+1) J_{2q+2n} (J_{2q} + J_{2q+2})}{\lambda_j^2 \omega^2 (2q+1)^2 + 1} \right] \end{aligned} \right) \\
& + \left(\begin{aligned} & -\sum_{p=1}^{n-1} \left[\frac{4(n-p) \lambda_j \omega J_{2p-1} J_{2n-2p}}{\lambda_j \dot{\gamma}^0 (4\lambda_j^2 \omega^2 (n-p)^2 + 1)} \right] \\ & +\sum_{q=1}^{\infty} \left[\frac{4q \lambda_j \omega J_{2q-1} J_{2q+2n-2}}{\lambda_j \dot{\gamma}^0 (4\lambda_j^2 \omega^2 q^2 + 1)} \right] \\ & +\sum_{q=1}^{\infty} \left[\frac{4(q+n-1) \lambda_j \omega J_{2q} J_{2q-1}}{\lambda_j \dot{\gamma}^0 (4\lambda_j^2 \omega^2 (q+n-1)^2 + 1)} \right] \\ & +\frac{J_0 (J_{2n} + J_{2n-2})}{\lambda_j^2 \omega^2 (2n-1)^2 + 1} + \sum_{p=1}^{n-1} \left[\frac{J_{2p} (J_{2n-2p} + J_{2n-2p-2})}{\lambda_j^2 \omega^2 (2n-2p-1)^2 + 1} \right] \\ & +\frac{J_{2n} (J_0 + J_2)}{\lambda_j^2 \omega^2 + 1} + \sum_{q=1}^{\infty} \left[\frac{J_{2q+2n} (J_{2q} + J_{2q+2})}{\lambda_j^2 \omega^2 (2q+1)^2 + 1} \right] \\ & +\sum_{q=1}^{\infty} \left[\frac{J_{2q} (J_{2q+2n} + J_{2q+2n-2})}{\lambda_j^2 \omega^2 (2q+2n-1)^2 + 1} \right] \end{aligned} \right) \cos(2n-1)\tau
\end{aligned} \tag{73}$$

from which exact expressions for the Fourier moduli defined in Eq. (10) are easily obtained:

$$G'_n \equiv \omega \sum_{j=1}^{\infty} \eta_{0,j} \left(\begin{aligned} & - \sum_{p=1}^{n-1} \left[\frac{8(n-p)^2 \lambda_j^2 \omega^2 J_{2p-1} J_{2n-2p}}{\lambda_j \dot{\gamma}^0 (4\lambda_j^2 \omega^2 (n-p)^2 + 1)} \right] - \sum_{q=1}^{\infty} \left[\frac{8q^2 \lambda_j^2 \omega^2 J_{2q+2n-1} J_{2q}}{\lambda_j \dot{\gamma}^0 (4\lambda_j^2 \omega^2 q^2 + 1)} \right] \\ & + \sum_{q=1}^{\infty} \left[\frac{8(q+n-1)^2 \lambda_j^2 \omega^2 J_{2q-1} J_{2q+2n-2}}{\lambda_j \dot{\gamma}^0 (4\lambda_j^2 \omega^2 (q+n-1)^2 + 1)} \right] + \frac{\lambda_j \omega (2n-1) J_0 (J_{2n} + J_{2n-2})}{\lambda_j^2 \omega^2 (2n-1)^2 + 1} \\ & - \frac{\lambda_j \omega J_{2n} (J_2 + J_0)}{\lambda_j^2 \omega^2 + 1} \\ & + \sum_{p=1}^{n-1} \left[\frac{\lambda_j \omega (2n-2p-1) J_{2p} (J_{2n-2p} + J_{2n-2p-2})}{\lambda_j^2 \omega^2 (2n-2p-1)^2 + 1} \right] \\ & + \sum_{q=1}^{\infty} \left[\frac{\lambda_j \omega (2q+2n-1) J_{2q} (J_{2q+2n} + J_{2q+2n-2})}{\lambda_j^2 \omega^2 (2q+2n-1)^2 + 1} \right] \\ & - \sum_{q=1}^{\infty} \left[\frac{\lambda_j \omega (2q+1) J_{2q+2n} (J_{2q+2} + J_{2q})}{\lambda_j^2 \omega^2 (2q+1)^2 + 1} \right] \end{aligned} \right) \quad (74)$$

and:

$$G''_n \equiv \omega \sum_{j=1}^{\infty} \eta_{0,j} \left(\begin{aligned} & - \sum_{p=1}^{n-1} \left[\frac{4(n-p) \lambda_j \omega J_{2p-1} J_{2n-2p}}{\lambda_j \dot{\gamma}^0 (4\lambda_j^2 \omega^2 (n-p)^2 + 1)} \right] + \sum_{q=1}^{\infty} \left[\frac{4q \lambda_j \omega J_{2q-1} J_{2q+2n-2}}{\lambda_j \dot{\gamma}^0 (4\lambda_j^2 \omega^2 q^2 + 1)} \right] \\ & + \sum_{q=1}^{\infty} \left[\frac{4(q+n-1) \lambda_j \omega J_{2q} J_{2q-1}}{\lambda_j \dot{\gamma}^0 (4\lambda_j^2 \omega^2 (q+n-1)^2 + 1)} \right] + \frac{J_0 (J_{2n} + J_{2n-2})}{\lambda_j^2 \omega^2 (2n-1)^2 + 1} \\ & + \sum_{p=1}^{n-1} \left[\frac{J_{2p} (J_{2n-2p} + J_{2n-2p-2})}{\lambda_j^2 \omega^2 (2n-2p-1)^2 + 1} \right] + \frac{J_{2n} (J_2 + J_0)}{\lambda_j^2 \omega^2 + 1} \\ & + \sum_{q=1}^{\infty} \left[\frac{J_{2q+2n} (J_{2q+2} + J_{2q})}{\lambda_j^2 \omega^2 (2q+1)^2 + 1} \right] + \sum_{q=1}^{\infty} \left[\frac{J_{2q} (J_{2q+2n} + J_{2q+2n-2})}{\lambda_j^2 \omega^2 (2q+2n-1)^2 + 1} \right] \end{aligned} \right) \quad (75)$$

These can in turn be used to explore loop intersection (see Section 9 of [5]; [16]).

VI. CONSISTENCY CHECKS

In this section, we perform consistency checks on the exact solution, for both the normal stress differences and the shear stress. We compare with approximate solutions, and we also examine limiting behaviors of the exact solutions. We begin with a comparison with the approximate solutions, Eqs. (20) and (21).

Figure 14 compares the exact solution for the alternant part of the normal stress differences with the approximate solution [Eq. (20)]. Though these nearly

match, we find an appreciable improvement with the exact solution, Eq. (56). Figure 15 and Figure 16 compare the exact solution for the alternant part of the shear stress response with the approximate solution [Eq. (21)]. Though these nearly match, we find an appreciable improvement with the exact solution, Eq. (66). Figure 16 shows the exact solution to be far further from the linear viscoelastic behavior, and thus that the truncation in the integral expansion method causes the predicted response to be much closer to the linear behavior than it should. Otherwise put, the truncation in the integral expansion discards fluid nonlinearity.

We next examine the limiting behaviors for alternance at small strain amplitude, $Wi/De \ll 1$. Eqs. (52) and (61) reduce to:

$$\mathbb{N}_1(\tau) = \frac{2}{De} e^{-\tau/De} \lim_{\frac{Wi}{De} \rightarrow 0} \left[I_1 - \lim_{\tau \rightarrow 0} I_1 \right] \quad (76)$$

and:

$$\mathbb{S}(\tau) = \frac{-1}{De} e^{-\tau/De} \lim_{\frac{Wi}{De} \rightarrow 0} \left[I_2 - \lim_{\tau \rightarrow 0} I_2 \right] \quad (77)$$

Also:

$$\lim_{\frac{Wi}{De} \rightarrow 0} J_0 = 1 \quad (78)$$

$$\lim_{\frac{Wi}{De} \rightarrow 0} J_n = 0 \quad ; n = 1, 2, 3, \dots \quad (79)$$

$$\lim_{\frac{Wi}{De} \rightarrow 0} \left[I_1 - \lim_{\tau \rightarrow 0} I_1 \right] = 0 \quad (80)$$

and:

$$\lim_{\frac{Wi}{De} \rightarrow 0} \left[I_2 - \lim_{\tau \rightarrow 0} I_2 \right] = \frac{De}{1 + De^2} \left(e^{\tau/De} (\cos \tau + De \sin \tau) - 1 \right) \quad (81)$$

Substituting Eqs. (80) and (81) into Eqs. (76) and (77) yields, for the normal stress differences:

$$\mathbb{N}_1(\tau) = 0 \quad (82)$$

which matches the corresponding limiting behavior of Eq. (20), as it should. For the shear stress:

$$\mathbb{S}(\tau) = \frac{1}{1 + De^2} e^{-\tau/De} - \left(\frac{1}{1 + De^2} \cos \tau + \frac{De}{1 + De^2} \sin \tau \right) \quad (83)$$

which matches the corresponding limit obtained from the approximate solution, the first line of Eq. (109) of [5], as it should.

Examining the exact solution numerically for steady shear flow (using $De \ll 1$) we can also report matches with Eq. (22), which can be recast as:

$$\begin{aligned} \mathbb{N}_1(\tau) &= -2\mathbb{N}_2(\tau) \\ &= -2Wi(1 - Wi^2 + Wi^4 - \dots) \\ &= \frac{-2Wi}{1 + Wi^2} \end{aligned} \quad (84)$$

and as:

$$\begin{aligned}
-\mathbb{S}(\tau) &= \frac{\dot{\gamma}}{\dot{\gamma}^0} (1 - Wi^2 + Wi^4 - \dots) \\
&= 1 - Wi^2 + Wi^4 - \dots \\
&= \frac{1}{1 + Wi^2}
\end{aligned} \tag{85}$$

as it should. Figure 17 and Figure 18 illustrate these matches.

Thus our exact solution does not exhibit any limiting misbehavior.

VII. COMPARISONS WITH EXPERIMENTAL DATA

In this section we compare with experimental data, both our own data, and also with an exhaustive (rarely cited) data set from a Russian laboratory.

a. Shear Stress Versus Shear Rate Loops

i. Startup

Figure 19 compares the exact solution for the shear stress response of the corotational Maxwell model (generalized for multiple relaxation times) to the startup of large-amplitude oscillatory shear flow with previously published measurements on molten high-density polyethylene. We find the exact solution to be a good match for the measured values. Also, unlike the truncated integral expansion (see Fig. 14 of [5]), the exact solution produces no spurious spikes.

ii. Alternance

Figure 20 through Figure 22 illustrate the excellent agreement for the alternant part of the shear stress response to large-amplitude oscillatory shear flow with previously published measurements on molten high-density polyethylene. We find the exact solution to be a good match for the measured values. However, under the severe flow conditions of elevated Weissenberg number, Figure 23 shows that the corotational Maxwell model breaks down. Specifically, the corotational Maxwell model is too far from the linear behavior. This sort of discrepancy has been misattributed to the truncation of the integral expansion (see Section 11 of [5]), but Figure 23 clearly suggests otherwise. We would expect the corotational Jeffreys model to fix this (to see how this might be done, see Section 8. of [5]).

b. Shear Stress Amplitude

At 5Hz in Figure 24 and 100Hz in Figure 23, we compare the peak values of the shear stress measured (and previously published) in strain sweep experiments using large-amplitude oscillatory shear flow at alternance for two molecular weights of polyisoprene and polybutadiene. Both figures illustrate the close agreement.

VIII. CONCLUSION

We derive what we believe to be the first exact analytical solution for the response of all components of the extra stress tensor in large-amplitude oscillatory shear flow. Our solution, unique and in closed form, thus includes both the normal stress differences [Eqs. (45) or (53)] and the shear stress [Eqs. (46) or (63)] for both startup and alternance. We then recast these results into Fourier series; one for the normal stress differences [Eq. (54) with Eqs. (55) and (56)], and another for the shear stress [Eq. (64) with Eqs. (65) and (66)]. We solve the corotational Maxwell model [Eqs. (15) with (16)] as a pair of nonlinear coupled ordinary differential equations [Eqs. (33)], simultaneously. We choose the corotational Maxwell model because this two-parameter model (η_0 and λ) is the simplest constitutive model relevant to large-amplitude oscillatory shear flow, and because it has previously been found to be accurate for molten plastics (see Section 11 of [5]). By *relevant* we mean that the model predicts higher harmonics. We find good agreement between the first few harmonics of our exact solution, and of our previous approximate expressions, obtained using the Goddard integral transform (see Section VI). Our exact solution is in good agreement with the measured behavior for molten plastics not only at alternance [Figure 20 through Figure 22, and Figure 24 and Figure 25], but also in startup [Figure 19]. Our exact solution does not exhibit any limiting misbehavior (see Section VI).

We here recall that our chosen model, the corotational Maxwell model, happens to be the simplest relevant model for large-amplitude oscillatory shear flow. We can report that our exact solution is both integrable and differentiable, and it thus provides a suitable starting point for exploring analytically many nonlinear problems in fluid physics, including especially the temperature rise (see Section I).

We close by pointing out that the Kovacic method might be equally useful for arriving at exact solutions to constitutive equations for polymeric liquids of higher complexity (and thus versatility) than the corotational Maxwell model. For instance, the corotational Jeffreys model might yield to this method (see end of Section VII.a.ii). Importantly, we would expect this approach to improve upon the discrepancy that we uncovered in Figure 23 (see end of Section VII.a.ii).

IX. ACKNOWLEDGMENT

We thank R. Byron Bird, Professor Emeritus of Chemical and Biological Engineering, of the Rheology Research Center of the University of Wisconsin-Madison for helpful discussions. We are also indebted to Professor Martin Guay and to Mr. Peter H. Gilbert of the Chemical Engineering Department of Queen's University in Canada, and to Dr. Andrew M. Schmalzer of the Los Alamos National Laboratory for helpful advice. The authors also acknowledge Jessada Tariboon, Professor of Mathematics, Faculty of Applied Science, King Mongkut's University of Technology North Bangkok, Thailand, for helpful discussion. The financial support of the Royal Golden Jubilee Program of the Thailand Research Fund for (Contract No. PHD/0116/2554) is also greatly appreciated. A.J. Giacomin is indebted to the Faculty of Applied Science and Engineering of Queen's University at Kingston, for its support through a

Research Initiation Grant (RIG). This research was undertaken, in part, thanks to funding from the Canada Research Chairs program of the Government of Canada for the Tier 1 Canada Research Chair in Rheology.

X. APPENDIX: FUNDAMENTAL MATRIX

Here we derive the fundamental matrix, Eq. (37), that we used in Section IV. We begin by differentiating Eqs. (30) with respect to τ :

$$\frac{d^2 \mathbb{N}_1}{d\tau^2} = -\frac{1}{\text{De}} \frac{d\mathbb{N}_1}{d\tau} - 2 \frac{\text{Wi}}{\text{De}} \mathbb{S} \sin \tau + 2 \frac{\text{Wi}}{\text{De}} \frac{d\mathbb{S}}{d\tau} \cos \tau \quad (86)$$

and we then substitute Eq. (32) into Eq. (86), to get:

$$\frac{d^2 \mathbb{N}_1}{d\tau^2} = -\frac{1}{\text{De}} \frac{d\mathbb{N}_1}{d\tau} - \frac{\text{Wi}^2}{\text{De}^2} \mathbb{N}_1 \cos^2 \tau + \left(-2 \frac{\text{Wi}}{\text{De}^2} \cos \tau - 2 \frac{\text{Wi}}{\text{De}} \sin \tau \right) \mathbb{S} \quad (87)$$

We then solve Eq. (87) for \mathbb{S} :

$$\mathbb{S} = \frac{1}{2 \frac{\text{Wi}}{\text{De}} \cos \tau} \frac{d\mathbb{N}_1}{d\tau} + \frac{1}{\text{De}} \frac{1}{2 \frac{\text{Wi}}{\text{De}} \cos \tau} \mathbb{N}_1 \quad (88)$$

Substituting Eq. (88) into Eq. (87), we get:

$$\begin{aligned} \frac{d^2 \mathbb{N}_1}{d\tau^2} = & -\frac{1}{\text{De}} \frac{d\mathbb{N}_1}{d\tau} - \frac{\text{Wi}^2}{\text{De}^2} \mathbb{N}_1 \cos^2 \tau \\ & + \left(-2 \frac{\text{Wi}}{\text{De}^2} \cos \tau - 2 \frac{\text{Wi}}{\text{De}} \sin \tau \right) \left(\frac{1}{2 \frac{\text{Wi}}{\text{De}} \cos \tau} \frac{d\mathbb{N}_1}{d\tau} + \frac{1}{\text{De}} \frac{1}{2 \frac{\text{Wi}}{\text{De}} \cos \tau} \mathbb{N}_1 \right) \end{aligned} \quad (89)$$

Simplifying and rearranging Eq. (89), we get:

$$\frac{d^2 \mathbb{N}_1}{d\tau^2} + \left(2 \frac{1}{\text{De}} + \frac{\sin \tau}{\cos \tau} \right) \frac{d\mathbb{N}_1}{d\tau} + \left(\frac{\text{Wi}^2}{\text{De}^2} \cos^2 \tau + \frac{1}{\text{De}^2} + \frac{1}{\text{De}} \frac{\sin \tau}{\cos \tau} \right) \mathbb{N}_1 = 0 \quad (90)$$

Letting:

$$\tau \equiv \arccos \mathcal{T} \quad (91)$$

and then using this to transform Eq. (90), gives:

$$\frac{d^2 \mathbb{N}_1}{d\mathcal{T}^2} + p(\mathcal{T}) \frac{d\mathbb{N}_1}{d\mathcal{T}} + q(\mathcal{T}) \mathbb{N}_1 = 0 \quad (92)$$

where:

$$p(\mathcal{T}) = \frac{(-8 \text{De} \mathcal{T} \sqrt{1 - \mathcal{T}^2} - 4 \text{De}^2)}{(4 \text{De}^2 \mathcal{T} - 4 \text{De}^2 \mathcal{T}^3)} \quad (93)$$

and:

$$q(\mathcal{T}) = \frac{(4 \text{Wi}^2 \mathcal{T}^3 + 4 \mathcal{T} + 4 \text{De} \sqrt{1 - \mathcal{T}^2})}{(4 \text{De}^2 \mathcal{T} - 4 \text{De}^2 \mathcal{T}^3)} \quad (94)$$

Introducing:

$$\mathbb{N}_1 \equiv e^{-\frac{1}{2} \int p(\mathcal{T}) d\mathcal{T}} z \quad (95)$$

so that:

$$\frac{d\mathbb{N}_1}{d\mathcal{T}} = e^{-\frac{1}{2} \int p(\mathcal{T}) d\mathcal{T}} \frac{dz}{d\mathcal{T}} - \frac{1}{2} p(\mathcal{T}) e^{-\frac{1}{2} \int p(\mathcal{T}) d\mathcal{T}} z \quad (96)$$

and so that:

$$\begin{aligned} \frac{d^2 \mathbb{N}_{\frac{1}{2}}}{d\mathcal{T}^2} &= e^{-\frac{1}{2} \int p(\mathcal{T}) d\mathcal{T}} \frac{d^2 z}{d\mathcal{T}^2} - \frac{1}{2} p(\mathcal{T}) e^{-\frac{1}{2} \int p(\mathcal{T}) d\mathcal{T}} \frac{dz}{d\mathcal{T}} \\ &\quad - \frac{1}{2} \frac{dp(\mathcal{T})}{d\mathcal{T}} e^{-\frac{1}{2} \int p(\mathcal{T}) d\mathcal{T}} z + \frac{1}{4} p(\mathcal{T})^2 e^{-\frac{1}{2} \int p(\mathcal{T}) d\mathcal{T}} z - \frac{1}{2} p(\mathcal{T}) e^{-\frac{1}{2} \int p(\mathcal{T}) d\mathcal{T}} \frac{dz}{d\mathcal{T}} \end{aligned} \quad (97)$$

We then substitute Eqs. (95) through (97) into Eq. (92) to get:

$$e^{-\frac{1}{2} \int p(\mathcal{T}) d\mathcal{T}} \frac{d^2 z}{d\mathcal{T}^2} - \frac{1}{2} \frac{dp(\mathcal{T})}{d\mathcal{T}} e^{-\frac{1}{2} \int p(\mathcal{T}) d\mathcal{T}} z - \frac{1}{4} p(\mathcal{T})^2 e^{-\frac{1}{2} \int p(\mathcal{T}) d\mathcal{T}} z + q(\mathcal{T}) e^{-\frac{1}{2} \int p(\mathcal{T}) d\mathcal{T}} z = 0 \quad (98)$$

and dividing through by the exponential term, we get:

$$\frac{d^2 z}{d\mathcal{T}^2} + \left[q(\mathcal{T}) - \frac{1}{4} p(\mathcal{T})^2 - \frac{1}{2} \frac{dp(\mathcal{T})}{d\mathcal{T}} \right] z = 0 \quad (99)$$

Substituting Eqs. (93) and (94) into Eq. (99) and then simplifying, we get:

$$\frac{d^2 z}{d\mathcal{T}^2} = \left[\begin{aligned} &\frac{Wi^2}{De^2} + \frac{3}{4\mathcal{T}^2} - \frac{8Wi^2 - 3De^2}{16De^2(\mathcal{T} + 1)} - \frac{3}{16(\mathcal{T} + 1)^2} \\ &\frac{-8Wi^2 + 3De^2}{16De^2(\mathcal{T} - 1)} - \frac{3}{16(\mathcal{T} - 1)^2} \end{aligned} \right] z \quad (100)$$

We then employ the Kovacic method (Case 2) (see Section 4 of [1]) to Eq. (100), by first defining:

$$r \equiv \frac{Wi^2}{De^2} + \frac{3}{4\mathcal{T}^2} - \frac{8Wi^2 - 3De^2}{16De^2(\mathcal{T} + 1)} - \frac{3}{16(\mathcal{T} + 1)^2} - \frac{-8Wi^2 + 3De^2}{16De^2(\mathcal{T} - 1)} - \frac{3}{16(\mathcal{T} - 1)^2} \quad (101)$$

whose poles c , each of order 2, are given by:

$$c = 0, -1, 1 \quad (102)$$

Table IV summarizes the Kovacic data set corresponding to each pole, E_c , and pole at infinity, E_∞ . From Table IV, we learn that for our problem there is just one family with non-negative d . Since we need only consider families with non-negative d , for our problem, we need only consider the ninth family in Table IV. We then calculate the *Kovacic rational function* (see fourth unnumbered equation from *Step 3* of Section 4.1 of [1]):

$$\theta = \frac{1}{2} \sum_{c \in \Gamma} \frac{e_c}{x - c} \quad (103)$$

$$= -\frac{1}{x} + \frac{1}{2x - 2} + \frac{1}{2x + 2} \quad (104)$$

Since the degree of the *Kovacic polynomial*, P , must equal the value of d of the ninth family in Table IV:

$$P = 1 \quad (105)$$

Substituting Eq. (104) into the definition:

$$\phi \equiv \theta + \frac{P'}{P} \quad (106)$$

gives:

$$\phi = -\frac{1}{x} + \frac{1}{2x - 2} + \frac{1}{2x + 2} \quad (107)$$

We now borrow (sixth unnumbered equation from *Step 3* of Section 4.1 of [1]):

$$\omega^2 - \phi\omega + \left(\frac{1}{2}\phi' + \frac{1}{2}\phi^2 - r\right) = 0 \quad (108)$$

Substituting Eqs. (101) and (107) into Eq. (108), and then solving for ω gives:

$$\omega = \frac{De \pm 2Wi \mathcal{T}^2 \sqrt{\mathcal{T}^2 - 1}}{2De \mathcal{T} (\mathcal{T} - 1)(\mathcal{T} + 1)} \quad (109)$$

Integrating Eq. (109) with respect to \mathcal{T} yields:

$$\int \omega d\mathcal{T} = \ln \left(\frac{(\mathcal{T}^2 - 1)^{1/4}}{\sqrt{\mathcal{T}}} \right) \pm i \frac{Wi}{De} \sqrt{1 - \mathcal{T}^2} \quad (110)$$

Still following [1], we now let:

$$z \equiv e^{\int \omega d\mathcal{T}} \quad (111)$$

and then substitute Eqs. (105) and (110) into Eq. (111) to get:

$$z = \left(\frac{(\mathcal{T}^2 - 1)^{1/4}}{\sqrt{\mathcal{T}}} \sin \left(\frac{Wi}{De} \sqrt{1 - \mathcal{T}^2} \right), \frac{(\mathcal{T}^2 - 1)^{1/4}}{\sqrt{\mathcal{T}}} \cos \left(\frac{Wi}{De} \sqrt{1 - \mathcal{T}^2} \right) \right) \quad (112)$$

Substituting Eqs. (93) and the first root of Eq. (112) into Eq. (95) gives:

$$\mathbb{N}_1 = e^{-\frac{\sqrt{-(\mathcal{T}-1)^2 - 2\mathcal{T} + 2}}{2De}} e^{\frac{\sqrt{-(\mathcal{T}+1)^2 + 2\mathcal{T} + 2}}{2De}} e^{\frac{\arcsin(\mathcal{T})}{De}} \sin \left(\frac{Wi}{De} \sqrt{1 - \mathcal{T}^2} \right) \quad (113)$$

Using Eq. (91), we transform Eq. (113) to:

$$\mathbb{N}_1 = e^{-\tau/De} \sin \left(\frac{Wi}{De} \sin \tau \right) \quad (114)$$

Similarly, for the second root in Eq. (112), we get:

$$\mathbb{N}_1 = e^{-\tau/De} \cos \left(\frac{Wi}{De} \sin \tau \right) \quad (115)$$

Adding the two fundamental solutions, Eqs. (114) and (115), yields:

$$\mathbb{N}_1 = C_1 e^{-\tau/De} \cos \left(\frac{Wi}{De} \sin \tau \right) + C_2 e^{-\tau/De} \sin \left(\frac{Wi}{De} \sin \tau \right) \quad (116)$$

Using the same procedure for the shear stress, \mathbb{S} , we get:

$$\mathbb{S} = C_3 e^{-\tau/De} \sin \left(\frac{Wi}{De} \sin \tau \right) + C_4 e^{-\tau/De} \cos \left(\frac{Wi}{De} \sin \tau \right) \quad (117)$$

Substituting Eqs. (116) and (117) into Eqs. (30) and (32), and then comparing coefficients, we see that:

$$C_3 = -\frac{1}{2}C_1 \quad (118)$$

and:

$$C_4 = \frac{1}{2}C_2 \quad (119)$$

Substituting Eqs. (118) and (119) into Eq. (117), we get:

$$\mathbb{S} = -\frac{1}{2}C_1 e^{-\tau/De} \sin \left(\frac{Wi}{De} \sin \tau \right) + \frac{1}{2}C_2 e^{-\tau/De} \cos \left(\frac{Wi}{De} \sin \tau \right) \quad (120)$$

According to Theorem 4 and Theorem 5, pp. 704 – 706 of chapter 9 in [38] the fundamental matrix is Eq. (37).

XI. APPENDIX: I_1 , I_2 AND THEIR LIMITS

Here we evaluate the quantities I_1 and I_2 from Eqs. (43) and (44) of Section IV, and their limits. For this we will need:

$$\cos\left(\frac{Wi}{De} \sin \tau\right) = J_0 + 2 \sum_{k=1}^{\infty} J_{2k} \cos 2k\tau \quad (121)$$

$$\equiv A_0 + \sum_{k=1}^{\infty} A_k \cos 2k\tau \quad (122)$$

where:

$$A_k \begin{cases} J_0 & ; k=0 \\ 2J_{2k} & ; k \geq 1 \end{cases} \quad (123)$$

from Eq. 9.1.42 of [39], and:

$$\sin\left(\frac{Wi}{De} \sin \tau\right) = 2 \sum_{k=1}^{\infty} J_{2k-1} \sin(2k-1)\tau \quad (124)$$

$$\equiv \sum_{k=1}^{\infty} B_k \sin(2k-1)\tau \quad (125)$$

where:

$$B_k = \begin{cases} 0 & ; k=0 \\ 2J_{2k-1} & ; k \geq 1 \end{cases} \quad (126)$$

from Eq. 9.1.43 of [39], where $J_m(z)$ is the m th order Bessel function of the first kind (see after Eqs. (5) of [36] or [37]):

$$J_m(z) \equiv \sum_{k=0}^{\infty} \frac{(-1)^k}{(m+k)!k!} \left(\frac{z}{2}\right)^{m+2k} \quad (127)$$

so that:

$$J_0(z) \equiv \sum_{k=0}^{\infty} \frac{(-1)^k}{(k!)^2} \left(\frac{z}{2}\right)^{2k} \quad (128)$$

Eq. (127) follows from Eq. (9.1.10) of [39]. In this paper, all Bessel functions are of Wi/De , so for brevity, we just write J_m and J_0 to mean $J_m(Wi/De)$ and $J_0(Wi/De)$.

We begin with I_1 from Eq. (43). Substituting Eqs. (121) and (124) into Eq. (43), and integrating yields:

$$I_1 = De e^{\tau/De} \sum_{k=1}^{\infty} \left[-\frac{2De k J_{2k-1}}{4De^2 k^2 + 1} \cos 2k\tau + \frac{J_{2k-1}}{4De^2 k^2 + 1} \sin 2k\tau \right] \\ + De e^{\tau/De} \sum_{k=1}^{\infty} \left[-\frac{2De(k-1)J_{2k-1}}{4De^2(k-1)^2 + 1} \cos 2(k-1)\tau + \frac{J_{2k-1}}{4De^2(k-1)^2 + 1} \sin 2(k-1)\tau \right] \quad (129)$$

In the second series of Eq. (129), the $k=1$ term is obviously zero. Hence:

$$I_1 = \text{De} e^{\tau/\text{De}} \sum_{k=1}^{\infty} \left[-\frac{2\text{De}k J_{2k-1}}{4\text{De}^2 k^2 + 1} \cos 2k\tau + \frac{J_{2k-1}}{4\text{De}^2 k^2 + 1} \sin 2k\tau \right] \\ + \text{De} e^{\tau/\text{De}} \sum_{k=2}^{\infty} \left[-\frac{2\text{De}(k-1) J_{2k-1}}{4\text{De}^2 (k-1)^2 + 1} \cos 2(k-1)\tau + \frac{J_{2k-1}}{4\text{De}^2 (k-1)^2 + 1} \sin 2(k-1)\tau \right] \quad (130)$$

To combine the two series in Eq. (130), we replace k with $k+1$ in the second to get:

$$I_1 = \text{De} e^{\tau/\text{De}} \sum_{k=1}^{\infty} \left[\frac{-8k^2 \text{De}^2 J_{2k}}{\text{Wi}(4\text{De}^2 k^2 + 1)} \cos 2k\tau + \frac{4k \text{De} J_{2k}}{\text{Wi}(4\text{De}^2 k^2 + 1)} \sin 2k\tau \right] \quad (131)$$

or:

$$I_1 = \text{De} e^{\tau/\text{De}} \sum_{k=1}^{\infty} \left[\alpha_k^{(1)} \cos 2k\tau + \beta_k^{(1)} \sin 2k\tau \right] \quad (132)$$

where:

$$\alpha_k^{(1)} \equiv \begin{cases} 0 & ; k = 0 \\ \frac{-8k^2 \text{De}^2 J_{2k}}{\text{Wi}(4\text{De}^2 k^2 + 1)} & ; k \geq 1 \end{cases} \quad (133)$$

and:

$$\beta_k^{(1)} \equiv \begin{cases} 0 & ; k = 0 \\ \frac{4k \text{De} J_{2k}}{\text{Wi}(4\text{De}^2 k^2 + 1)} & ; k \geq 1 \end{cases} \quad (134)$$

and thus:

$$\lim_{\tau \rightarrow 0} I_1 = -\text{De} \sum_{k=1}^{\infty} \left[J_{2k-1} \left(\frac{2\text{De}k}{4\text{De}^2 k^2 + 1} - \frac{2\text{De}(k-1)}{4\text{De}^2 (k-1)^2 + 1} \right) \right] \quad (135)$$

or:

$$\lim_{\tau \rightarrow 0} I_1 = \text{De} \sum_{k=1}^{\infty} \alpha_k^{(1)} \quad (136)$$

We continue with I_2 from Eq. (44). Substituting Eqs. (121) and (124) into Eq. (44), and integrating yields:

$$I_2 = \text{De} e^{\tau/\text{De}} \left(\frac{J_0 + J_2}{1 + \text{De}^2} \right) \cos \tau + \text{De} e^{\tau/\text{De}} \left(\frac{\text{De} J_0 + \text{De} J_2}{1 + \text{De}^2} \right) \sin \tau \\ + \text{De} e^{\tau/\text{De}} \sum_{k=2}^{\infty} \left[\frac{\text{De}(2k-1) J_{2k}}{\text{De}^2 (2k-1)^2 + 1} \sin(2k-1)\tau + \frac{J_{2k}}{\text{De}^2 (2k-1)^2 + 1} \cos(2k-1)\tau \right] \\ + \text{De} e^{\tau/\text{De}} \sum_{k=1}^{\infty} \left[\frac{\text{De}(2k+1) J_{2k}}{\text{De}^2 (2k+1)^2 + 1} \sin(2k+1)\tau + \frac{J_{2k}}{\text{De}^2 (2k+1)^2 + 1} \cos(2k+1)\tau \right] \quad (137)$$

To combine two series in Eq. (137), we replace k with $k-1$ in the second to get:

$$\begin{aligned}
I_2 = & \text{De} e^{\tau/\text{De}} \left(\frac{2\text{De}J_1}{\text{Wi}(1+\text{De}^2)} \right) \cos \tau + \text{De} e^{\tau/\text{De}} \left(\frac{2\text{De}^2 J_1}{\text{Wi}(1+\text{De}^2)} \right) \sin \tau \\
& + \text{De} e^{\tau/\text{De}} \sum_{k=2}^{\infty} \left[\begin{aligned} & \frac{J_{2k} + J_{2k-2}}{\text{De}^2 (2k-1)^2 + 1} \cos(2k-1)\tau \\ & + \frac{\text{De}(2k-1)(J_{2k} + J_{2k-2})}{\text{De}^2 (2k-1)^2 + 1} \sin(2k-1)\tau \end{aligned} \right] \quad (138)
\end{aligned}$$

or:

$$\begin{aligned}
I_2 = & \text{De} e^{\tau/\text{De}} \alpha_1^{(2)} \cos \tau + \text{De} e^{\tau/\text{De}} \beta_1^{(2)} \sin \tau \\
& + \text{De} e^{\tau/\text{De}} \sum_{k=2}^{\infty} \left[\alpha_k^{(2)} \cos(2k-1)\tau + \beta_k^{(2)} \sin(2k-1)\tau \right] \quad (139)
\end{aligned}$$

where:

$$\alpha_k^{(2)} = \begin{cases} 0 & ; k = 0 \\ \frac{J_{2k} + J_{2k-2}}{\text{De}^2 (2k-1)^2 + 1} & ; k \geq 1 \end{cases} \quad (140)$$

and:

$$\beta_k^{(2)} = \begin{cases} 0 & ; k = 0 \\ \frac{\text{De}(2k-1)(J_{2k} + J_{2k-2})}{\text{De}^2 (2k-1)^2 + 1} & ; k \geq 1 \end{cases} \quad (141)$$

and thus:

$$\begin{aligned}
\lim_{\tau \rightarrow 0} I_2 = & \frac{J_0 \text{De}}{1 + \text{De}^2} + \text{De} \sum_{k=1}^{\infty} \left[\frac{J_{2k}}{\text{De}^2 (2k-1)^2 + 1} + \frac{J_{2k}}{\text{De}^2 (2k+1)^2 + 1} \right] \\
= & \frac{\text{De} J_0}{1 + \text{De}^2} + \text{De} \sum_{k=1}^{\infty} J_{2k} \left[\frac{1}{\text{De}^2 (2k-1)^2 + 1} + \frac{1}{\text{De}^2 (2k+1)^2 + 1} \right] \quad (142) \\
= & \text{De} \left\{ \frac{J_0}{1 + \text{De}^2} + \sum_{k=1}^{\infty} J_{2k} \left[\frac{1}{\text{De}^2 (2k-1)^2 + 1} + \frac{1}{\text{De}^2 (2k+1)^2 + 1} \right] \right\}
\end{aligned}$$

or:

$$\lim_{\tau \rightarrow 0} I_2 = \text{De} \sum_{k=1}^{\infty} \alpha_k^{(2)} \quad (143)$$

We use Eqs. (132) [with Eqs. (133) and (134)], (139) [with Eqs. (140) and (141)], (136) and (143) throughout Sections V.a and V.b.

XII. APPENDIX: FOURIER ANALYSIS OF COMPACT FORMS

In this appendix, we Fourier analyze Eqs. (51) and (63), and for this, we will need the following identities (Eqs. 4.3.31-4.3.33 of [39]):

$$\cos n\tau \cos m\tau = \frac{1}{2} \cos(n-m)\tau + \frac{1}{2} \cos(n+m)\tau \quad (144)$$

$$\sin n\tau \cos m\tau = \frac{1}{2} \sin(n-m)\tau + \frac{1}{2} \sin(n+m)\tau \quad (145)$$

$$\sin n\tau \sin m\tau = \frac{1}{2} \cos(n-m)\tau - \frac{1}{2} \cos(n+m)\tau \quad (146)$$

a. Normal Stress Differences

We begin by rewriting the compact form, Eq. (51), as:

$$\mathbb{N}_1(\tau) = \mathbb{N}_1^{(1)}(\tau) + \mathbb{N}_1^{(2)}(\tau) + \mathbb{N}_1^{(3)}(\tau) + \mathbb{N}_1^{(4)}(\tau) \quad (147)$$

where the transient parts are given by:

$$\mathbb{N}_1^{(1)}(\tau) = -\frac{2}{\text{De}} e^{-\tau/\text{De}} \cos\left(\frac{W_i}{\text{De}} \sin \tau\right) \lim_{\tau \rightarrow 0} I_1 \quad (148)$$

$$\mathbb{N}_1^{(2)}(\tau) = \frac{2}{\text{De}} e^{-\tau/\text{De}} \sin\left(\frac{W_i}{\text{De}} \sin \tau\right) \lim_{\tau \rightarrow 0} I_2 \quad (149)$$

and the alternant parts by:

$$\mathbb{N}_1^{(3)}(\tau) = \frac{2}{\text{De}} e^{-\tau/\text{De}} \cos\left(\frac{W_i}{\text{De}} \sin \tau\right) I_1 \quad (150)$$

$$\mathbb{N}_1^{(4)}(\tau) = -\frac{2}{\text{De}} e^{-\tau/\text{De}} \sin\left(\frac{W_i}{\text{De}} \sin \tau\right) I_2 \quad (151)$$

i. Transient parts of Eq. (147)

Substituting Eqs. (122) and (135) into the first transient part, Eq. (148), of Eq. (147), gives:

$$\mathbb{N}_1^{(1)}(\tau) = -2 \sum_{k=1}^{\infty} \alpha_k^{(1)} e^{-\tau/\text{De}} A_0 - e^{-\tau/\text{De}} \sum_{k=1}^{\infty} \left[\left(\sum_{k=1}^{\infty} \alpha_k^{(1)} \right) A_k \cos 2k\tau \right] \quad (152)$$

and substituting Eqs. (125) and (142) into the second transient part, Eq. (149), gives:

$$\mathbb{N}_1^{(2)}(\tau) = 2e^{-\tau/\text{De}} \sum_{k=0}^{\infty} \alpha_k^{(2)} \sum_{k=1}^{\infty} B_k \sin(2k\tau - \tau) \quad (153)$$

ii. First alternant part of Eq. (147)

Substituting Eqs. (122) and (136) into the first alternant part of Eq. (147), Eq. (150), gives:

$$\mathbb{N}_1^{(3)}(\tau) = 2 \left(A_0 + \sum_{k=1}^{\infty} A_k \cos(2k\tau) \right) \left(\sum_{k=1}^{\infty} \alpha_k^{(1)} \cos(2k\tau) + \beta_k^{(1)} \sin(2k\tau) \right) \quad (154)$$

Expanding Eq. (154) yields:

$$\begin{aligned}
\mathbb{N}_1^{(3)}(\tau) = & 2\left(A_0\alpha_1^{(1)}\cos 2\tau + A_0\alpha_2^{(1)}\cos 4\tau + A_0\alpha_3^{(1)}\cos 6\tau + \dots\right) \\
& + 2\left(A_1\alpha_1^{(1)}\cos 2\tau\cos 2\tau + A_1\alpha_2^{(1)}\cos 2\tau\cos 4\tau + A_1\alpha_3^{(1)}\cos 2\tau\cos 6\tau + \dots\right) \\
& + 2\left(A_2\alpha_1^{(1)}\cos 4\tau\cos 2\tau + A_2\alpha_2^{(1)}\cos 4\tau\cos 4\tau + A_2\alpha_3^{(1)}\cos 4\tau\cos 6\tau + \dots\right) \\
& + 2\left(A_3\alpha_1^{(1)}\cos 6\tau\cos 2\tau + A_3\alpha_2^{(1)}\cos 6\tau\cos 4\tau + A_3\alpha_3^{(1)}\cos 6\tau\cos 6\tau + \dots\right) \\
& + 2\left(A_0\beta_1^{(1)}\sin 2\tau + A_0\beta_2^{(1)}\sin 4\tau + A_0\beta_3^{(1)}\sin 6\tau + \dots\right) \\
& + 2\left(A_1\beta_1^{(1)}\sin 2\tau\cos 2\tau + A_1\beta_2^{(1)}\sin 4\tau\cos 2\tau + A_1\beta_3^{(1)}\sin 6\tau\cos 2\tau + \dots\right) \\
& + 2\left(A_2\beta_1^{(1)}\sin 2\tau\cos 4\tau + A_2\beta_2^{(1)}\sin 4\tau\cos 4\tau + A_2\beta_3^{(1)}\sin 6\tau\cos 4\tau + \dots\right) \\
& + 2\left(A_3\beta_1^{(1)}\sin 2\tau\cos 6\tau + A_3\beta_2^{(1)}\sin 4\tau\cos 6\tau + A_3\beta_3^{(1)}\sin 6\tau\cos 6\tau + \dots\right)
\end{aligned} \tag{155}$$

Applying the identities Eqs. (144) and (145) to Eq. (155) then gives:

$$\begin{aligned}
\mathbb{N}_1^{(3)}(\tau) = & \left(A_0\alpha_0^{(1)} + A_1\alpha_1^{(1)} + A_2\alpha_2^{(1)} + \dots\right)\cos 0\tau + \left(A_0\alpha_0^{(1)}\right)\cos 0\tau \\
& + \left(A_0\alpha_1^{(1)} + A_1\alpha_2^{(1)} + A_2\alpha_3^{(1)} + \dots + A_3\alpha_2^{(1)} + A_2\alpha_1^{(1)} + A_1\alpha_0^{(1)}\right)\cos 2\tau \\
& + \left(A_0\alpha_1^{(1)} + A_1\alpha_0^{(1)}\right)\cos 2\tau \\
& + \left(A_0\alpha_2^{(1)} + A_1\alpha_3^{(1)} + A_2\alpha_4^{(1)} + \dots + A_4\alpha_2^{(1)} + A_3\alpha_1^{(1)} + A_2\alpha_0^{(1)}\right)\cos 4\tau \\
& + \left(A_0\alpha_2^{(1)} + A_1\alpha_1^{(1)} + A_2\alpha_0^{(1)}\right)\cos 4\tau \\
& + \left(A_0\beta_1^{(1)} + A_1\beta_2^{(1)} + A_2\beta_3^{(1)} + \dots - A_3\beta_2^{(1)} - A_2\beta_1^{(1)} - A_1\beta_0^{(1)}\right)\sin 2\tau \\
& + \left(A_0\beta_1^{(1)} + A_1\beta_0^{(1)}\right)\sin 2\tau \\
& + \left(A_0\beta_2^{(1)} + A_1\beta_3^{(1)} + A_2\beta_4^{(1)} + \dots - A_4\beta_2^{(1)} - A_3\beta_1^{(1)} - A_2\beta_0^{(1)}\right)\sin 4\tau \\
& + \left(A_0\beta_2^{(1)} + A_1\beta_1^{(1)} + A_2\beta_0^{(1)}\right)\sin 4\tau \\
& + \dots
\end{aligned} \tag{156}$$

which leads us to the general expression:

$$\mathbb{N}_1^{(3)}(\tau) = \sum_{n=0}^{\infty} \left[\phi_{\mathbb{N}_1, n}^{(3)} \cos 2n\tau + \psi_{\mathbb{N}_1, n}^{(3)} \sin 2n\tau \right] \tag{157}$$

where:

$$\phi_{\mathbb{N}_1, 0}^{(3)} = A_0\alpha_0^{(1)} + \sum_{q=0}^{\infty} A_q\alpha_q^{(1)} \tag{158}$$

$$\phi_{\mathbb{N}_1, 1}^{(3)} = \sum_{p=0}^1 A_p\alpha_{1-p}^{(1)} + \sum_{q=0}^{\infty} A_q\alpha_{q+1}^{(1)} + \sum_{q=0}^{\infty} A_{q+1}\alpha_q^{(1)} \tag{159}$$

$$\phi_{\mathbb{N}_1, 2}^{(3)} = \sum_{p=0}^2 A_p\alpha_{2-p}^{(1)} + \sum_{q=0}^{\infty} A_q\alpha_{q+2}^{(1)} + \sum_{q=0}^{\infty} A_{q+2}\alpha_q^{(1)} \tag{160}$$

and thus:

$$\phi_{\mathbb{N}_1, n}^{(3)} = \sum_{p=0}^n A_p \alpha_{n-p}^{(1)} + \sum_{q=0}^{\infty} A_q \alpha_{q+n}^{(1)} + \sum_{q=0}^{\infty} A_{q+n} \alpha_q^{(1)} \quad ; n \geq 1 \quad (161)$$

so that:

$$\phi_{\mathbb{N}_1, n}^{(3)} = \begin{cases} A_0 \alpha_0^{(1)} + \sum_{q=0}^{\infty} A_q \alpha_q^{(1)} & ; n = 0 \\ \sum_{p=0}^n A_p \alpha_{n-p}^{(1)} + \sum_{q=0}^{\infty} A_q \alpha_{q+n}^{(1)} + \sum_{q=0}^{\infty} A_{q+n} \alpha_q^{(1)} & ; n \geq 1 \end{cases} \quad (162)$$

$$= \begin{cases} 2A_0 \alpha_0^{(1)} + \sum_{q=1}^{\infty} A_q \alpha_q^{(1)} & ; n = 0 \\ \left[\begin{array}{l} A_0 \alpha_n^{(1)} + \sum_{p=1}^{n-1} A_p \alpha_{n-p}^{(1)} + A_0 \alpha_n^{(1)} \\ + \sum_{q=1}^{\infty} A_q \alpha_{q+n}^{(1)} + A_n \alpha_0^{(1)} + \sum_{q=1}^{\infty} A_{q+n} \alpha_q^{(1)} \end{array} \right] & ; n \geq 1 \end{cases} \quad (163)$$

Now, substituting Eqs. (123) and (133) into Eq. (163), we get:

$$\phi_{\mathbb{N}_1, n}^{(3)} = \begin{cases} -\sum_{q=1}^{\infty} \frac{16q^2 \text{De}^2 J_{2q}^2}{\text{Wi}(4\text{De}^2 q^2 + 1)} & ; n = 0 \\ \left[\begin{array}{l} \frac{-16n^2 \text{De}^2 J_0 J_{2n}}{\text{Wi}(4\text{De}^2 n^2 + 1)} + \sum_{p=1}^{n-1} \frac{-16(n-p)^2 \text{De}^2 J_{2p} J_{2(n-p)}}{\text{Wi}(4\text{De}^2 (n-p)^2 + 1)} \\ + \sum_{q=1}^{\infty} \frac{-16(q+n)^2 \text{De}^2 J_{2q} J_{2(q+n)}}{\text{Wi}(4\text{De}^2 (q+n)^2 + 1)} + \sum_{q=1}^{\infty} \frac{-16q^2 \text{De}^2 J_{2(q+n)} J_{2q}}{\text{Wi}(4\text{De}^2 q^2 + 1)} \end{array} \right] & ; n \geq 1 \end{cases} \quad (164)$$

and where, in Eq. (157):

$$\psi_{\mathbb{N}_1, 0}^{(3)} = 0 \quad (165)$$

$$\psi_{\mathbb{N}_1, 1}^{(3)} = \sum_{p=0}^1 A_p \beta_{1-p}^{(1)} + \sum_{q=0}^{\infty} A_q \beta_{q+1}^{(1)} - \sum_{q=0}^{\infty} A_{q+1} \beta_q^{(1)} \quad (166)$$

$$\psi_{\mathbb{N}_1, 2}^{(3)} = \sum_{p=0}^2 A_p \beta_{2-p}^{(1)} + \sum_{q=0}^{\infty} A_q \beta_{q+2}^{(1)} - \sum_{q=0}^{\infty} A_{q+2} \beta_q^{(1)} \quad (167)$$

and thus:

$$\psi_{\mathbb{N}_1, n}^{(3)} = \sum_{p=0}^n A_p \beta_{n-p}^{(1)} + \sum_{q=0}^{\infty} A_q \beta_{q+n}^{(1)} - \sum_{q=0}^{\infty} A_{q+n} \beta_q^{(1)} \quad ; n \geq 1 \quad (168)$$

so that:

$$\psi_{\mathbb{N}_1, n}^{(3)} = \begin{cases} 0 & ; n = 0 \\ \sum_{p=0}^n A_p \beta_{n-p}^{(1)} + \sum_{q=0}^{\infty} A_q \beta_{q+n}^{(1)} - \sum_{q=0}^{\infty} A_{q+n} \beta_q^{(1)} & ; n \geq 1 \end{cases} \quad (169)$$

$$= \begin{cases} 0 & ; n = 0 \\ \begin{bmatrix} A_0 \beta_n^{(1)} + \sum_{p=1}^{n-1} A_p \beta_{n-p}^{(1)} + A_0 \beta_n^{(1)} \\ - \sum_{q=1}^{\infty} A_q \beta_{q+n}^{(1)} - A_n \beta_0^{(1)} - \sum_{q=1}^{\infty} A_{q+n} \beta_q^{(1)} \end{bmatrix} & ; n \geq 1 \end{cases} \quad (170)$$

Substituting Eqs. (123) and (134) into Eq. (170), we then get:

$$\psi_{\mathbb{N}_1, n}^{(3)} = \begin{cases} 0 & ; n = 0 \\ \begin{bmatrix} \frac{8n \text{De} J_0 J_{2n}}{\text{Wi}(4 \text{De}^2 n^2 + 1)} + \sum_{p=1}^{n-1} \frac{8(n-p) \text{De} J_{2p} J_{2(n-p)}}{\text{Wi}(4 \text{De}^2 (n-p)^2 + 1)} \\ - \sum_{q=1}^{\infty} \frac{8(n+q) \text{De} J_{2q} J_{2(n+q)}}{\text{Wi}(4 \text{De}^2 (n+q)^2 + 1)} - \sum_{q=1}^{\infty} \frac{8q \text{De} J_{2q} J_{2(q+n)}}{\text{Wi}(4 \text{De}^2 q^2 + 1)} \end{bmatrix} & ; n \geq 1 \end{cases} \quad (171)$$

iii. Second alternant part of Eq. (147)

Substituting Eqs. (125) and (139) into the second alternant part of Eq. (147), Eq. (151), gives:

$$\mathbb{N}_1^{(4)}(\tau) = -2 \sum_{k=1}^{\infty} B_k \sin(2k\tau - \tau) \times \begin{bmatrix} \alpha_1^{(2)} \cos \tau + \text{De} e^{\tau/\text{De}} \beta_1^{(2)} \sin \tau \\ + \sum_{k=2}^{\infty} \left[\alpha_k^{(2)} \cos(2k\tau - \tau) + \beta_k^{(2)} \sin(2k\tau - \tau) \right] \end{bmatrix} \quad (172)$$

Expanding Eq. (172) yields:

$$\begin{aligned} \mathbb{N}_1^{(4)}(\tau) = & -2 \left(B_1 \alpha_1^{(2)} \sin \tau \cos \tau + B_1 \alpha_2^{(2)} \sin \tau \cos 3\tau + B_1 \alpha_3^{(2)} \sin \tau \cos 5\tau + \dots \right) \\ & -2 \left(B_2 \alpha_1^{(2)} \sin 3\tau \cos \tau + B_2 \alpha_2^{(2)} \sin 3\tau \cos 3\tau + B_2 \alpha_3^{(2)} \sin 3\tau \cos 5\tau + \dots \right) \\ & -2 \left(B_3 \alpha_1^{(2)} \sin 5\tau \cos \tau + B_3 \alpha_2^{(2)} \sin 5\tau \cos 3\tau + B_3 \alpha_3^{(2)} \sin 5\tau \cos 5\tau + \dots \right) \\ & -2 \left(B_1 \beta_1^{(2)} \sin \tau \sin \tau + B_1 \beta_2^{(2)} \sin \tau \sin 3\tau + B_1 \beta_3^{(2)} \sin \tau \sin 5\tau + \dots \right) \\ & -2 \left(B_2 \beta_1^{(2)} \sin 3\tau \sin \tau + B_2 \beta_2^{(2)} \sin 3\tau \sin 3\tau + B_2 \beta_3^{(2)} \sin 3\tau \sin 5\tau + \dots \right) \\ & -2 \left(B_3 \beta_1^{(2)} \sin 5\tau \sin \tau + B_3 \beta_2^{(2)} \sin 5\tau \sin 3\tau + B_3 \beta_3^{(2)} \sin 5\tau \sin 5\tau + \dots \right) \end{aligned} \quad (173)$$

Applying identities Eqs. (145) and (146) to Eq. (173) gives:

$$\begin{aligned}
\mathbb{N}_1^{(4)}(\tau) = & -\left(B_2\alpha_1^{(2)} + B_3\alpha_2^{(2)} + B_4\alpha_3^{(2)} + \dots - B_3\alpha_4^{(2)} - B_2\alpha_3^{(2)} - B_1\alpha_2^{(2)}\right)\sin 2\tau \\
& -\left(B_1\alpha_1^{(2)}\right)\sin 2\tau \\
& -\left(B_3\alpha_1^{(2)} + B_4\alpha_2^{(2)} + B_5\alpha_3^{(2)} + \dots - B_3\alpha_5^{(2)} - B_2\alpha_4^{(2)} - B_1\alpha_3^{(2)}\right)\sin 4\tau \\
& -\left(B_1\alpha_2^{(2)} + B_2\alpha_1^{(2)}\right)\sin 4\tau \\
& -\left(B_4\alpha_1^{(2)} + B_5\alpha_2^{(2)} + B_6\alpha_3^{(2)} + \dots - B_3\alpha_6^{(2)} - B_2\alpha_5^{(2)} - B_1\alpha_4^{(2)}\right)\sin 6\tau \\
& -\left(B_1\alpha_3^{(2)} + B_2\alpha_2^{(2)} + B_3\alpha_1^{(2)}\right)\sin 6\tau + \dots \\
& -\left(B_1\beta_1^{(2)} + B_2\beta_2^{(2)} + B_3\beta_3^{(2)} + \dots\right)\cos 0\tau \\
& -\left(B_1\beta_2^{(2)} + B_2\beta_3^{(2)} + B_3\beta_4^{(2)} + \dots + B_4\beta_3^{(2)} + B_3\beta_2^{(2)} + B_2\beta_1^{(2)}\right)\cos 2\tau \\
& +\left(B_1\beta_1^{(2)}\right)\cos 2\tau \\
& -\left(B_1\beta_3^{(2)} + B_2\beta_4^{(2)} + B_3\beta_5^{(2)} + \dots + B_5\beta_3^{(2)} + B_4\beta_2^{(2)} + B_3\beta_1^{(2)}\right)\cos 4\tau \\
& +\left(B_1\beta_2^{(2)} + B_2\beta_1^{(2)}\right)\cos 4\tau \\
& -\left(B_1\beta_4^{(2)} + B_2\beta_5^{(2)} + B_3\beta_6^{(2)} + \dots + B_6\beta_3^{(2)} + B_5\beta_2^{(2)} + B_4\beta_1^{(2)}\right)\cos 6\tau \\
& +\left(B_1\beta_3^{(2)} + B_2\beta_2^{(2)} + B_3\beta_1^{(2)}\right)\cos 6\tau + \dots
\end{aligned} \tag{174}$$

which leads us to the general expression:

$$\mathbb{N}_1^{(4)}(\tau) = \sum_{n=0}^{\infty} \left[\phi_{\mathbb{N}_1, n}^{(4)} \cos 2n\tau + \psi_{\mathbb{N}_1, n}^{(4)} \sin 2n\tau \right] \tag{175}$$

where:

$$\phi_{\mathbb{N}_1, 0}^{(4)} = -\sum_{q=1}^{\infty} B_q \beta_q^{(2)} \tag{176}$$

$$\phi_{\mathbb{N}_1, 1}^{(4)} = B_1 \beta_1^{(2)} - \sum_{q=1}^{\infty} \left[B_q \beta_{q+1}^{(2)} + B_{q+1} \beta_q^{(2)} \right] \tag{177}$$

$$\phi_{\mathbb{N}_1, 2}^{(4)} = \sum_{p=1}^2 B_p \beta_{2-p+1}^{(2)} - \sum_{q=1}^{\infty} \left[B_q \beta_{q+2}^{(2)} + B_{q+2} \beta_q^{(2)} \right] \tag{178}$$

and thus:

$$\phi_{\mathbb{N}_1, n}^{(4)} = \begin{cases} -\sum_{q=1}^{\infty} B_q \beta_q^{(2)} & ; n = 0 \\ \sum_{p=1}^n B_p \beta_{n-p+1}^{(2)} - \sum_{q=1}^{\infty} \left[B_q \beta_{q+n}^{(2)} + B_{q+n} \beta_q^{(2)} \right] & ; n \geq 1 \end{cases} \tag{179}$$

$$= \begin{cases} -\sum_{q=1}^{\infty} B_q \beta_q^{(2)} & ; n=0 \\ \sum_{p=1}^n B_p \beta_{n-p+1}^{(2)} - \sum_{q=1}^{\infty} B_q \beta_{q+n}^{(2)} - \sum_{q=1}^{\infty} B_{q+n} \beta_q^{(2)} & ; n \geq 1 \end{cases} \quad (180)$$

Substituting Eqs. (126) and (141) into Eq. (180):

$$\phi_{N_1, n}^{(4)} = \begin{cases} -\sum_{q=1}^{\infty} \frac{2De J_{2q-1} (2q-1) (J_{2q} + J_{2q-2})}{De^2 (2q-1)^2 + 1} & ; n=0 \\ \left[\begin{aligned} & \sum_{p=1}^n \frac{2De J_{2p-1} (2n-2p+1) (J_{2n-2p+2} + J_{2n-2p})}{De^2 (2n-2p+1)^2 + 1} \\ & - \sum_{q=1}^{\infty} \frac{2De J_{2q-1} (2n+2q-1) (J_{2n+2q} + J_{2n+2q-2})}{De^2 (2n+2q-1)^2 + 1} \\ & - \sum_{q=1}^{\infty} \frac{2De J_{2n+2q-1} (2q-1) (J_{2q} + J_{2q-2})}{De^2 (2q-1)^2 + 1} \end{aligned} \right] & ; n \geq 1 \end{cases} \quad (181)$$

and where, in Eq. (175):

$$\psi_{N_1, 0}^{(4)} = 0 \quad (182)$$

$$\psi_{N_1, 1}^{(4)} = -B_1 \alpha_1^{(2)} - \sum_{q=1}^{\infty} [B_{q+1} \alpha_q^{(2)} - B_q \alpha_{q+1}^{(2)}] \quad (183)$$

$$\psi_{N_1, 2}^{(4)} = -\sum_{p=1}^2 B_p \alpha_{2-p+1}^{(2)} - \sum_{q=1}^{\infty} [B_{q+2} \alpha_q^{(2)} - B_q \alpha_{q+2}^{(2)}] \quad (184)$$

and thus:

$$\psi_{N_1, n}^{(4)} = \begin{cases} 0 & ; n=0 \\ -\sum_{p=1}^n B_p \alpha_{n-p+1}^{(2)} - \sum_{q=1}^{\infty} [B_{q+n} \alpha_q^{(2)} - B_q \alpha_{q+n}^{(2)}] & ; n \geq 1 \end{cases} \quad (185)$$

$$= \begin{cases} 0 & ; n=0 \\ \left[\begin{aligned} & -\sum_{p=1}^n \frac{2J_{2p-1} (J_{2n-2p+2} + J_{2n-2p})}{De^2 (2n-2p+1)^2 + 1} - \sum_{q=1}^{\infty} \frac{2J_{2n+2q-1} (J_{2q} + J_{2q-2})}{De^2 (2q-1)^2 + 1} \\ & + \sum_{q=1}^{\infty} \frac{2J_{2q-1} (J_{2q+2n} + J_{2q+2n-2})}{De^2 (2n+2q-1)^2 + 1} \end{aligned} \right] & ; n \geq 1 \end{cases} \quad (186)$$

Using Eqs. (152), (153), (164) and (171), with Eqs. (164), (170), (181) and (186), we get Eq. (56).

b. Shear Stress

We begin by rewriting the compact form, Eq. (63), as:

$$\mathbb{S}(\tau) = \mathbb{S}^{(1)}(\tau) + \mathbb{S}^{(2)}(\tau) + \mathbb{S}^{(3)}(\tau) + \mathbb{S}^{(4)}(\tau) \quad (187)$$

where the transient parts are given by:

$$\mathbb{S}^{(1)}(\tau) = \frac{1}{D_e} e^{-\tau/D_e} \sin\left(\frac{W_i}{D_e} \sin \tau\right) \lim_{\tau \rightarrow 0} I_1 \quad (188)$$

$$\mathbb{S}^{(2)}(\tau) = \frac{1}{D_e} e^{-\tau/D_e} \cos\left(\frac{W_i}{D_e} \sin \tau\right) \lim_{\tau \rightarrow 0} I_2 \quad (189)$$

and the alternant parts by:

$$\mathbb{S}^{(3)}(\tau) = -\frac{1}{D_e} e^{-\tau/D_e} \sin\left(\frac{W_i}{D_e} \sin \tau\right) I_1 \quad (190)$$

$$\mathbb{S}^{(4)}(\tau) = -\frac{1}{D_e} e^{-\tau/D_e} \cos\left(\frac{W_i}{D_e} \sin \tau\right) I_2 \quad (191)$$

i. Transient parts of Eq. (187)

Substituting Eqs. (125) and (135) into the first transient part, Eq. (188), of Eq. (187), gives:

$$\mathbb{S}^{(1)}(\tau) = e^{-\tau/D_e} \sum_{k=1}^{\infty} \alpha_k^{(1)} \sum_{k=1}^{\infty} B_k \sin(2k\tau - \tau) \quad (192)$$

and substituting Eqs. (122) and (142) into the second transient part, Eq. (189), gives:

$$\mathbb{S}^{(2)}(\tau) = e^{-\tau/D_e} \sum_{k=1}^{\infty} \alpha_k^{(2)} A_0 + e^{-\tau/D_e} \sum_{k=1}^{\infty} \alpha_k^{(2)} \sum_{k=1}^{\infty} A_k \cos(2k\tau) \quad (193)$$

ii. First alternant part of Eq. (187)

Substituting Eqs. (125) and (135) into the first alternant part of Eq. (187), Eq. (190), gives:

$$\mathbb{S}^{(3)}(\tau) = -\sum_{k=1}^{\infty} B_k \sin(2k\tau - \tau) \sum_{k=1}^{\infty} \left[\alpha_k^{(1)} \cos(2k\tau) + \beta_k^{(1)} \sin(2k\tau) \right] \quad (194)$$

Expanding Eq. (194) yields:

$$\begin{aligned} \mathbb{S}^{(3)}(\tau) = & -\left(B_1 \alpha_1^{(1)} \sin \tau \cos 2\tau + B_1 \alpha_2^{(1)} \sin \tau \cos 4\tau + B_1 \alpha_3^{(1)} \sin \tau \cos 6\tau + \dots \right) \\ & -\left(B_2 \alpha_1^{(1)} \sin 3\tau \cos 2\tau + B_2 \alpha_2^{(1)} \sin 3\tau \cos 4\tau + B_2 \alpha_3^{(1)} \sin 3\tau \cos 6\tau + \dots \right) \\ & -\left(B_3 \alpha_1^{(1)} \sin 5\tau \cos 2\tau + B_3 \alpha_2^{(1)} \sin 5\tau \cos 4\tau + B_3 \alpha_3^{(1)} \sin 5\tau \cos 6\tau + \dots \right) \\ & -\left(B_1 \beta_1^{(1)} \sin \tau \sin 2\tau + B_1 \beta_2^{(1)} \sin \tau \sin 4\tau + B_1 \beta_3^{(1)} \sin \tau \sin 6\tau + \dots \right) \\ & -\left(B_2 \beta_1^{(1)} \sin 3\tau \sin 2\tau + B_2 \beta_2^{(1)} \sin 3\tau \sin 4\tau + B_2 \beta_3^{(1)} \sin 3\tau \sin 6\tau + \dots \right) \\ & -\left(B_3 \beta_1^{(1)} \sin 5\tau \sin 2\tau + B_3 \beta_2^{(1)} \sin 5\tau \sin 4\tau + B_3 \beta_3^{(1)} \sin 5\tau \sin 6\tau + \dots \right) \end{aligned} \quad (195)$$

Applying the identities Eqs. (145) and (146) to Eq. (195) then gives:

$$\begin{aligned}
\mathbb{S}^{(3)}(\tau) = & -\frac{1}{2}(B_2\alpha_1^{(1)} + B_3\alpha_2^{(1)} + B_4\alpha_3^{(1)} + \dots - B_1\alpha_1^{(1)} - B_2\alpha_2^{(1)} - B_3\alpha_3^{(1)} - \dots)\sin\tau \\
& -\frac{1}{2}(B_3\alpha_1^{(1)} + B_4\alpha_2^{(1)} + B_5\alpha_3^{(1)} + \dots - B_1\alpha_2^{(1)} - B_2\alpha_3^{(1)} - B_3\alpha_4^{(1)} - \dots)\sin 3\tau \\
& -\frac{1}{2}(B_1\alpha_1^{(1)})\sin 3\tau \\
& -\frac{1}{2}(B_4\alpha_1^{(1)} + B_5\alpha_2^{(1)} + B_6\alpha_3^{(1)} + \dots - B_1\alpha_3^{(1)} - B_2\alpha_4^{(1)} - B_3\alpha_5^{(1)} - \dots)\sin 5\tau \\
& -\frac{1}{2}(B_1\alpha_2^{(1)} + B_2\alpha_1^{(1)})\sin 5\tau + \dots \\
& -\frac{1}{2}(B_2\beta_1^{(1)} + B_3\beta_2^{(1)} + B_4\beta_3^{(1)} + \dots + B_1\beta_1^{(1)} + B_2\beta_2^{(1)} + B_3\beta_3^{(1)} + \dots)\cos\tau \\
& -\frac{1}{2}(B_3\beta_1^{(1)} + B_4\beta_2^{(1)} + B_5\beta_3^{(1)} + \dots + B_1\beta_2^{(1)} + B_2\beta_3^{(1)} + B_3\beta_4^{(1)} + \dots)\cos 3\tau \\
& -\frac{1}{2}(-B_1\beta_1^{(1)})\cos 3\tau \\
& -\frac{1}{2}(B_4\beta_1^{(1)} + B_5\beta_2^{(1)} + B_6\beta_3^{(1)} + \dots + B_1\beta_3^{(1)} + B_2\beta_4^{(1)} + B_3\beta_5^{(1)} + \dots)\cos 5\tau \\
& -\frac{1}{2}(-B_1\beta_2^{(1)} - B_2\beta_1^{(1)})\cos 5\tau + \dots
\end{aligned} \tag{196}$$

which leads us to the general expression:

$$\mathbb{S}^{(3)}(\tau) = -\frac{1}{2} \sum_{n=0}^{\infty} \left[\phi_{\mathbb{S},n}^{(3)} \cos(2n\tau - \tau) + \psi_{\mathbb{S},n}^{(3)} \sin(2n\tau - \tau) \right] \tag{197}$$

where

$$\phi_{\mathbb{S},1}^{(3)} = \sum_{k=1}^{\infty} [B_{k+1}\beta_k^{(1)} + B_k\beta_k^{(1)}] \tag{198}$$

$$\phi_{\mathbb{S},2}^{(3)} = -\sum_{k=1}^{2-1} B_k\beta_{2-k}^{(1)} + \sum_{k=1}^{\infty} [B_{k+2}\beta_k^{(1)} + B_k\beta_{k+2-1}^{(1)}] \tag{199}$$

$$\phi_{\mathbb{S},3}^{(3)} = -\sum_{k=1}^{3-1} B_k\beta_{3-k}^{(1)} + \sum_{k=1}^{\infty} [B_{k+3}\beta_k^{(1)} + B_k\beta_{k+3-1}^{(1)}] \tag{200}$$

and thus:

$$\phi_{\mathbb{S},n}^{(3)} = -\sum_{k=1}^{n-1} B_k\beta_{n-k}^{(1)} + \sum_{k=1}^{\infty} [B_{k+n}\beta_k^{(1)} + B_k\beta_{k+n-1}^{(1)}] \quad ; n \geq 1 \tag{201}$$

so that:

$$\phi_{\mathbb{S},n}^{(3)} = \begin{cases} 0 & ; n = 0 \\ -\sum_{k=0}^{n-1} B_k\beta_{n-k}^{(1)} + \sum_{k=0}^{\infty} [B_{k+n}\beta_k^{(1)} + B_k\beta_{k+n-1}^{(1)}] & ; n \geq 1 \end{cases} \tag{202}$$

$$= \begin{cases} 0 & ;n=0 \\ -\sum_{p=1}^{n-1} \frac{8(n-p)\text{De} J_{2p-1} J_{2n-2p}}{\text{Wi}(4\text{De}^2(n-p)^2+1)} & \\ +\sum_{q=1}^{\infty} \left[\frac{8q\text{De} J_{2q} J_{2q+2n-1}}{\text{Wi}(4\text{De}^2 q^2+1)} + \frac{8(q+n-1)\text{De} J_{2q-1} J_{2q+2n-2}}{\text{Wi}(4\text{De}^2(q+n-1)^2+1)} \right] & ;n \geq 1 \end{cases} \quad (203)$$

and where, in Eq. (197):

$$\psi_{S,1}^{(3)} = \sum_k [B_{k+1}\alpha_k^{(1)} - B_k\alpha_k^{(1)}] \quad (204)$$

$$\psi_{S,2}^{(3)} = \sum_k^{2-1} B_k\alpha_{2-k}^{(1)} + \sum_k [B_{k+2}\alpha_k^{(1)} - B_k\alpha_{k+2-1}^{(1)}] \quad (205)$$

$$\psi_{S,3}^{(3)} = \sum_k^{3-1} B_k\alpha_{3-k}^{(1)} + \sum_k [B_{k+3}\alpha_k^{(1)} - B_k\alpha_{k+3-1}^{(1)}] \quad (206)$$

and thus:

$$\psi_{S,n}^{(3)} = \sum_k^{n-1} B_k\alpha_{n-k}^{(1)} + \sum_k [B_{k+n}\alpha_k^{(1)} - B_k\alpha_{k+n-1}^{(1)}] \quad (207)$$

so that:

$$\psi_{S,n}^{(3)} = \begin{cases} 0 & n=0 \\ \sum_{k=0}^{n-1} B_k\alpha_{n-k}^{(1)} + \sum_{k=0}^{\infty} [B_{k+n}\alpha_k^{(1)} - B_k\alpha_{k+n-1}^{(1)}] & n \geq 1 \end{cases} \quad (208)$$

$$= \begin{cases} 0 & ;n=0 \\ \sum_{p=1}^{n-1} \frac{-16(n-p)^2 \text{De}^2 J_{2p-1} J_{2n-2p}}{\text{Wi}(4\text{De}^2(n-p)^2+1)} & \\ +\sum_{q=1}^{\infty} \left[\frac{-16q^2 \text{De}^2 J_{2q+2n-1} J_{2q}}{\text{Wi}(4\text{De}^2 q^2+1)} + \frac{16(q+n-1)^2 \text{De}^2 J_{2q-1} J_{2q+2n-2}}{\text{Wi}(4\text{De}^2(q+n-1)^2+1)} \right] & ;n \geq 1 \end{cases} \quad (209)$$

iii. Second alternant part of Eq. (187)

Substituting Eqs. (122) and (139) into the second alternant part of Eq. (187), Eq. (191), gives:

$$\mathbb{S}^{(4)}(\tau) = - \left[A_0 + \sum_{k=1}^{\infty} A_k \cos(2k\tau) \right] \times \left[\begin{aligned} &\alpha_1^{(2)} \cos \tau + \beta_1^{(2)} \sin \tau \\ &+ \sum_{k=2}^{\infty} \left[\alpha_k^{(2)} \cos(2k\tau - \tau) + \beta_k^{(2)} \sin(2k\tau - \tau) \right] \end{aligned} \right] \quad (210)$$

Expanding Eq. (210) yields:

$$\begin{aligned} \mathbb{S}^{(4)}(\tau) = & - \left(A_0 \alpha_1^{(2)} \cos \tau + A_0 \alpha_2^{(2)} \cos 3\tau + A_0 \alpha_3^{(2)} \cos 5\tau + \dots \right) \\ & - \left(A_1 \alpha_1^{(2)} \cos 2\tau \cos \tau + A_1 \alpha_2^{(2)} \cos 2\tau \cos 3\tau + A_1 \alpha_3^{(2)} \cos 2\tau \cos 5\tau + \dots \right) \\ & - \left(A_2 \alpha_1^{(2)} \cos 4\tau \cos \tau + A_2 \alpha_2^{(2)} \cos 4\tau \cos 3\tau + A_2 \alpha_3^{(2)} \cos 4\tau \cos 5\tau + \dots \right) \\ & - \left(A_3 \alpha_1^{(2)} \cos 6\tau \cos \tau + A_3 \alpha_2^{(2)} \cos 6\tau \cos 3\tau + A_3 \alpha_3^{(2)} \cos 6\tau \cos 5\tau + \dots \right) \\ & - \left(A_0 \beta_1^{(2)} \sin \tau + A_0 \beta_2^{(2)} \sin 3\tau + A_0 \beta_3^{(2)} \sin 5\tau + \dots \right) \\ & - \left(A_1 \beta_1^{(2)} \sin \tau \cos 2\tau + A_1 \beta_2^{(2)} \sin 3\tau \cos 2\tau + A_1 \beta_3^{(2)} \sin 5\tau \cos 2\tau + \dots \right) \\ & - \left(A_2 \beta_1^{(2)} \sin \tau \cos 4\tau + A_2 \beta_2^{(2)} \sin 3\tau \cos 4\tau + A_2 \beta_3^{(2)} \sin 5\tau \cos 4\tau + \dots \right) \\ & - \left(A_3 \beta_1^{(2)} \sin \tau \cos 6\tau + A_3 \beta_2^{(2)} \sin 3\tau \cos 6\tau + A_3 \beta_3^{(2)} \sin 5\tau \cos 6\tau + \dots \right) \end{aligned} \quad (211)$$

Applying identities Eqs. (123) and (141) to Eq. (211) gives:

$$\begin{aligned} \mathbb{S}^{(4)}(\tau) = & -\frac{1}{2} \left(A_0 \alpha_1^{(2)} + A_1 \alpha_2^{(2)} + A_2 \alpha_3^{(2)} + \dots + A_1 \alpha_1^{(2)} + A_2 \alpha_2^{(2)} + A_3 \alpha_3^{(2)} + \dots \right) \cos \tau \\ & -\frac{1}{2} \left(A_0 \alpha_2^{(2)} + A_1 \alpha_3^{(2)} + A_2 \alpha_4^{(2)} + \dots + A_2 \alpha_1^{(2)} + A_3 \alpha_2^{(2)} + A_4 \alpha_3^{(2)} + \dots \right) \cos 3\tau \\ & -\frac{1}{2} \left(A_0 \alpha_3^{(2)} + A_1 \alpha_4^{(2)} + A_2 \alpha_5^{(2)} + \dots + A_3 \alpha_1^{(2)} + A_4 \alpha_2^{(2)} + A_5 \alpha_3^{(2)} + \dots \right) \cos 5\tau \\ & -\frac{1}{2} \left(A_0 \alpha_1^{(2)} \right) \cos \tau \\ & -\frac{1}{2} \left(A_0 \alpha_2^{(2)} + A_1 \alpha_1^{(2)} \right) \cos 3\tau \\ & -\frac{1}{2} \left(A_0 \alpha_3^{(2)} + A_1 \alpha_2^{(2)} + A_2 \alpha_1^{(2)} \right) \cos 5\tau \\ & -\frac{1}{2} \left(A_0 \beta_1^{(2)} + A_1 \beta_2^{(2)} + A_2 \beta_3^{(2)} + \dots - A_1 \beta_1^{(2)} - A_2 \beta_2^{(2)} - A_3 \beta_3^{(2)} - \dots \right) \sin \tau \\ & -\frac{1}{2} \left(A_0 \beta_2^{(2)} + A_1 \beta_3^{(2)} + A_2 \beta_4^{(2)} + \dots - A_2 \beta_1^{(2)} - A_3 \beta_2^{(2)} - A_4 \beta_3^{(2)} - \dots \right) \sin 3\tau \\ & -\frac{1}{2} \left(A_0 \beta_3^{(2)} + A_1 \beta_4^{(2)} + A_2 \beta_5^{(2)} + \dots - A_3 \beta_1^{(2)} - A_4 \beta_2^{(2)} - A_5 \beta_3^{(2)} - \dots \right) \sin 5\tau \\ & -\frac{1}{2} \left(A_0 \beta_1^{(2)} \right) \sin \tau \\ & -\frac{1}{2} \left(A_0 \beta_2^{(2)} + A_1 \beta_1^{(2)} \right) \sin 3\tau \\ & -\frac{1}{2} \left(A_0 \beta_3^{(2)} + A_1 \beta_2^{(2)} + A_2 \beta_1^{(2)} \right) \sin 5\tau \end{aligned} \quad (212)$$

which leads us to the general expression:

$$\mathbb{S}^{(4)}(\tau) = -\frac{1}{2} \sum_{n=1}^{\infty} \left[\phi_{\mathbb{S},n}^{(4)} \cos(2n\tau - \tau) + \psi_{\mathbb{S},n}^{(4)} \sin(2n\tau - \tau) \right] \quad (213)$$

where:

$$\phi_{\mathbb{S},1}^{(4)} = \sum_{k=0}^{1-1} A_k \alpha_{1-k}^{(2)} + \sum_{k=0}^{\infty} \left[A_k \alpha_{k+1}^{(2)} + A_{k+1} \alpha_{k+1}^{(2)} \right] \quad (214)$$

$$\phi_{\mathbb{S},2}^{(4)} = \sum_{k=0}^{2-1} A_k \alpha_{2-k}^{(2)} + \sum_{k=0}^{\infty} \left[A_k \alpha_{k+2}^{(2)} + A_{k+2} \alpha_{k+1}^{(2)} \right] \quad (215)$$

$$\phi_{\mathbb{S},3}^{(4)} = \sum_{k=0}^{3-1} A_k \alpha_{3-k}^{(2)} + \sum_{k=0}^{\infty} \left[A_k \alpha_{k+3}^{(2)} + A_{k+3} \alpha_{k+1}^{(2)} \right] \quad (216)$$

and thus:

$$\phi_{\mathbb{S},n}^{(4)} = \begin{cases} 0 & n = 0 \\ \sum_{k=0}^{n-1} A_k \alpha_{n-k}^{(2)} + \sum_{k=0}^{\infty} \left[A_k \alpha_{k+n}^{(2)} + A_{k+n} \alpha_{k+1}^{(2)} \right] & n \geq 1 \end{cases} \quad (217)$$

$$= \begin{cases} 0 & ; n = 0 \\ \sum_{p=0}^{n-1} A_p \alpha_{n-p}^{(2)} + \sum_{q=0}^{\infty} \left[A_q \alpha_{q+n}^{(2)} + A_{q+n} \alpha_{q+1}^{(2)} \right] & ; n \geq 1 \end{cases} \quad (218)$$

Substituting Eqs. (123) and (133) into Eq. (218):

$$\phi_{\mathbb{S},n}^{(4)} = \begin{cases} 0 & ; n = 0 \\ \frac{2J_0(J_{2n} + J_{2n-2})}{\text{De}^2(2n-1)^2 + 1} + \sum_{p=1}^{n-1} \left[\frac{2J_{2p}(J_{2n-2p} + J_{2n-2p-2})}{\text{De}^2(2n-2p-1)^2 + 1} \right] + \frac{2J_{2n}(J_2 + J_0)}{\text{De}^2 + 1} & ; n \geq 1 \\ + \sum_{q=1}^{\infty} \left[\frac{2J_{2q}(J_{2q+2n} + J_{2q+2n-2})}{\text{De}^2(2q+2n-1)^2 + 1} + \frac{2J_{2q+2n}(J_{2q+2} + J_{2q})}{\text{De}^2(2q+1)^2 + 1} \right] & ; n \geq 1 \end{cases} \quad (219)$$

and where, in Eq. (213):

$$\psi_{\mathbb{S},1}^{(4)} = \sum_{k=0}^{1-1} A_k \beta_{1-k}^{(2)} + \sum_{k=0}^{\infty} \left[A_k \beta_{k+1}^{(2)} - A_{k+1} \beta_{k+1}^{(2)} \right] \quad (220)$$

$$\psi_{\mathbb{S},2}^{(4)} = \sum_{k=0}^{2-1} A_k \beta_{2-k}^{(2)} + \sum_{k=0}^{\infty} \left[A_k \beta_{k+2}^{(2)} - A_{k+2} \beta_{k+1}^{(2)} \right] \quad (221)$$

$$\psi_{\mathbb{S},3}^{(4)} = \sum_{k=0}^{3-1} A_k \beta_{3-k}^{(2)} + \sum_{k=0}^{\infty} \left[A_k \beta_{k+3}^{(2)} - A_{k+3} \beta_{k+1}^{(2)} \right] \quad (222)$$

and thus:

$$\psi_{\mathbb{S},n}^{(4)} = \begin{cases} 0 & ; n = 0 \\ \sum_{k=0}^{n-1} A_k \beta_{n-k}^{(2)} + \sum_{k=0}^{\infty} \left[A_k \beta_{k+n}^{(2)} - A_{k+n} \beta_{k+1}^{(2)} \right] & ; n \geq 1 \end{cases} \quad (223)$$

$$= \left\{ \begin{array}{l} 0 \qquad \qquad \qquad ; n = 0 \\ \frac{2J_0 \operatorname{De}(2n-1)(J_{2n} + J_{2n-2})}{\operatorname{De}^2(2n-1)^2 + 1} - \frac{2\operatorname{De}J_{2n}(J_2 + J_0)}{\operatorname{De}^2 + 1} \\ + \sum_{p=1}^{n-1} \frac{2\operatorname{De}(2n-2p-1)J_{2p}(J_{2n-2p} + J_{2n-2p-2})}{\operatorname{De}^2(2n-2p-1)^2 + 1} \\ + \sum_{q=1}^{\infty} \left[\frac{2\operatorname{De}(2q+2n-1)J_{2q}(J_{2q+2n} + J_{2q+2n-2})}{\operatorname{De}^2(2q+2n-1)^2 + 1} \right] \\ - \sum_{q=1}^{\infty} \left[\frac{2\operatorname{De}(2q+1)J_{2q+2n}(J_{2q+2} + J_{2q})}{\operatorname{De}^2(2q+1)^2 + 1} \right] \end{array} \right. \qquad ; n \geq 1 \qquad (224)$$

Using Eqs. (192), (193), (197) and (213), with Eqs. (203), (209), (219) and (224), we get Eq. (66).

Table I: Literature on Analytical Solution for Large-Amplitude Oscillatory Shear Flow.

| | Model | First | Third | Fifth | Zeroth | Second | Fourth | Startup | Notation Eq. | Form | [Ref.] (Correction to) |
|--|-----------------------|-----------------------|-------|-------|-----------------------------------|----------------|--------|---------|--------------|----------|------------------------|
| | | Shear Stress Harmonic | | | Normal Stress Difference Harmonic | | | | | | |
| Kirkwood and Plock (1956, 1967); Plock (1957) | RD,SK | n | | | | | | | (12) | \equiv | [40,41,42] |
| Lodge (1961, 1964) | L^\dagger | ℓ | | | N_1 | N_1 | | | | $=$ | [31,32] |
| Spriggs (1966) | NGJ | ℓ | | | N_1 | N_1 | | | | $=$ | [43] |
| Spriggs (1966) | CJ | ℓ | | | N_1 N_2 | N_1 N_2 | | | | $=$ | [43] |
| Williams and Bird (1962) | O_s | ℓ | | | | N_1 | | | | $=$ | [44] |
| Williams and Bird (1964) | O_s | ℓ | | | N_1 | N_1 | | | | $=$ | [45] |
| Spriggs (1965) | O_s^\dagger | ℓ | | | N_1 N_2 | N_1 N_2 | | | | $=$ | [46] |
| Akers and Williams (1969) | RZ | | | | N_1 | N_1 | | | | $=$ | [47] |
| Paul (1969); Paul (1970); Bharadwaj (2012) | RD,SK | n | X | | | | | | (12) | \equiv | [48,49,50] (40,42) |
| Paul and Mazo (1969), Paul (1970) | RR | n | X | | | | | | (12) | \equiv | [51,49] |
| MacDonald, Marsh and Ashare (1969) | BC, OWFS [†] | n | | | | | | | | \equiv | [52] |
| Bird, Warner and Evans (1971) | RD | n | | | N_1 N_2 | N_1 N_2 | | | (12) | \equiv | [53] |
| Abdel-Khalik <i>et al.</i> (1974); Bird <i>et al.</i> (1974) | GE+SK | n | | | N_1 N_2 | N_1 N_2 | | | | \equiv | [54,55] |
| Bird <i>et al.</i> (1977) | BHS | ℓ | 0 | 0 | | | | | | $=$ | Table 11.4-2 [56] |
| Mou and Mazo (1977) | RR | | | | N_1 N_2 | N_1 N_2 | | | | \equiv | [57](51) |

| | | | | | | | | | | | |
|--|-------------------------|--------|---|---|----------------|----------------|----------------|---|------|---------|------------|
| Pearson and Rochefort (1982); Helfand and Rochefort (1982) | R [†] | n | X | | | | | | (11) | \cong | [9,10] |
| Fan and Bird (1984) | CB [†] | n | X | | | | | | (12) | \cong | [12](10) |
| Phan-Thien <i>et al.</i> (2000) | Dough | ℓ | | | | | | | | = | [58] |
| Yu <i>et al.</i> (2002); Zhou (2004) | SE | n | X | | N_1 | N_1 | N_1 | | | \cong | [59,60] |
| Cho <i>et al.</i> (2010) | K-BKZ | | | | | | | | (11) | | [61] |
| Hoyle (2010) | PP | n | | | | | | | (11) | \cong | [62] |
| Wagner <i>et al.</i> (2011) | R | n | X | | | | | | (11) | \cong | [63] |
| Gurnon and Wagner (2012) | G | ℓ | X | | N_1 N_2 | N_1 N_2 | | | (11) | \cong | [64] |
| Giacomin <i>et al.</i> (2011) | CM [†] , CJ | n | X | X | N_1 N_2 | N_1 N_2 | N_1 N_2 | X | (12) | \cong | [5](65) |
| Giacomin and Bird (2011) | ANSR | n | X | X | N_1 N_2 | N_1 N_2 | N_1 N_2 | X | (12) | \cong | [34] |
| Bird <i>et al.</i> (2014) | RD | n | X | | | | | | (12) | \cong | [66] |
| Schmalzer <i>et al.</i> (2014) | RD | | | | N_1 N_2 | N_1 N_2 | N_1 N_2 | | (12) | \cong | [67,68,69] |
| This paper | CM | n | X | X | N_1 N_2 | N_1 N_2 | N_1 N_2 | X | | = | |

Legend: ANSR \equiv corotational ANSR; BC \equiv Bird-Carreau; BHS \equiv Bead-Hookean spring; CB \equiv Curtiss-Bird; CJ \equiv corotational Jeffreys; CM \equiv corotational Maxwell; SE \equiv simple emulsion; GE \equiv Goddard integral expansion; L \equiv Lodge rubberlike; NGJ \equiv nonlinear Generalized Jeffreys; O₃ \equiv 3-constant Oldroyd; OWFS \equiv modified Oldroyd-Walters-Fredrickson-Spriggs; PP \equiv pompom; R \equiv reptation; RD \equiv rigid dumbbell; RR \equiv planar rigid ring; RZ \equiv Rouse-Zimm; SK \equiv shish-kebab; N_1, N_2 \equiv first and second normal stress differences; $n \equiv \eta^*(\omega, \gamma_0)$; $\ell \equiv \eta^*(\omega)$; † \equiv multiple relaxation times; = \equiv exact; \cong \equiv approximate.

Table II: Dimensional Variables

| | | |
|---|------------|------------------------------------|
| Angular frequency | t^{-1} | ω |
| Cartesian coordinate | | x, y, z |
| Dynamic viscosity | $FL^{-2}t$ | η |
| Dynamic viscosity, j th spectrum | $FL^{-2}t$ | $\eta_{0,j}$ |
| Extra stress tensor* | FL^{-2} | $\boldsymbol{\tau}$ |
| Extra stress, ij th component | FL^{-2} | τ_{ij} |
| First normal stress difference | FL^{-2} | $N_1 \equiv \tau_{11} - \tau_{22}$ |
| Relaxation time | t | λ |
| Relaxation time, j th spectrum | t | λ_j |
| Second normal stress difference | FL^{-2} | $N_2 \equiv \tau_{22} - \tau_{33}$ |
| Shear stress, j th spectrum | FL^{-2} | τ_j |
| Shear stress, alternant part, j th spectrum | FL^{-2} | $\tau_{j,al}$ |
| Shear stress, transient part, j th spectrum | FL^{-2} | $\tau_{j,tr}$ |
| Storage and loss moduli, m th component | FL^{-2} | η'_{mn}, η''_{mn} |
| Strain rate tensor | t^{-1} | $\dot{\boldsymbol{\gamma}}$ |
| Strain rate, ij th component | t^{-1} | $\dot{\gamma}_{ij}$ |
| Strain rate, ij th component | t^{-1} | $\dot{\gamma}_{ij}$ |
| Strain rate, amplitude | t^{-1} | $\dot{\gamma}^0$ |
| Strain rate, amplitude | t^{-1} | $\dot{\gamma}^0$ |
| Time | t | t |
| Velocity vector | t^{-1} | \mathbf{v} |
| Velocity, i th-components | Lt^{-1} | v_i |
| Vorticity tensor | t^{-1} | $\boldsymbol{\omega}$ |
| Zero shear rate viscosity | $FL^{-2}t$ | η_0 |

Legend: F force; L length; t time; T temperature

* Where τ_{ij} is the force exerted in the j th direction on a unit area of fluid surface of constant x_i by fluid in the region lesser x_i on fluid in the region greater x_i [70].

Table III: Dimensionless Variables and Groups

| | |
|--|---|
| Bessel function of first kind, m th order | $J_m(z) \equiv \sum_{k=0}^{\infty} \frac{(-1)^k}{(m+k)!k!} \left(\frac{z}{2}\right)^{m+2k}$ |
| Bessel function of first kind, m th order with argument Wi/De | $J_m \equiv J_m(Wi/De)$ |
| Coefficient, Eq. (123) | A_k |
| Coefficient, Eq. (126) | B_k |
| Coefficient, Eq. (133) | $\alpha_k^{(1)}$ |
| Coefficient, Eq. (140) | $\alpha_k^{(2)}$ |
| Coefficient, Eq. (134) | $\beta_k^{(1)}$ |
| Coefficient, Eq. (141) | $\beta_k^{(2)}$ |
| Coefficient, first derivative, Eq. (93) | p |
| Coefficient, second derivative, Eq. (94) | q |
| Cosine coefficient of first normal stress difference, fourth part, n th component, Eq. (181) | $\phi_{N_1,n}^{(4)}$ |
| Cosine coefficient of first normal stress difference, third part, n th component, Eq. (164) | $\phi_{N_1,n}^{(3)}$ |
| Cosine coefficient of shear stress, fourth part, n th component, Eq. (219) | $\phi_{S,n}^{(4)}$ |
| Cosine coefficient of shear stress, third part, n th component, Eq. (203) | $\phi_{S,n}^{(3)}$ |
| Data set correspond to pole c | E_c, E_{∞} |
| Deborah number | $De \equiv \lambda\omega$ |
| Elastic Fourier modulus | G'_n |
| First normal stress difference | $N_1 \equiv N_1/\eta_0\dot{\gamma}^0$ |
| First normal stress difference, n th harmonic | $N_{1,n}$ |
| First normal stress difference, alternant part | $N_{1,al}$ |
| First normal stress difference, Fourier form, first component | $N_1^{(1)}$ |
| First normal stress difference, Fourier form, fourth component | $N_1^{(4)}$ |
| First normal stress difference, Fourier form, second component | $N_1^{(2)}$ |

| | |
|--|--|
| First normal stress difference, Fourier form, third component | $\mathbb{N}_1^{(3)}$ |
| First normal stress difference, homogeneous part | $\mathbb{N}_{1,h}$ |
| First normal stress difference, particular part | $\mathbb{N}_{1,p}$ |
| First normal stress difference, transient part | $\mathbb{N}_{1,tr}$ |
| Function, Eq. (95) | z |
| Function, Eq. (106) | ϕ |
| Function, Eq. (109) | ω |
| Fundamental matrix | Φ |
| Generalized non-Newtonianness | $\mathbb{G}n$ |
| Inclination of the non-Newtonianness | ϕ |
| Integral, Eq. (43) | I_1 |
| Integral, Eq. (44) | I_2 |
| Integrating constant | C_n |
| Kovacic polynomial, Eq. (105) | P |
| Pole, Kovacic rational function, Eq. (102) | c |
| Rational function, Eq. (101) | r |
| Second normal stress difference | $\mathbb{N}_2 \equiv N_2/\eta_0\dot{\gamma}^0$ |
| Shear stress | $\mathbb{S} \equiv \tau_{21}/\eta_0\dot{\gamma}^0$ |
| Shear stress, alternant part | \mathbb{S}_{al} |
| Shear stress, Fourier form, first component | $\mathbb{S}^{(1)}$ |
| Shear stress, Fourier form, first component | $\mathbb{S}^{(2)}$ |
| Shear stress, Fourier form, first component | $\mathbb{S}^{(3)}$ |
| Shear stress, Fourier form, first component | $\mathbb{S}^{(4)}$ |
| Shear stress, homogeneous part | \mathbb{S}_h |
| Shear stress, particular part | \mathbb{S}_p |
| Shear stress, transient part | \mathbb{S}_{tr} |
| Sine coefficient of first normal stress difference, fourth part, n th component, Eq. (186) | $\psi_{\mathbb{N}_1,n}^{(4)}$ |
| Sine coefficient of first normal stress difference, third part, n th component, Eq. (171) | $\psi_{\mathbb{N}_1,n}^{(3)}$ |
| Sine coefficient of shear stress, | $\psi_{\mathbb{S},n}^{(4)}$ |

| | |
|---|------------------------------------|
| fourth part, n th component, Eq. (224) | |
| Sine coefficient of shear stress, third part, n th component, Eq. (209) | $\psi_{s,n}^{(3)}$ |
| Strain amplitude | γ_0 |
| Time | $\tau \equiv \omega t$ |
| Transformed time | \mathcal{T} |
| Viscous Fourier modulus | G_n'' |
| Weissenberg number | $Wi \equiv \lambda \dot{\gamma}^0$ |

Table IV: Intermediate Results for Kovacic Method (Case 2)

| | E_0 | E_{-1} | E_1 | E_∞ | d |
|----|---------------|----------|-------|------------|--------------------------|
| 1 | 2 | 2 | 2 | 0 | -3 |
| 2 | 2 | 2 | 1 | 0 | $-\frac{5}{2}$ |
| 3 | 2 | 2 | -1 | 0 | $-\frac{3}{2}$ |
| 4 | 2 | 1 | 2 | 0 | $-\frac{5}{2}$ |
| 5 | 2 | 1 | 1 | 0 | -2 |
| 6 | 2 | 1 | -1 | 0 | -1 |
| 7 | 2 | -1 | 2 | 0 | $-\frac{3}{2}$ |
| 8 | 2 | -1 | 1 | 0 | -1 |
| 9 | 2 | -1 | -1 | 0 | 0 |
| 10 | $2\sqrt{2}i$ | 2 | 2 | 0 | $-2-\sqrt{2}i$ |
| 11 | $2\sqrt{2}i$ | 2 | 1 | 0 | $-\frac{3}{2}-\sqrt{2}i$ |
| 12 | $2\sqrt{2}i$ | 2 | -1 | 0 | $-\frac{1}{2}-\sqrt{2}i$ |
| 13 | $2\sqrt{2}i$ | 1 | 2 | 0 | $-\frac{3}{2}-\sqrt{2}i$ |
| 14 | $2\sqrt{2}i$ | 1 | 1 | 0 | $-1-\sqrt{2}i$ |
| 15 | $2\sqrt{2}i$ | 1 | -1 | 0 | $-\sqrt{2}i$ |
| 16 | $2\sqrt{2}i$ | -1 | 2 | 0 | $-\frac{1}{2}-\sqrt{2}i$ |
| 17 | $2\sqrt{2}i$ | -1 | 1 | 0 | $-\sqrt{2}i$ |
| 18 | $2\sqrt{2}i$ | -1 | -1 | 0 | $1-1\sqrt{2}i$ |
| 19 | $-2\sqrt{2}i$ | 2 | 2 | 0 | $-2+\sqrt{2}i$ |
| 20 | $-2\sqrt{2}i$ | 2 | 1 | 0 | $-\frac{3}{2}+\sqrt{2}i$ |
| 21 | $-2\sqrt{2}i$ | 2 | -1 | 0 | $-\frac{1}{2}+\sqrt{2}i$ |
| 22 | $-2\sqrt{2}i$ | 1 | 2 | 0 | $-\frac{3}{2}+\sqrt{2}i$ |
| 23 | $-2\sqrt{2}i$ | 1 | 1 | 0 | $-1+\sqrt{2}i$ |
| 24 | $-2\sqrt{2}i$ | 1 | -1 | 0 | $\sqrt{2}i$ |
| 25 | $-2\sqrt{2}i$ | -1 | 2 | 0 | $-\frac{1}{2}+\sqrt{2}i$ |
| 26 | $-2\sqrt{2}i$ | -1 | 1 | 0 | $\sqrt{2}i$ |
| 27 | $-2\sqrt{2}i$ | -1 | -1 | 0 | $1+\sqrt{2}i$ |

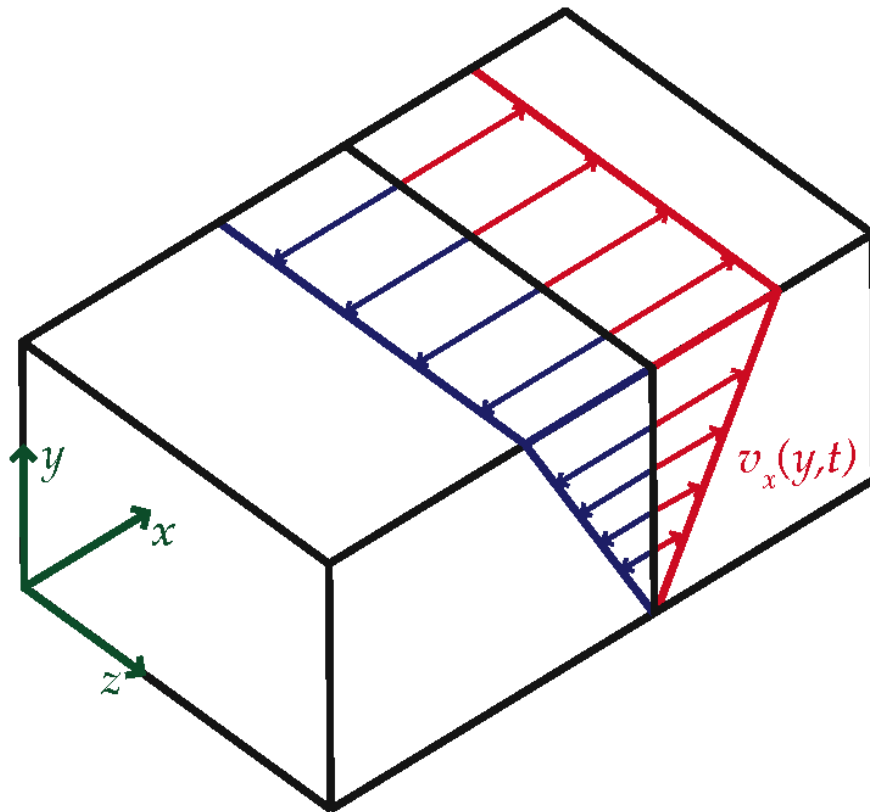


Figure 1: Orthomorphic isometric sketch of alternating velocity profile in oscillatory shear flow [Eq. (1)]. Cartesian coordinates with origin on the stationary plate. The linear velocity profile results from the assumption that inertial effects can be neglected.

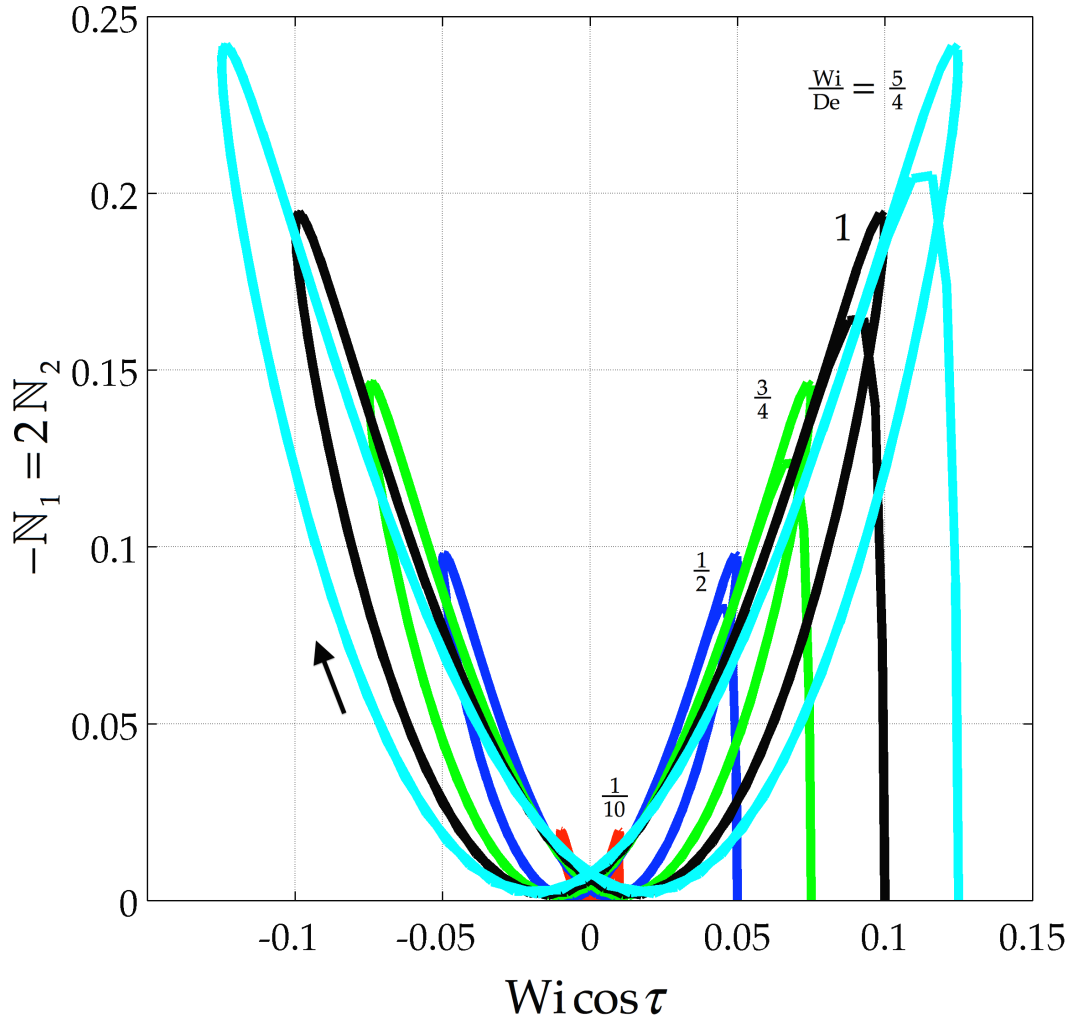


Figure 2. Exact solution [Eq. (54) with Eqs. (55) and (56)] using 40 even harmonics, 0 through 78, and 40 odd ones, 1 through 79, for startup (first two cycles). Minus dimensionless first normal stress differences, $-\mathbb{N}_1 = 2\mathbb{N}_2$, versus dimensionless shear rate, $\lambda\dot{\gamma}$, calculated for the 2-constant corotational Maxwell model, for a Deborah number of $\lambda\omega = \frac{1}{10}$.

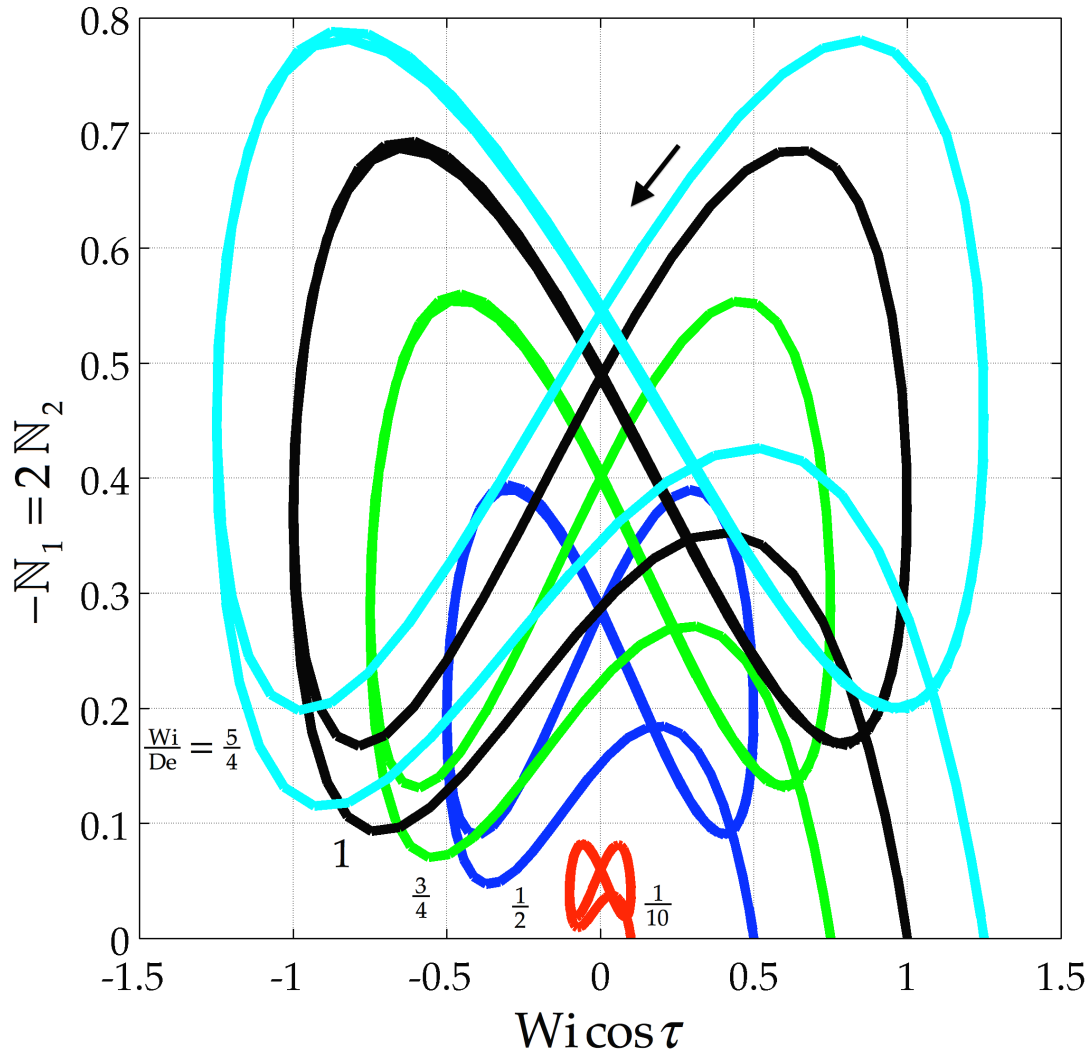


Figure 3. Exact solution [Eq. (54) with Eqs. (55) and (56)] using 40 even harmonics, 0 through 78, and 40 odd ones, 1 through 79, for startup (first two cycles). Minus dimensionless first normal stress differences, $-N_1 = 2N_2$, versus dimensionless shear rate, $\lambda\dot{\gamma}$, calculated for the 2-constant corotational Maxwell model, for a Deborah number of $\lambda\omega = 1$.

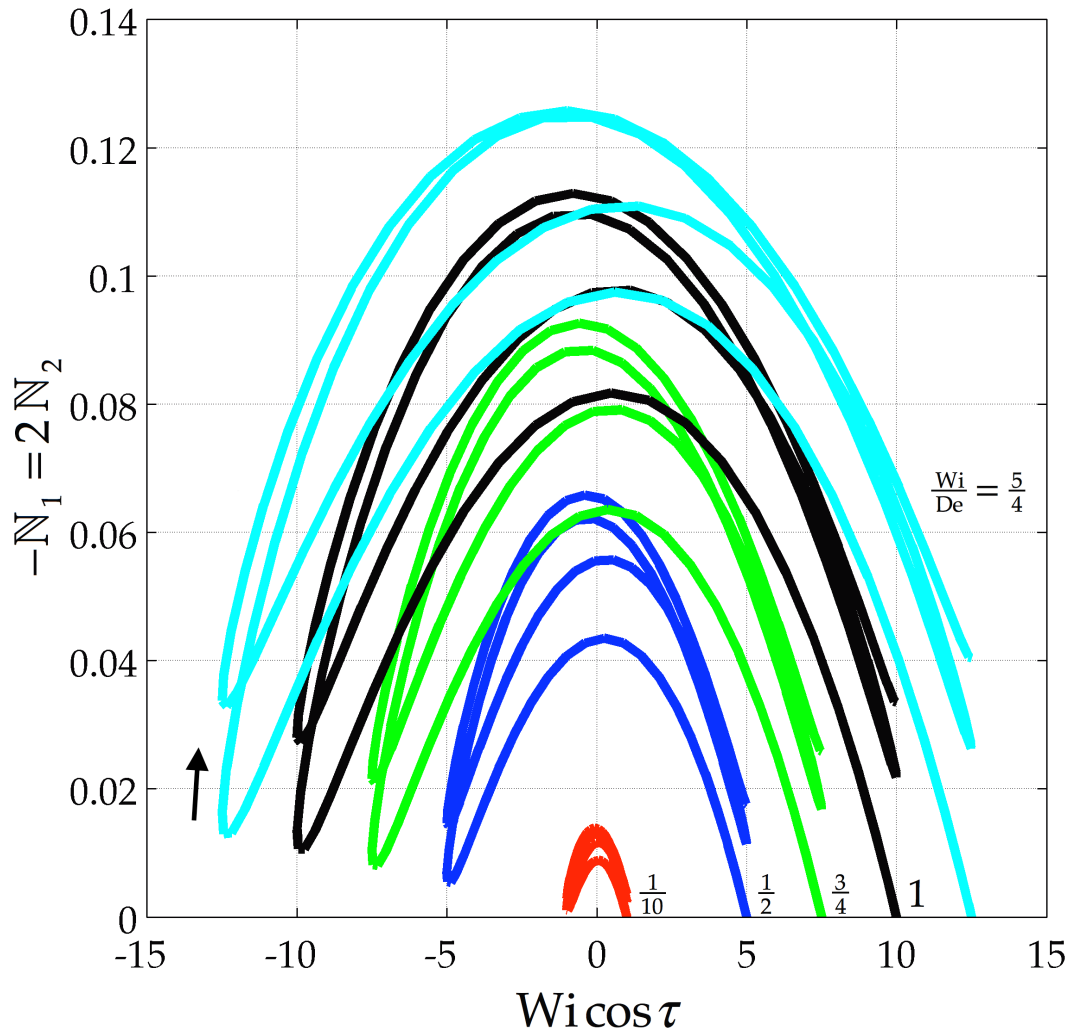


Figure 4. Exact solution [Eq. (54) with Eqs. (55) and (56)] using 40 even harmonics, 0 through 78, and 40 odd ones, 1 through 79, for startup (first two cycles). Minus dimensionless first normal stress differences, $-\mathbb{N}_1 = 2\mathbb{N}_2$, versus dimensionless shear rate, $\lambda\dot{\gamma}$, calculated for the 2-constant corotational Maxwell model, for a Deborah number of $\lambda\omega = 10$.

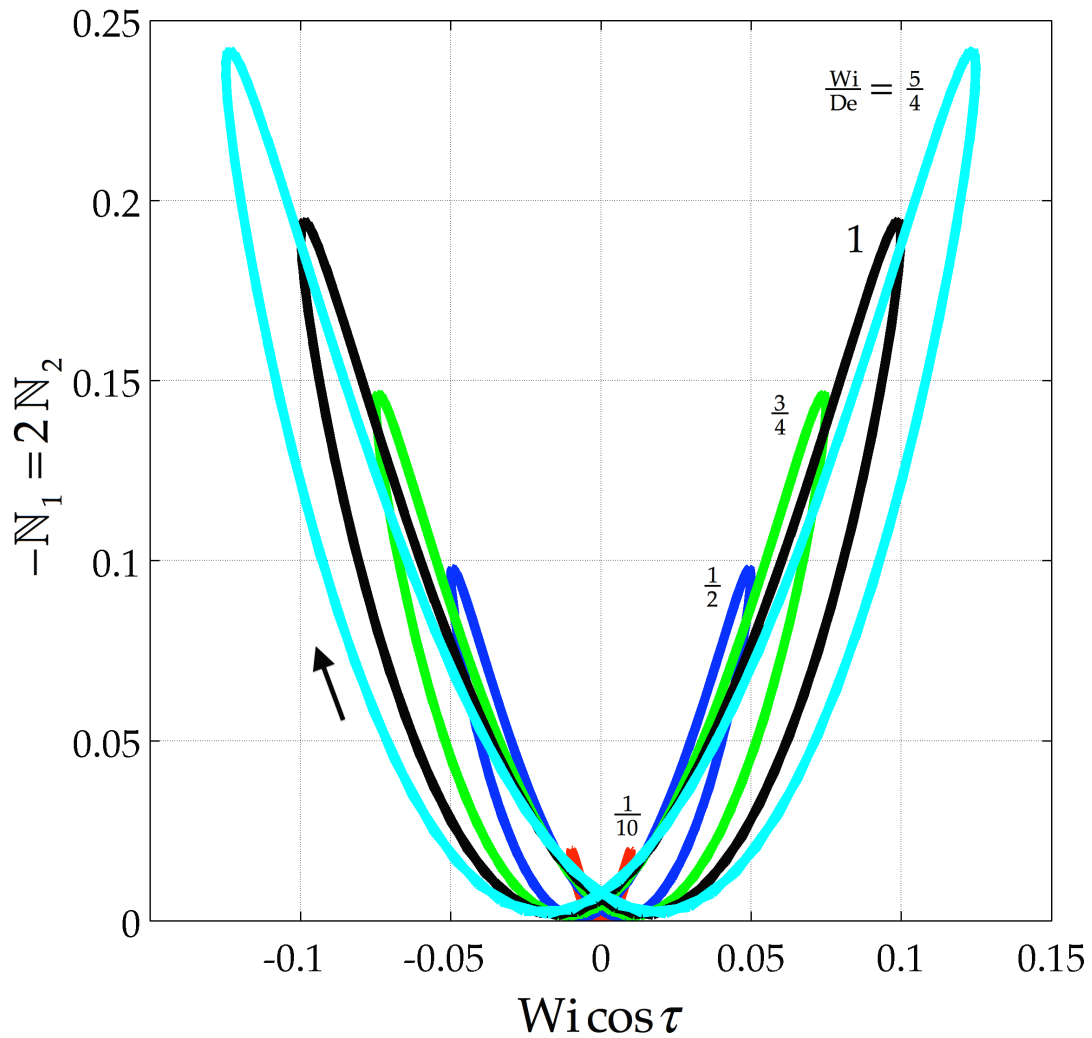


Figure 5. Exact solution [Eq. (56)] using 40 even harmonics, 0 through 78, for alternance. Minus dimensionless first normal stress differences, $-\mathbb{N}_1 = 2\mathbb{N}_2$, *versus* dimensionless shear rate, $\lambda\dot{\gamma}$, left-clockwise loops calculated for the 2-constant corotational Maxwell model, for a Deborah number of $\lambda\omega = \frac{1}{10}$.

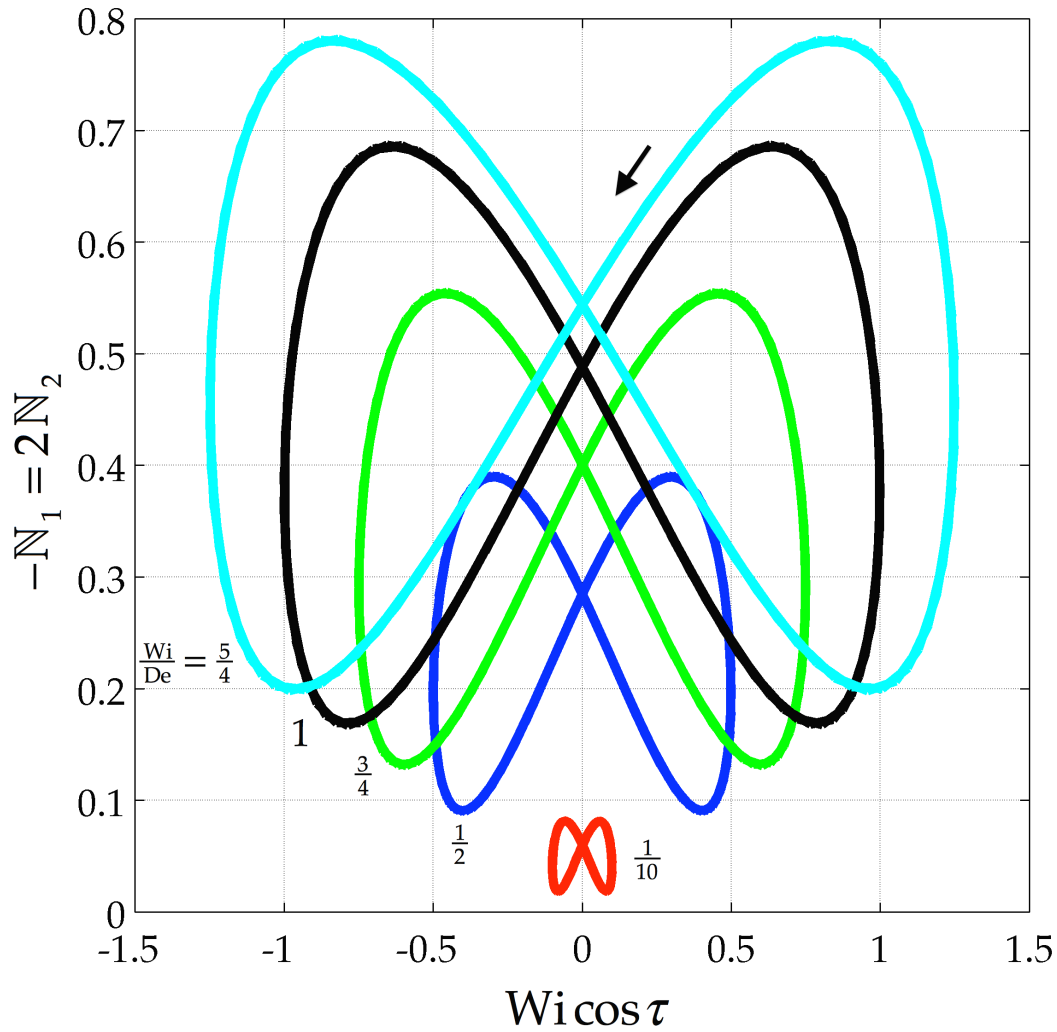


Figure 6. Exact solution [Eq. (56)] using 40 even harmonics, 0 through 78, for alternance. Minus dimensionless first normal stress differences, $-N_1 = 2N_2$, versus dimensionless shear rate, $\lambda\dot{\gamma}$, left-clockwise loops calculated for the 2-constant corotational Maxwell model, for a Deborah number of $\lambda\omega = 1$.

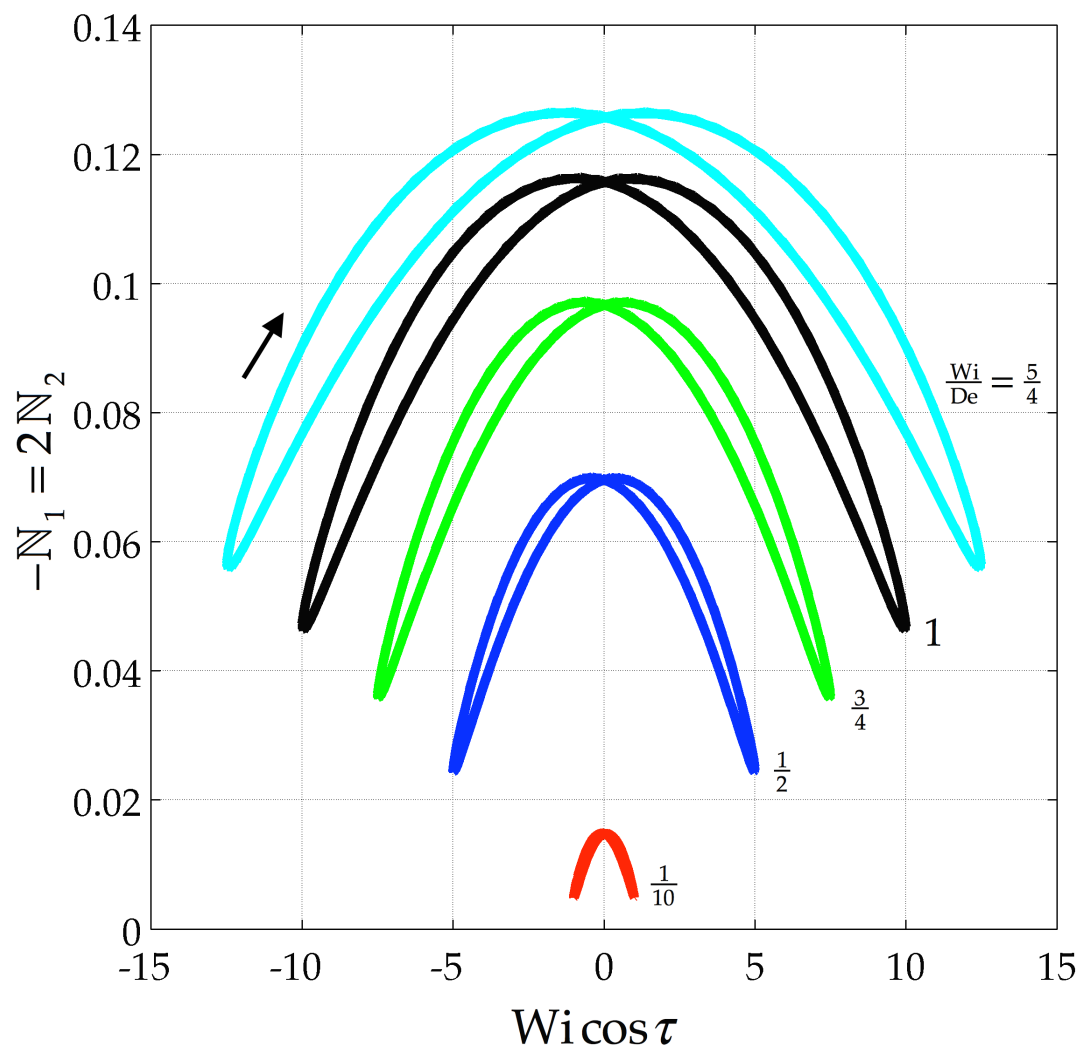


Figure 7. Exact solution [Eq. (56)] using 40 even harmonics, 0 through 78, for alternance. Minus dimensionless first normal stress differences, $-N_1 = 2N_2$, versus dimensionless shear rate, $\lambda\dot{\gamma}$, left-clockwise loops calculated for the 2-constant corotational Maxwell model, for a Deborah number of $\lambda\omega = 10$.

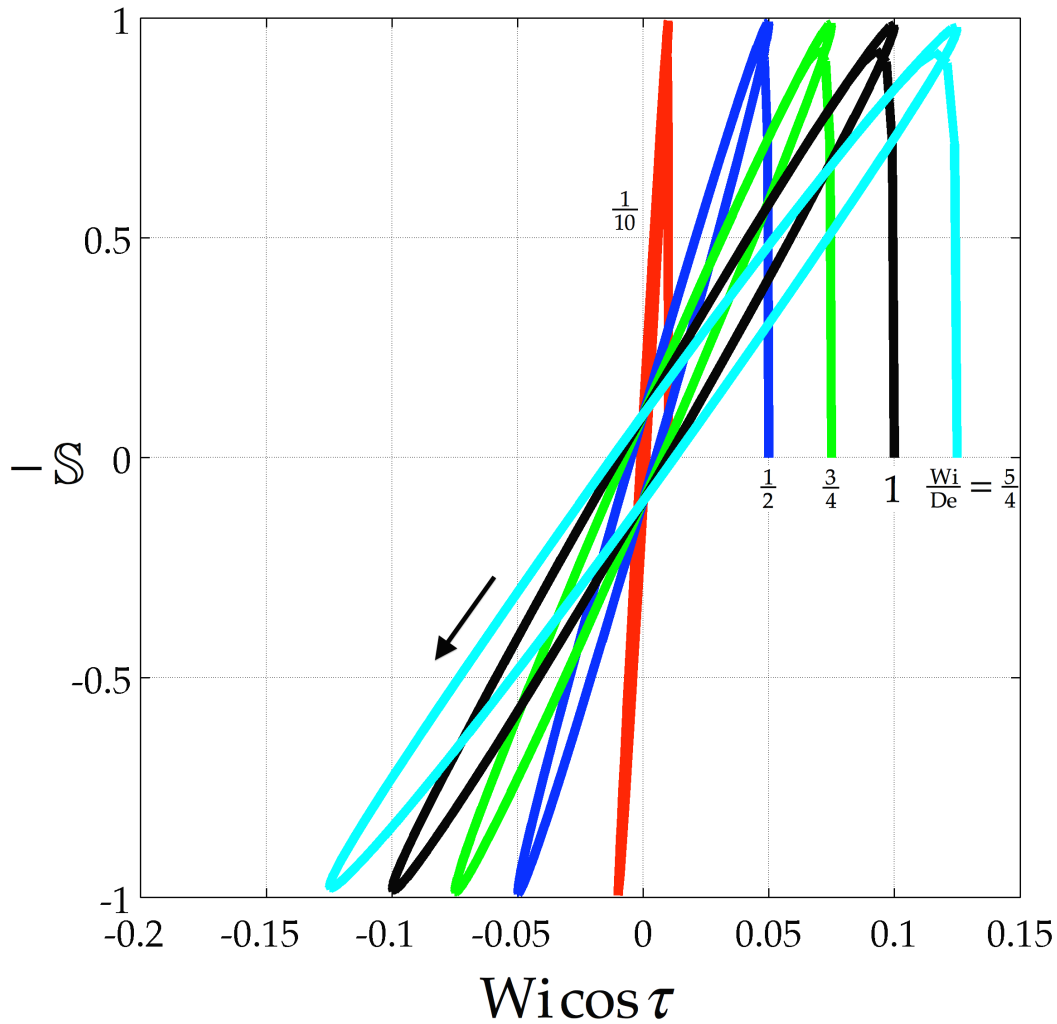


Figure 8. Exact solution [Eq. (64) with Eqs. (65) and (66)] using 40 even harmonics, 0 through 78, and 40 odd ones, 1 through 79, for startup (first two cycles). Minus dimensionless shear stress, $-S$, versus dimensionless shear rate, $\lambda\dot{\gamma}$, calculated for the 2-constant corotational Maxwell model with a Deborah number of $\lambda\omega = \frac{1}{10}$.

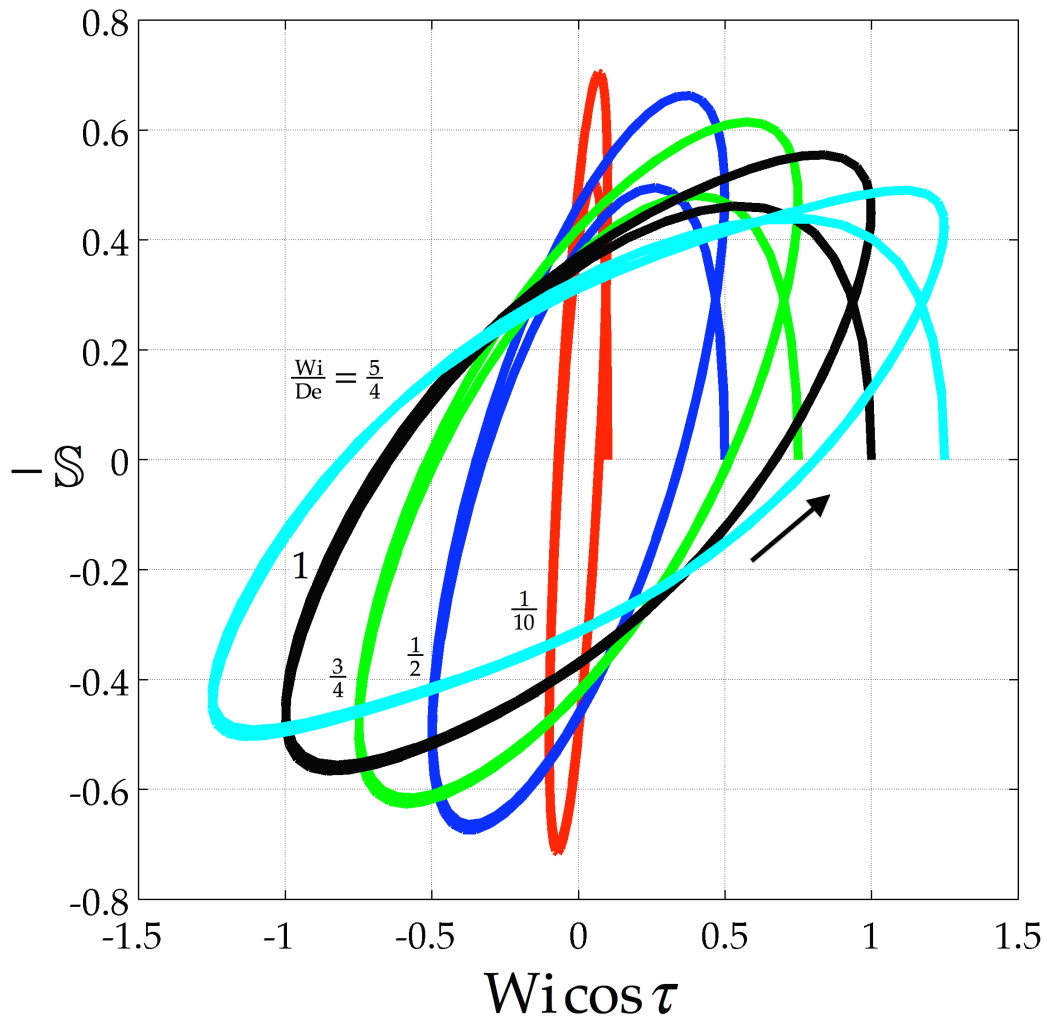


Figure 9. Exact solution [Eq. (64) with Eqs. (65) and (66)] using 40 even harmonics, 0 through 78, and 40 odd ones, 1 through 79, for startup (first two cycles). Minus dimensionless shear stress, $-S$, versus dimensionless shear rate, $\lambda\dot{\gamma}$, calculated for the 2-constant corotational Maxwell model with a Deborah number of $\lambda\omega = 1$.

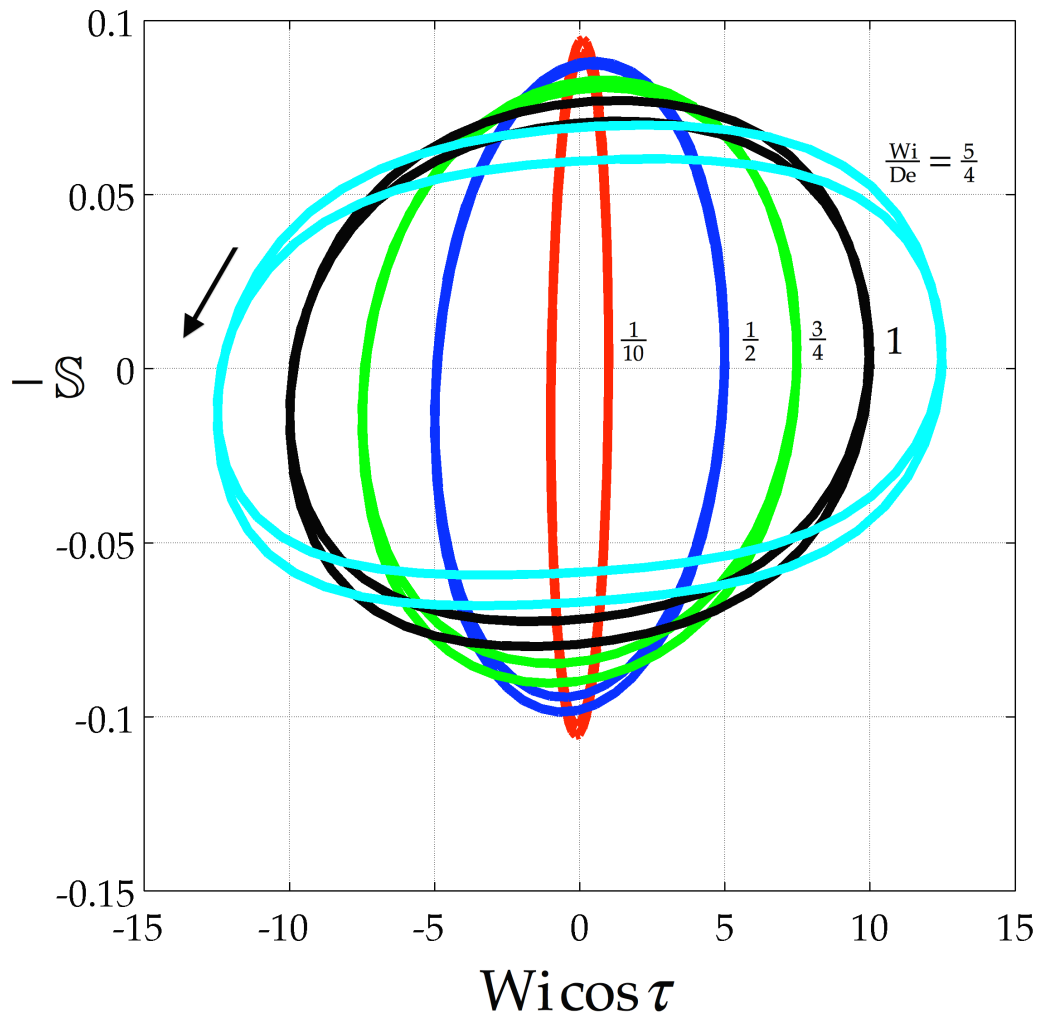


Figure 10. Exact solution [Eq. (64) with Eqs. (65) and (66)] using 40 even harmonics, 0 through 78, and 40 odd ones, 1 through 79, for startup (first two cycles). Minus dimensionless shear stress, $-S$, versus dimensionless shear rate, $\lambda\dot{\gamma}$, calculated for the 2-constant corotational Maxwell model with a Deborah number of $\lambda\omega = 10$.

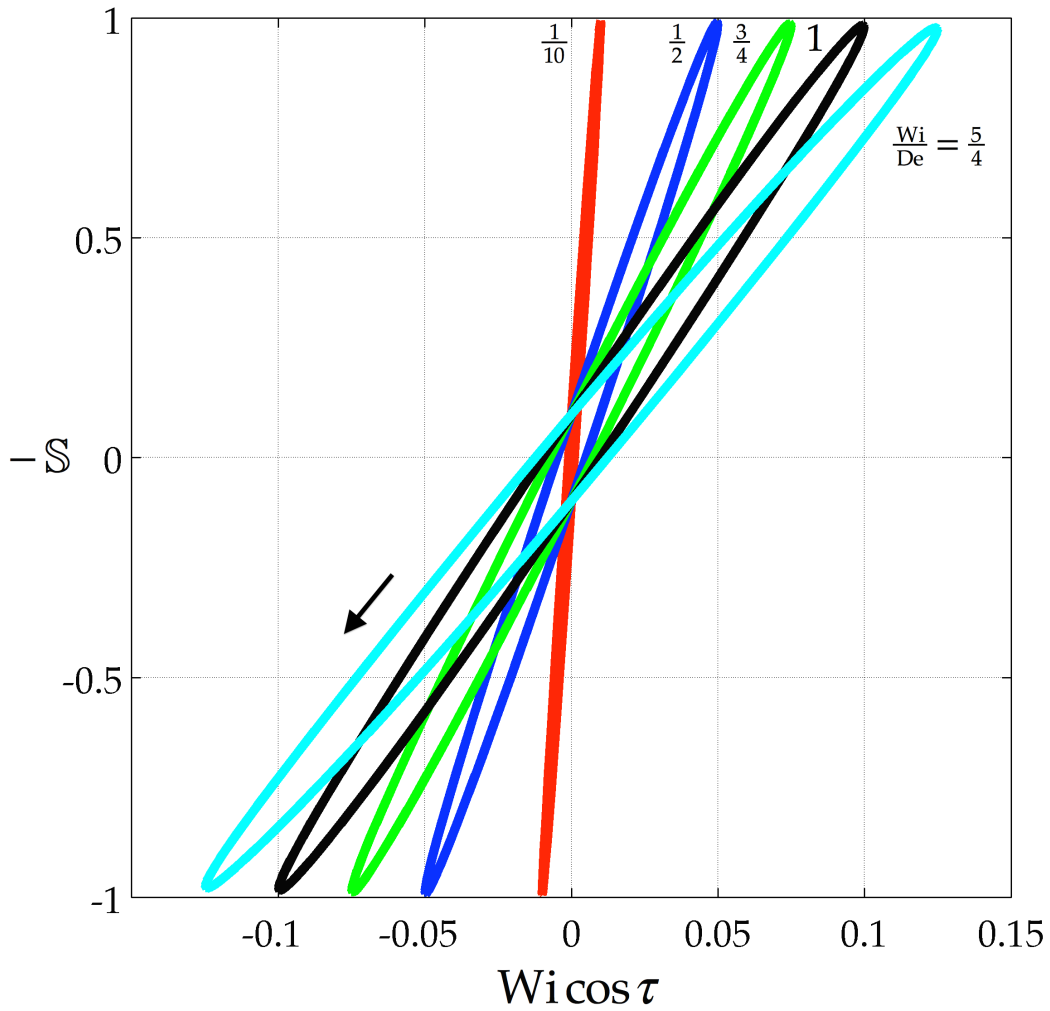


Figure 11. Exact solution [Eq. (66)] using 40 odd harmonics, 1 through 79, for alternance. Counterclockwise loops of minus dimensionless shear stress, $-\mathcal{S}$, *versus* dimensionless shear rate, $\lambda\dot{\gamma}$, calculated for the 2-constant corotational Maxwell model with a Deborah number of $\lambda\omega = \frac{1}{10}$.

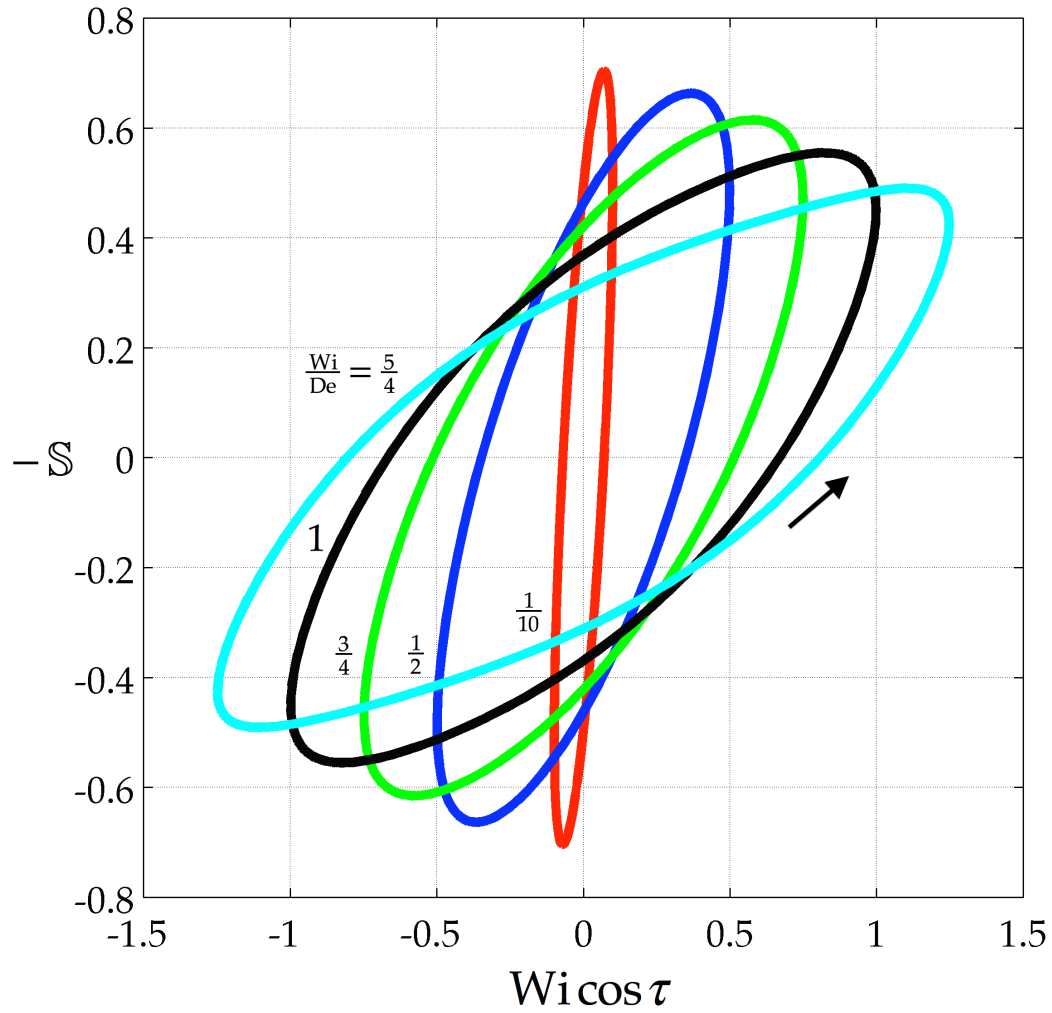


Figure 12. Exact solution [Eq. (66)] using 40 odd harmonics, 1 through 79, for alternance. Counterclockwise loops of minus dimensionless shear stress, $-S$, *versus* dimensionless shear rate, $\lambda\dot{\gamma}$, calculated for the 2-constant corotational Maxwell model with a Deborah number of $\lambda\omega = 1$.

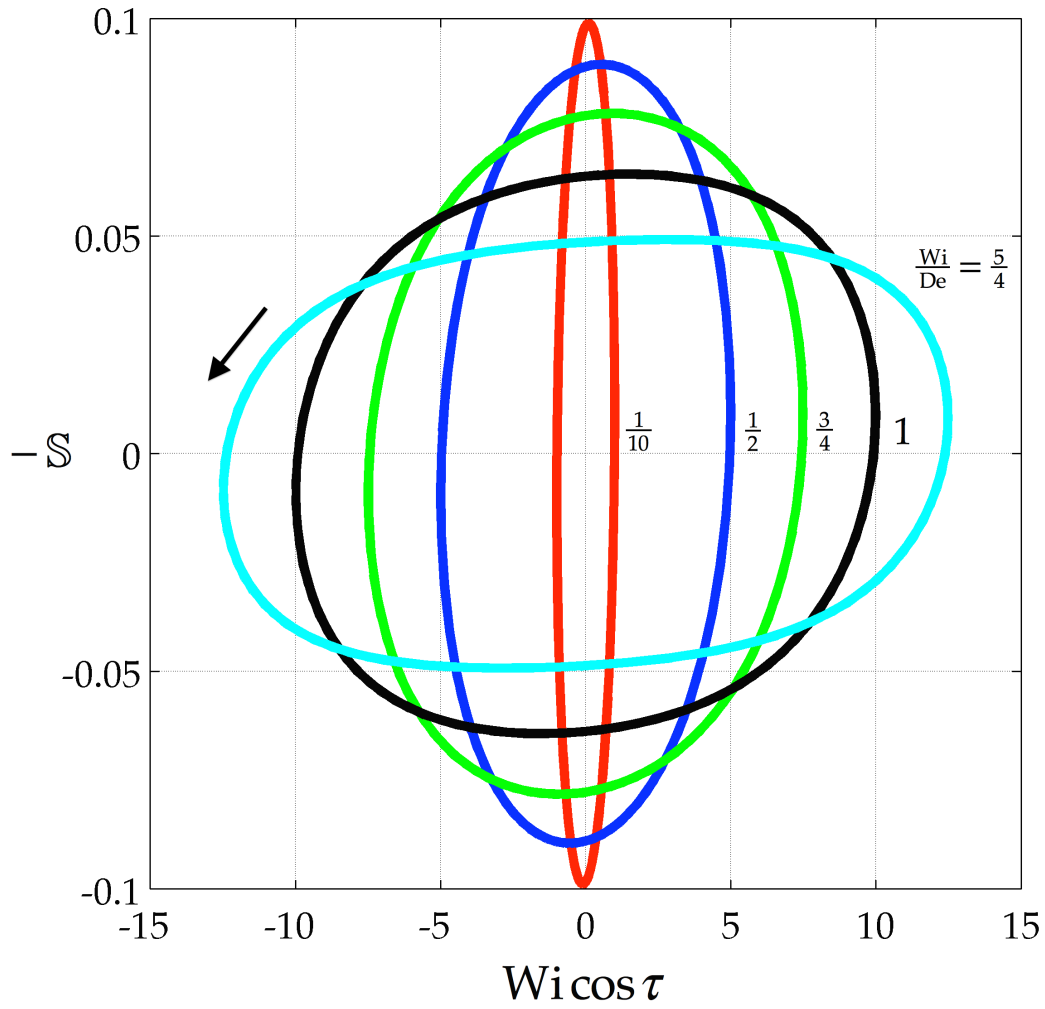


Figure 13. Exact solution [Eq. (66)] using 40 odd harmonics, 1 through 79, for alternance. Counterclockwise loops of minus dimensionless shear stress, $-\mathcal{S}$, *versus* dimensionless shear rate, $\lambda\dot{\gamma}$, calculated for the 2-constant corotational Maxwell model with a Deborah number of $\lambda\omega = 10$.

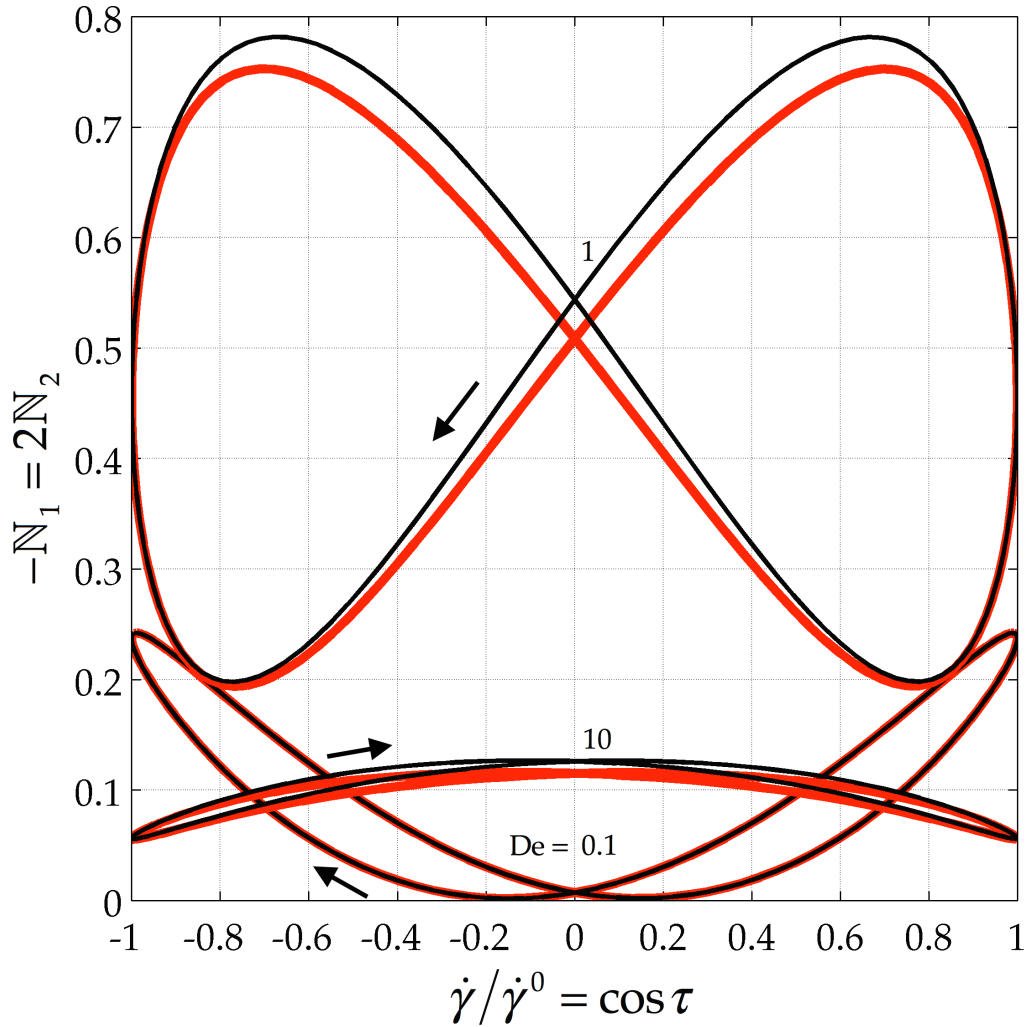


Figure 14. Comparison of exact solution (**black**) [Eq. (56) with 40 harmonics, 0 through 78] with approximate solution (**red**) [Eq. (20)] for loops of minus dimensionless first normal stress differences, $-N_1 = 2N_2$, versus normalized shear rate, $\dot{\gamma}/\dot{\gamma}^0 = \cos \tau$, left-clockwise loops calculated for the 2-constant corotational Maxwell model with a Deborah number of $\lambda\omega = 10$ for $Wi/De = 5/4$ and $\lambda\omega = \frac{1}{10}, 1, 10$. For the normal stress differences, the exact solution is an improvement over the approximate solution.

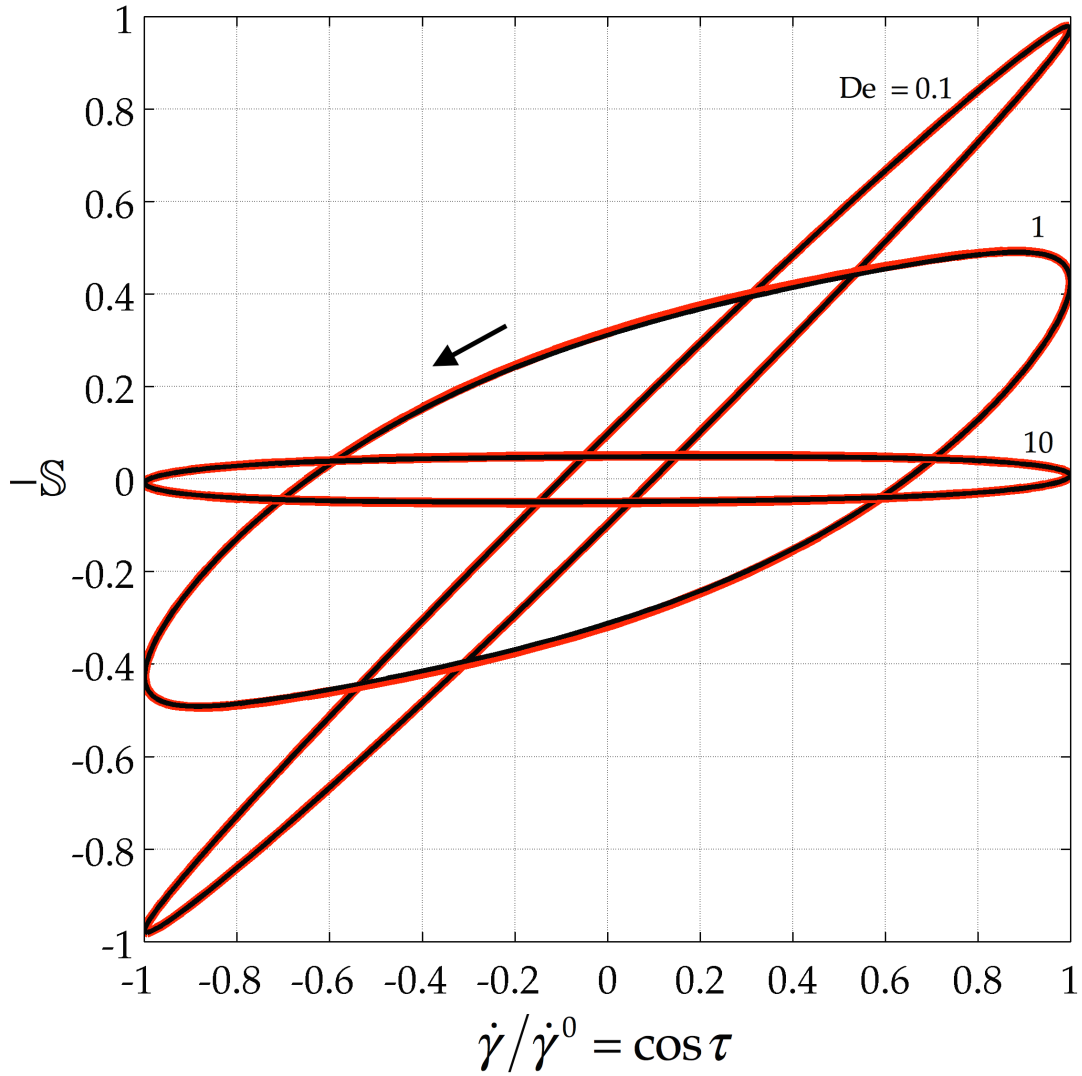


Figure 15. Comparison of exact solution (**black**) [Eq. (66) using 40 harmonics, 1 through 79] with approximate solution (**red**) [Eq. (21)] for counterclockwise loops of minus dimensionless shear stress, $-\mathcal{S}$, versus dimensionless shear rate, $\lambda\dot{\gamma}$, calculated for the 2-constant corotational Maxwell model with a Deborah number of $\lambda\omega = 10$ for $Wi/De = 5/4$ and $\lambda\omega = \frac{1}{10}, 1, 10$. For the shear stress, the exact and approximate solutions nearly match.

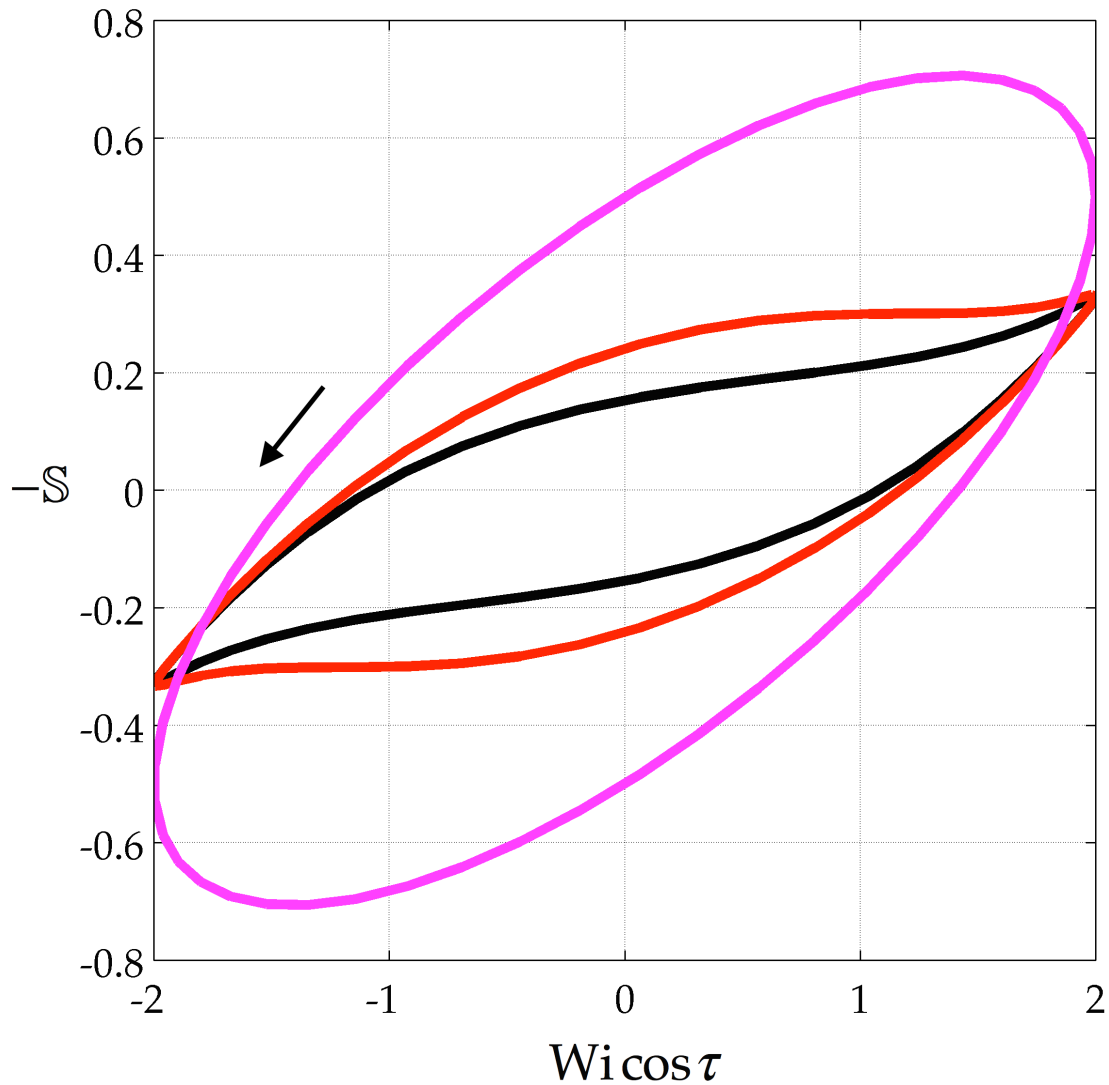


Figure 16. Comparison of exact solution (**black**) [Eq. (66) using 40 harmonics, 1 through 79] with approximate solution (**red**) [Eq. (21)] for counterclockwise loops of minus dimensionless shear stress, $-S$, versus dimensionless shear rate, $\lambda\dot{\gamma}$, calculated for the 2-constant corotational Maxwell model with a Deborah number of $\lambda\omega = 10$ for $Wi/De = 2$ and $\lambda\omega = 1$. **Pink** curve shows corresponding linear viscoelastic behavior [alternant part of Eq. (83)]. The exact solution is a significant improvement over the approximate one, and specifically, is much further from the corresponding linear response.

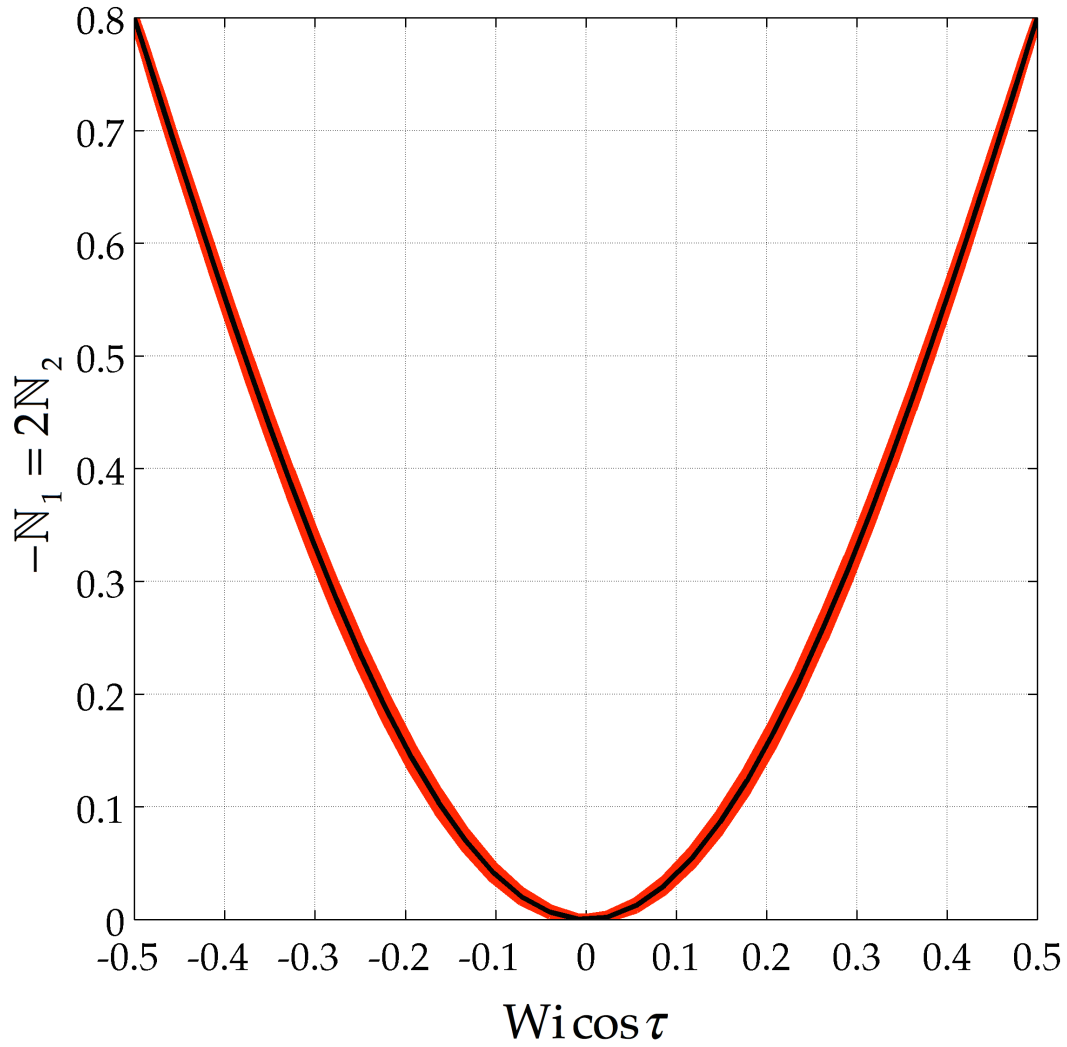


Figure 17. Exact solution (**black**) [Eq. (56) with 40 harmonics, 0 through 78] with approximate solution (**red**) [Eq. (20)], with $\lambda\omega = \frac{1}{10}$ and $\lambda\dot{\gamma}^0 = \frac{1}{2}$, compared with exact solution for steady shear flow (**red**) (Eq. (84) of [5]). Left-clockwise loops of minus dimensionless first normal stress differences, $-\mathbb{N}_1 = 2\mathbb{N}_2$, versus dimensionless shear rate, $\lambda\dot{\gamma}$, calculated for the 2-constant corotational Maxwell model. Curves nearly overlap, as they should.

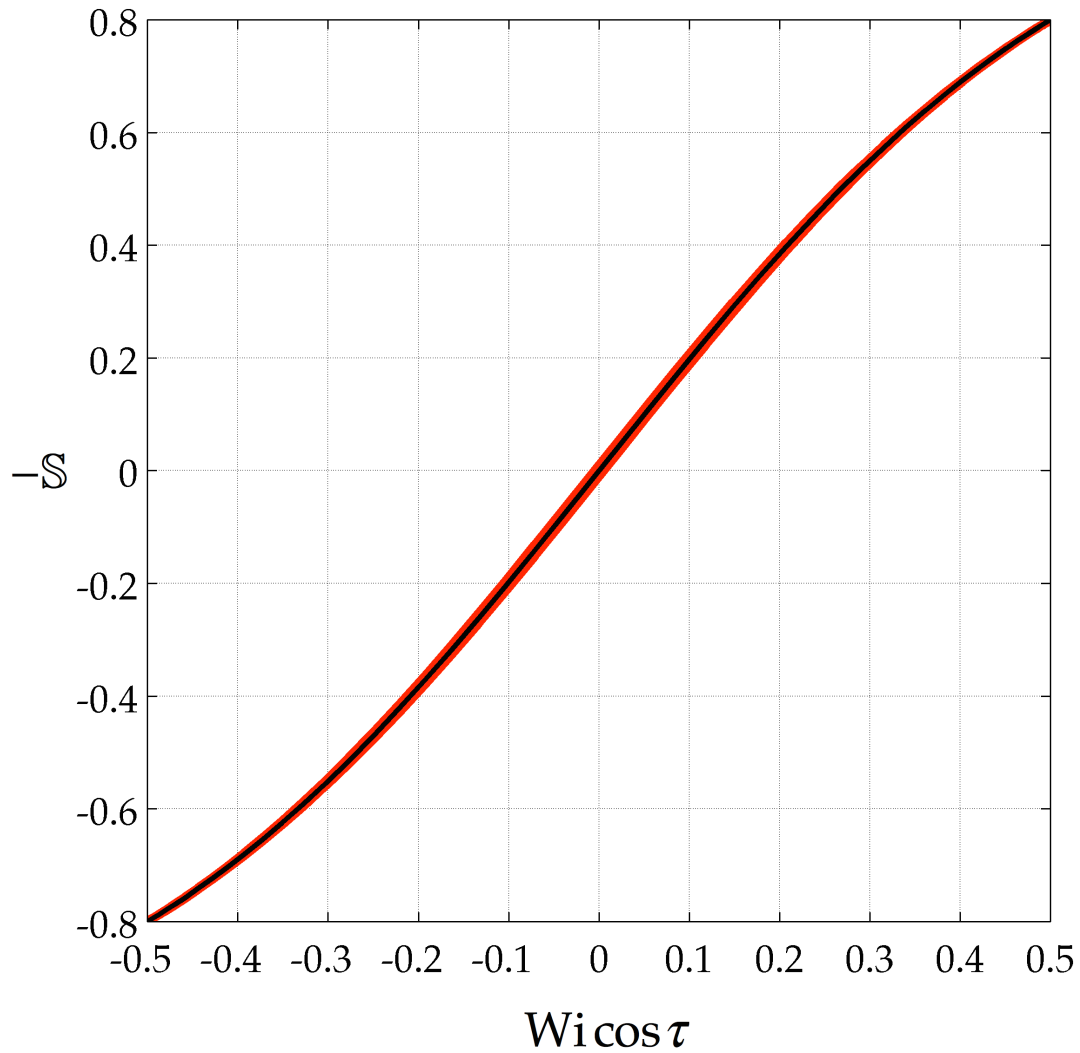


Figure 18. Comparison of exact solution (**black**) [Eq. (66) using 40 harmonics, 1 through 79] with approximate solution (**red**) [Eq. (21)] with $\lambda\omega = \frac{1}{10}$ and $\lambda\dot{\gamma}^0 = \frac{1}{2}$, with exact solution for steady shear flow (**red**) (Eq. (84) of [5]). Counterclockwise loops of minus dimensionless shear stress, $-\mathbb{S}$, versus dimensionless shear rate, $\lambda\dot{\gamma}$, calculated for the 2-constant corotational Maxwell model. Curves nearly overlap, as they should.

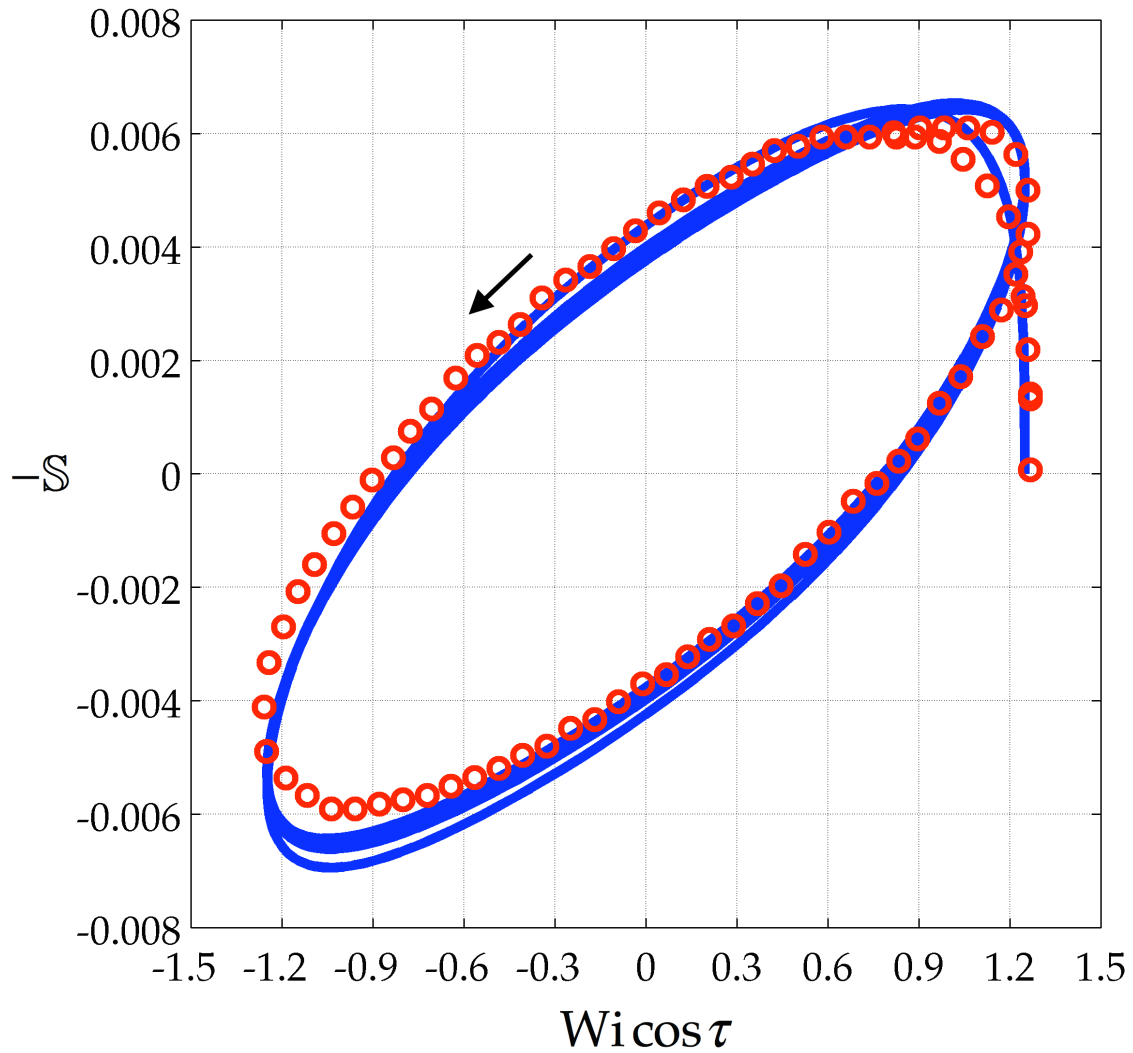


Figure 19. Exact solution (blue response is Eq. (71) using 40 even harmonics, 0 through 78, and 40 odd ones, 1 through 79, for startup and evaluated for multiple relaxation times, taken from Table 4 of [5]) for counterclockwise response of minus dimensionless shear stress, $-S$, versus dimensionless shear rate, $\lambda\dot{\gamma}$, calculated for the generalized corotational Maxwell model and compared with measured behavior of molten HDPE (red dots). $Wi = \bar{\lambda}\dot{\gamma}^0 = 1.25$ and $De = \bar{\lambda}\omega = 1.0$.

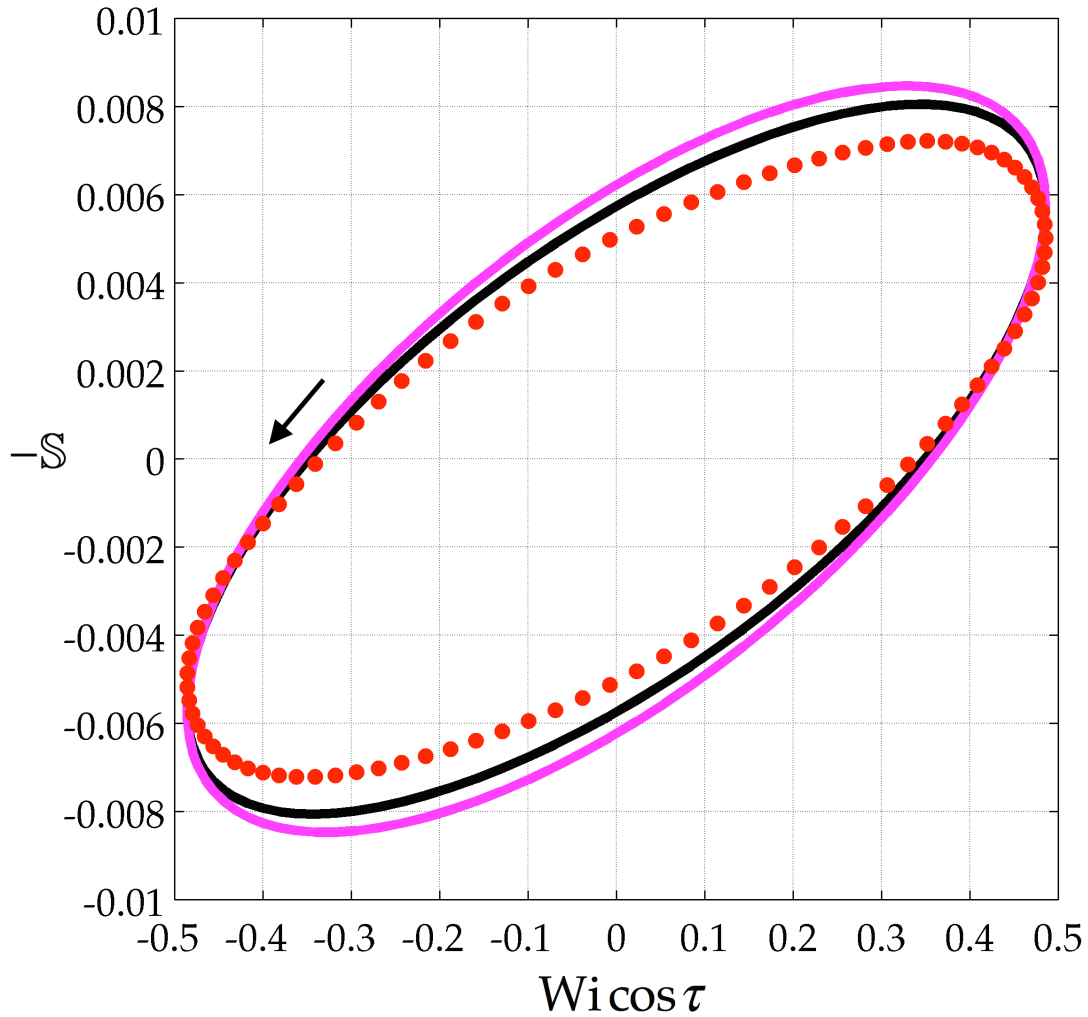


Figure 20. Exact solution (**black** loop is Eq. (73) with 40 harmonics, 1 through 79 and evaluated for multiple relaxation times, taken from Table 4 of [5]) for counterclockwise loops of minus dimensionless shear stress, $-S$, versus dimensionless shear rate, $\lambda\dot{\gamma}$, calculated for the generalized corotational Maxwell model and compared with measured behavior of molten HDPE (**red** dots). $Wi = \bar{\lambda}\dot{\gamma}^0 = 0.486$ and $De = \bar{\lambda}\omega = 1.0$. **Pink** curve shows corresponding linear viscoelastic behavior [alternant part of Eq. (83)].

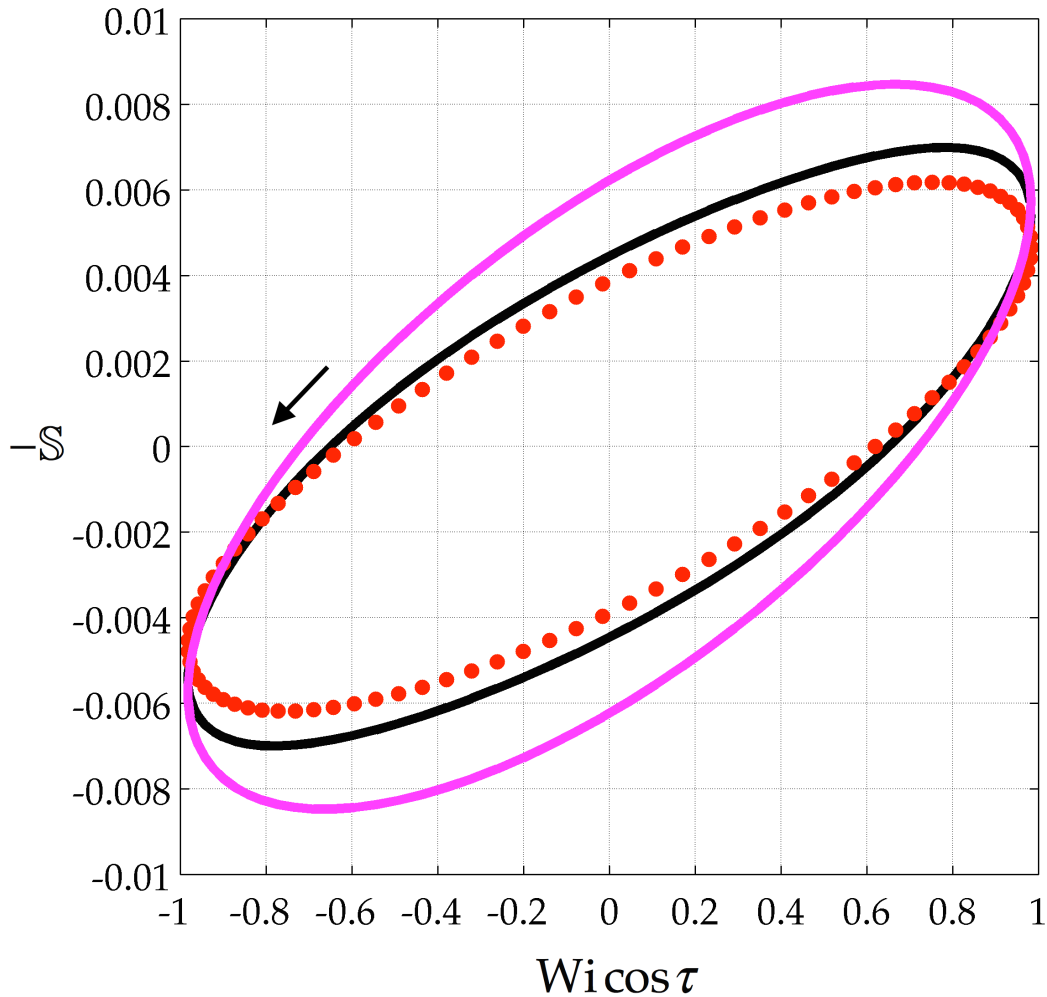


Figure 21. Exact solution (**black** loop is Eq. (73) with 40 harmonics, 1 through 79 and evaluated for multiple relaxation times, taken from Table 4 of [5]) for counterclockwise loops of minus dimensionless shear stress, $-S$, versus dimensionless shear rate, $\lambda\dot{\gamma}$, calculated for the generalized corotational Maxwell model and compared with measured behavior of molten HDPE (**red** dots). $Wi = \bar{\lambda}\dot{\gamma}^0 = 0.983$ and $De = \bar{\lambda}\omega = 1.0$. **Pink** curve shows corresponding linear viscoelastic behavior [alternant part of Eq. (83)].

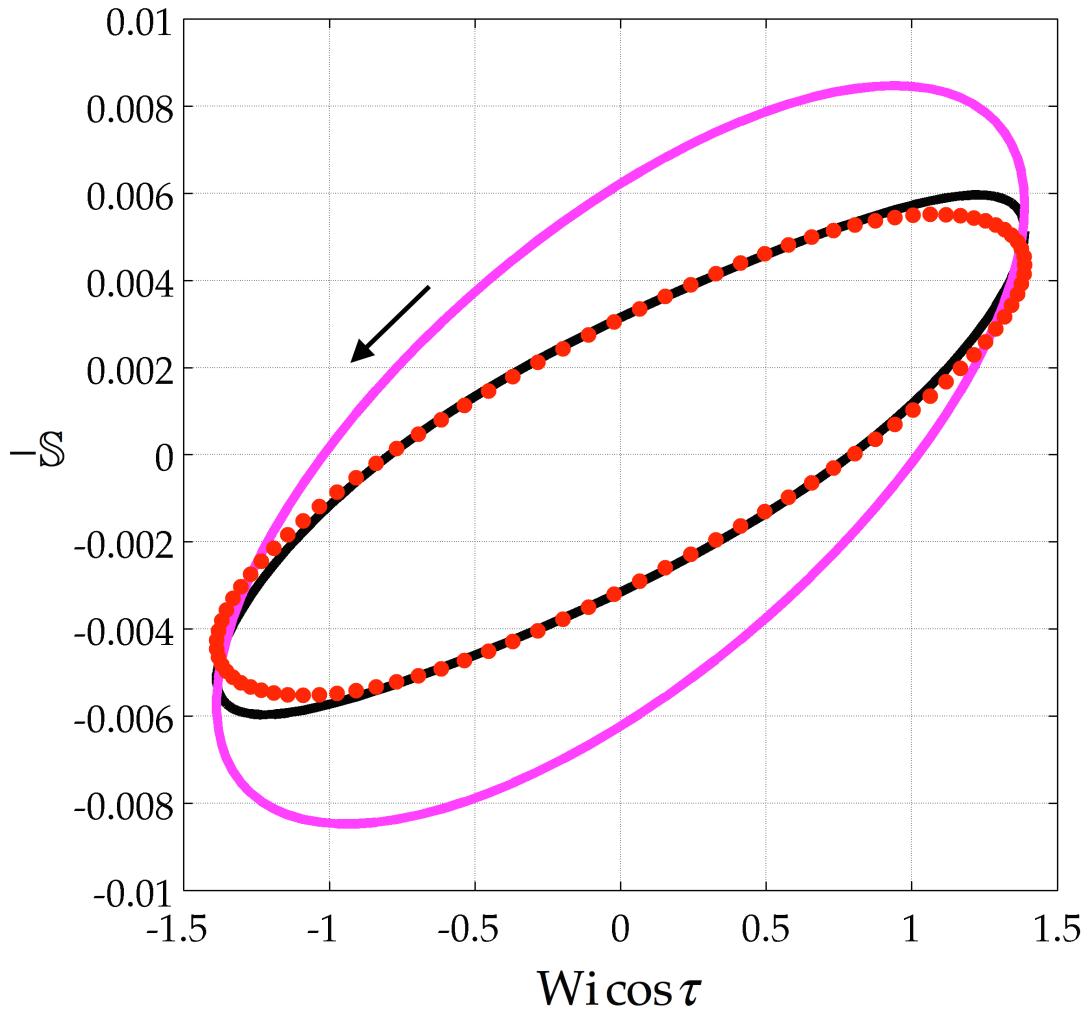


Figure 22. Exact solution (**black** loop is Eq. (73) with 40 harmonics, 1 through 79 and evaluated for multiple relaxation times, taken from Table 4 of [5]) for counterclockwise loops of minus dimensionless shear stress, $-S$, versus dimensionless shear rate, $\lambda\dot{\gamma}$, calculated for the generalized corotational Maxwell model and compared with measured behavior of molten HDPE (**red** dots). $Wi = \bar{\lambda}\dot{\gamma}^0 = 1.388$ and $De = \bar{\lambda}\omega = 1.0$. **Pink** curve shows corresponding linear viscoelastic behavior [alternant part of Eq. (83)].

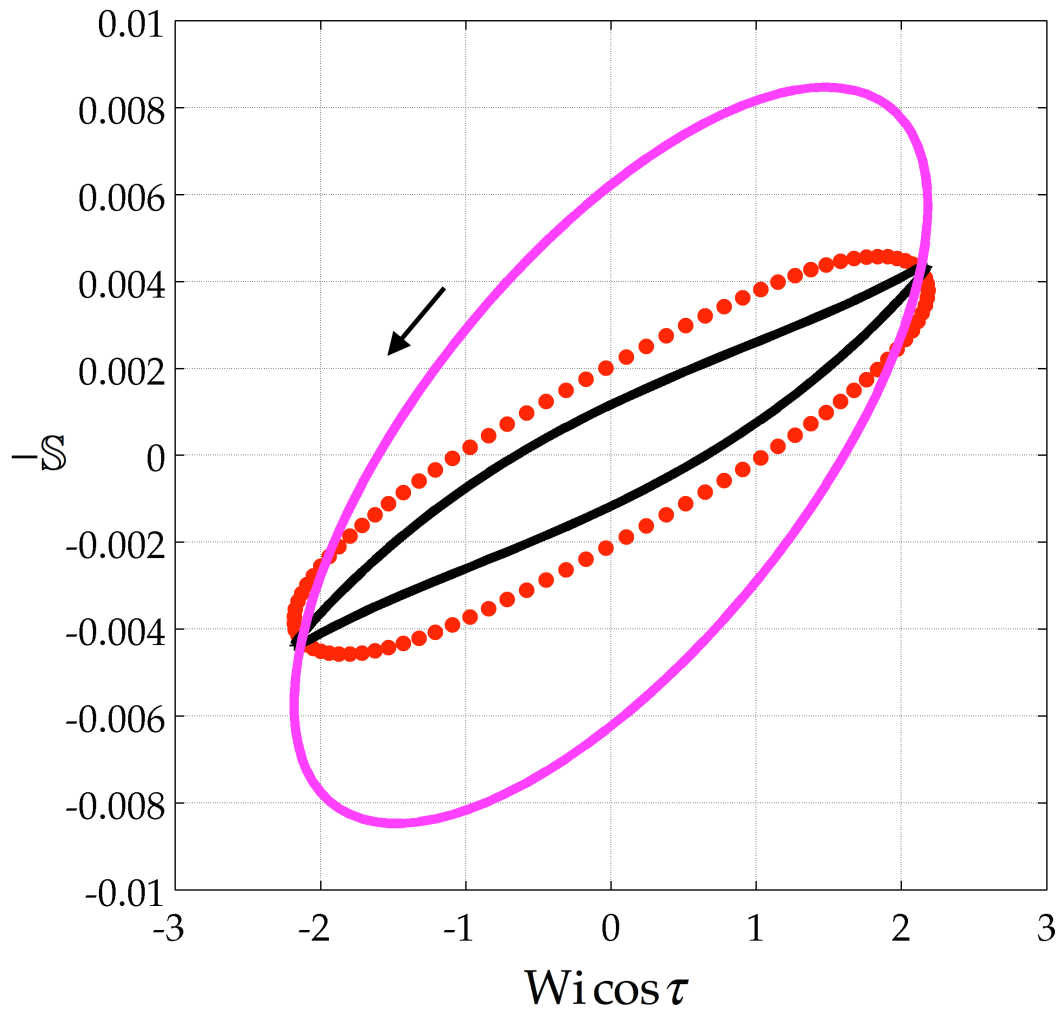


Figure 23. Exact solution (**black** loop is Eq. (73) with 40 harmonics, 1 through 79 and evaluated for multiple relaxation times, taken from Table 4 of [5]) for counterclockwise alternance loops of minus dimensionless shear stress, $-S$, versus dimensionless shear rate, $\lambda\dot{\gamma}$, calculated for the generalized corotational Maxwell model and compared with measured behavior of molten HDPE (**red** dots). $Wi = \bar{\lambda}\dot{\gamma}^0 = 2.183$ and $De = \bar{\lambda}\omega = 1.0$. **Pink** curve shows corresponding linear viscoelastic behavior [alternant part of Eq. (83)].

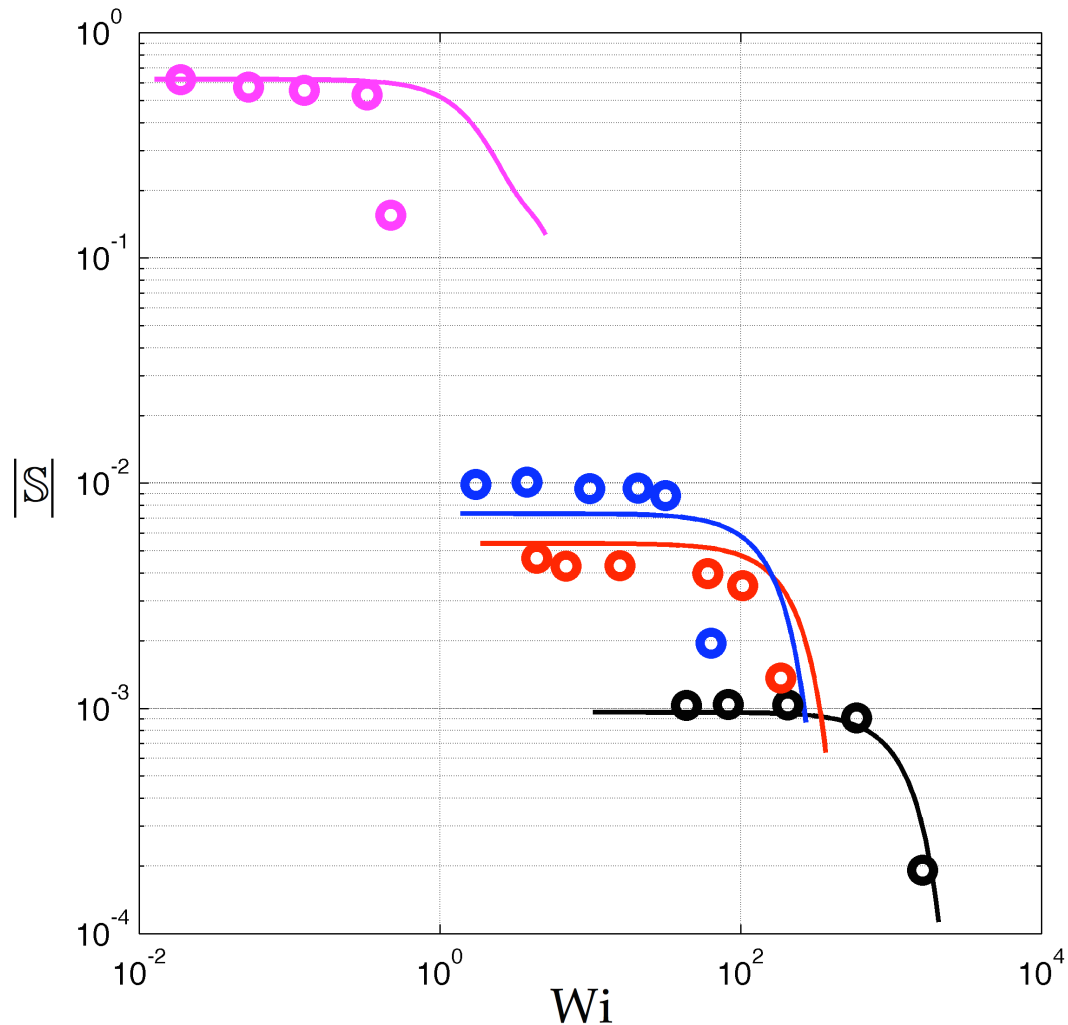


Figure 24. Comparison of exact solution [Eq. (71) with Eqs. (72) and (73) using 40 odd harmonics, 1 through 79] with experimental measurements of the maximum value of the shear stress response in large-amplitude oscillatory shear flow at $\omega = 10\pi$ rad/s (from Fig. 1 of [36] or *Puc. 1.* of [37]). **Black** line is polyisoprene ($\eta_0 = 1.0 \times 10^7$ Pa·s, $\lambda = 33.12$ s) with $De = 1040$. **Red** line is polyisoprene ($\eta_0 = 2.87 \times 10^6$ Pa·s, $\lambda = 5.89$ s) with $De = 902$. **Blue** line is polybutadiene ($\eta_0 = 3.0 \times 10^6$ Pa·s, $\lambda = 4.34$ s) $De = 139$. **Pink** line is polybutadiene ($\eta_0 = 3.0 \times 10^4$ Pa·s, $\lambda = 0.04$ s) with $De = 1.26$.

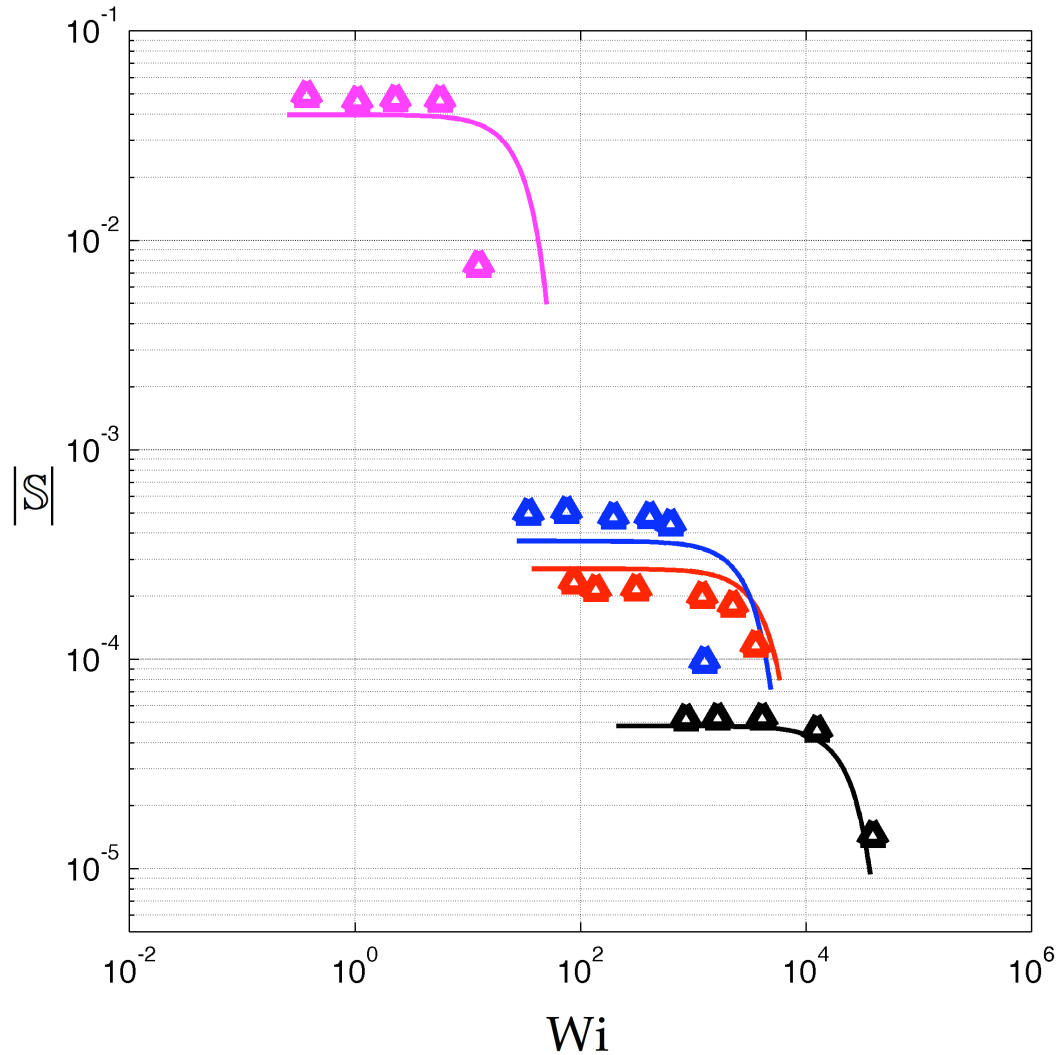


Figure 25. Comparison of exact solution [Eq. (71) with Eqs. (72) and (73) using 40 odd harmonics, 1 through 79] with experimental measurements of the maximum value of the shear stress response in large-amplitude oscillatory shear flow at $\omega = 200\pi$ rad/s (from Fig. 1 of [36] or *Puc. 1.* of [37]). **Black** line is polyisoprene ($\eta_0 = 1.0 \times 10^7$ Pa·s, $\lambda = 33.12$ s) with $De = 20,810$. **Red** line is polyisoprene ($\eta_0 = 2.87 \times 10^6$ Pa·s, $\lambda = 5.89$ s) with $De = 18,033$. **Blue** line is polybutadiene ($\eta_0 = 3.0 \times 10^6$ Pa·s, $\lambda = 4.34$ s) with $De = 2,727$. **Pink** line is polybutadiene ($\eta_0 = 3.0 \times 10^4$ Pa·s, $\lambda = 0.04$ s) with $De = 25$.

XIII. REFERENCES

- ¹ J.J. Kovacic, "An Algorithm for Solving Second Order Linear Homogeneous Differential Equations," *J. Symbolic Computation*, **2**, 3-43 (1986); Erratum: " $\omega^2 + \phi\omega + \left(\frac{1}{2}\phi' + \frac{1}{2}\phi^2 - r\right) = 0$ " should be " $\omega^2 - \phi\omega + \left(\frac{1}{2}\phi' + \frac{1}{2}\phi^2 - r\right) = 0$ " for the last equation on p. 18.
- ² A. Gemant, "Komplexe Viskosität.," *Naturwissenschaften* **25**, 406-407 (1935).
- ³ A. Gemant, "The conception of a complex viscosity and its application to dielectrics," *Transactions of the Faraday Society*, No. 175, **XXXI**, Part II, 1582-1590 (November, 1935b); Erratum: The footnote on p. 1583, "¹⁵A. Gemant, *Naturwiss.*, 1935, **23**, 406." should be "¹⁵A. Gemant, *Naturwiss.*, 1935, **25**, 406."
- ⁴ R.B. Bird and A.J. Giacomin, "Who Conceived the Complex Viscosity?," *Rheologica Acta*, **51**(6), 481-486 (2012).
- ⁵ A.J. Giacomin, R.B. Bird, L.M. Johnson and A.W. Mix, "Large-Amplitude Oscillatory Shear Flow from the Corotational Maxwell Model," *Journal of Non-Newtonian Fluid Mechanics*, **166**(19-20), 1081-1099 (2011). Errata: after Eq. (20), Ref. [10] should be [13]; in Eq. (66), " $20De^2$ " and " $10De^2 - 50De^4$ " should be " $20De$ " and " $10De - 50De^3$ "; after Eq. (119), " $(\zeta\alpha)$ " should be " $\zeta(\alpha)$ "; In Eq. (147), " $n - 1$ " should be " $n = 1$ "; In Eqs. (76) and (77), Ψ' and Ψ'' should be Ψ_1' and Ψ_1'' ; Throughout, Ψ_1^d , Ψ_1' and Ψ_1'' should be Ψ_1^d , Ψ_1' and Ψ_1'' ; In Eqs. (181) and (182), "1,21" should be "1,2"; on the ordinates of Figs. 5-7, $\frac{1}{2}$ should be 2; see also [65] below.
- ⁶ A.J. Giacomin and J.M. Dealy, "Large-amplitude oscillatory shear," Chapter 4, Collyer, A.A., ed., *Techniques in Rheological Measurement*, Chapman and Hall, London & New York, pp. 99-121 (1993); Kluwer Academic Publishers, Dordrecht, pp. 99-121 (1993).
- ⁷ A.J. Giacomin and J.M. Dealy, "Using large-amplitude oscillatory shear," Chapter 11, Collyer, A.A. and D.W. Clegg, eds., *Rheological Measurement*, 2nd ed., Kluwer Academic Publishers, Dordrecht, Netherlands, pp. 327-356 (1998).
- ⁸ K. Hyun, M. Wilhelm, C.O. Klein, K.S. Cho, J.G. Nam, K.H. Ahn, S.J. Lee, R.H. Ewoldt, G.H. McKinley, "A review of nonlinear oscillatory shear tests: analysis and application of large amplitude oscillatory shear (LAOS)," *Prog. Polym. Sci.* **36**, 1697-1753 (2011).

- ⁹ D.S. Pearson and W.E. Rochefort, "Behavior of concentrated polystyrene solutions in large-amplitude oscillating shear fields," *J. Polym. Sci.: Pol. Phys. Ed.*, **20**, 83-98 (1982); Errata: on p. 95, $e^{i\omega t}$ should be $e^{-i\omega t}$ in Eq. (A2); after Eq. (A.10), α should be $\sqrt{\omega \tau_d/2}$; and in Eq. (A.11), $\cos x$ should be $\cosh x$.
- ¹⁰ E. Helfand and D.S. Pearson, "Calculation of the nonlinear stress of polymers in oscillatory shear fields," *J. Polym. Sci.: Pol. Phys. Ed.*, **20**, 1249-1258 (1982).
- ¹¹ W.M. Davis and C.W. Macosko, "Nonlinear dynamic mechanical moduli for polycarbonate and PMMA," *J. Rheol.*, **22**, 53-71 (1978).
- ¹² X.-J. Fan and R.B. Bird, "A kinetic theory for polymer melts VI. calculation of additional material functions," *J. Non-Newton. Fluid Mech.*, **15**, 341-373 (1984).
- ¹³ M. Wilhelm, K. Reinheimer and J. Kübel, "Optimizing the sensitivity of FT-rheology to quantify and differentiate for the first time the nonlinear mechanical response of dispersed beer foams of light and dark beer," *Zeitschrift für physikalische Chemie*, **226**, 547-567 (2012).
- ¹⁴ A.J. Giacomin, R.B. Bird, C. Aumnate, A.M. Mertz, A.M. Schmalzer and A.W. Mix, "Viscous Heating in Large Amplitude Oscillatory Shear Flow," *Physics of Fluids*, **24**, 103101 (2012); doi: 10.1063/1.4752777
- ¹⁵ A.J. Giacomin, R.B. Bird and H.M. Baek (백형민), "Temperature Rise in Large-Amplitude Oscillatory Shear Flow from Shear Stress Measurements," *Industrial & Engineering Chemistry Research*, **52**, 2008-2017 (2013).
- ¹⁶ R.H. Ewoldt and G.H. McKinley, "On secondary loops in LAOS via self-intersection of Lissajous-Bowditch curves," *Rheol. Acta*, **49**, 213-219 (2010).
- ¹⁷ K. Schultz, "Ermittlung des physikalischen Verhaltens von hochviskosen Flüssigkeiten bei harmonischer Schubwechselbeanspruchung." *Rheol. Acta*, **17**, 33 (1978).
- ¹⁸ J.C. Georgian, "Torsional Viscous Friction Dampers," *Trans. Am. Soc. Mech. Eng.*, **71**, 389 (1949).
- ¹⁹ K. Wakabayashi, Y. Honda, T. Kodama and S. Iwamoto, "The dynamic characteristics of torsional viscous-friction dampers on reciprocating engine shaftings," SAE Technical Paper Series, 921726, SAE International, International Off-Highway & Powerplant Congress & Exhibition, Milwaukee, WI (September 14-17, 1992), pp. 1-21 (1992).

- ²⁰ R. Andrä and Spurk, J.H. "Complex viscosity of viscoelastic damping fluids," *Rheol. Acta*, **21**, 530 (1982).
- ²¹ E.J. Nestorides, *A Handbook on Torsional Vibration*; Cambridge University Press: Cambridge (1958).
- ²² K.E. Hagner and Maass, H. *Torsionsschwingungen in der Verbrennungskraftmaschine*; Springer-Verlag, Vienna (1985).
- ²³ G. Böhme, *Strömungsmechanik nicht-newtonscher Fluide*, B.G. Teubner, Stuttgart, (1981).
- ²⁴ G. Böhme, *Non-Newtonian Fluid Mechanics*, Translated from German by J.C. Harvey; Elsevier Science Publisher B.V., Amsterdam (1987).
- ²⁵ R.B. Bird, R.C. Armstrong and O. Hassager, *Dynamics of Polymeric Liquids*, Vol. 1, First Edition, Wiley, New York (1977).
- ²⁶ J.G. Oldroyd, "Non-Newtonian effects in steady motion of some idealized elastico-viscous liquids," *Proc. Roy. Soc.*, **A245**, 278-297 (1958).
- ²⁷ 吴其晔 and 巫静安, "高分子材料流变学 *Polymer Rheology*," 高等教育出版社, 北京市 (2002).
- ²⁸ R.G. Larson, *Constitutive Equations for Polymer Melts and Solutions*, Butterworths, Boston (1988).
- ²⁹ C.D. Han, *Rheology and Processing of Polymeric Materials: Volume I Polymer Rheology*, Oxford University Press, New York (2007).
- ³⁰ G. Böhme, *Strömungsmechanik nicht-newtonscher Fluide*, B.G. Teubner, Stuttgart (1981).
- ³¹ A.S. Lodge, *Elastic Liquids*, Academic Press, London (1964). Errata: Eq. (6.40a) should be $s = \alpha \{ \sin \omega t (1 - \cos \omega \tau) + \cos \omega t \sin \omega \tau \}$; Eq. (6.40b) should be $s^2 = \alpha^2 \{ 1 + \cos 2\omega \tau \cos \omega \tau + \sin 2\omega t \sin \omega \tau \} (1 - \cos \omega \tau)$; Eq. (6.41a) should be $p_{11} - p_{22} = \alpha^2 \{ A + B \cos 2\omega t + C \sin 2\omega t \}$; Eq. (6.41b) should be $p_{21} = \alpha \{ D \cos \omega t + A \sin \omega t \}$; in line 4 of p. 113, $\alpha A \cos \omega t$ should be $\alpha D \cos \omega t$; in the sentence preceding Eq. (6.43), and also in Eq. (6.43), "the out-of-phase part of p_{21} " should be "the part of p_{21} that is in-phase with s ".
- ³² A.S. Lodge, "Recent network theories of the rheological properties of

moderately concentrated polymer solutions," in *Phénomènes de Relaxation et de Fluage en Rhéologie Non-linéaire*, Editions du C.N.R.S., Paris, (1961), pp. 51-63.

³³ J.D. Goddard and C. Miller, "An inverse for the Jaumann derivative and some applications to the rheology of viscoelastic fluids," *Rheol. Acta*, **5**, 177-184 (1966).

³⁴ A.J. Giacomin and R.B. Bird, "Normal Stress Differences in Large-Amplitude Oscillatory Shear Flow for the Corotational "ANSR" Model," *Rheologica Acta*, **50**(9), 741-752 (2011); Errata: In Eqs. (47) and (48), "20De²" and "10De² - 50De⁴" should be "20De" and "10De - 50De³".

³⁵ L.M. Johnson, A.J. Giacomin and A.W. Mix, "Viscoelasticity in Thermoforming," *Journal of Polymer Engineering*, **32**(4-5), 245-258 (June 2012).

³⁶ V.N. Burlii and É.É. Yakobson, "Thermodynamic Examination of the Periodic Shear Strain of Melts of Linear Polymers of Narrow Molecular-Mass Distribution," *Mechanics of Composite Materials*, **25**(4), 542-548 (1990). Erratum: In the abscissa label to Fig. 1, $\log|\alpha_{12}|$ should be $\log_{10}|\sigma_{12}|$, where $|\sigma_{12}|$ represents the amplitude of the first harmonic.

³⁷ В.Н. бурлий and Э.Э. Якобсон, "Термодинамическое Рассмотрение Периодического Сдвигового Деформирования Расплавов Линейных Полимеров Узкого Молекулярно-Массового Распределения," *Механика Композитных Материалов*, **4**, 718-723 (1989). Addendum: In the abscissa label to the first figure, *Рис. 1.*, $\lg|\sigma_{12}|$ should be $\lg_{10}|\sigma_{12}|$, where $|\sigma_{12}|$ represents the amplitude of the first harmonic.

³⁸ W.A. Adkins and M.G. Davidson, *Ordinary Differential Equations*, Springer, New York (2010).

³⁹ M. Abramowitz and I.A. Stegun, *Handbook of Mathematical Functions with Formulas, Graphs, and Mathematical Tables*, 10th ed., Applied Mathematics Series, National Bureau of Standards, Government Printing Office, Washington DC, p. 361 (1972).

⁴⁰ J.G. Kirkwood and R.J. Plock, "Non-Newtonian viscoelastic properties of rod-like macromolecules in solution," *J. Chem. Phys.*, **24**, 665-669 (1956).

⁴¹ P.L. Auer, (Ed.), *Macromolecules (John Gamble Kirkwood Collected Works)*, J. G. Kirkwood and R. J. Plock, "Non-Newtonian viscoelastic properties of rod-like macromolecules in solution," Gordon and Breach, New York (1967). Errata: On the left side of Eq. (1) on p. 113, ϵ should be $\dot{\epsilon}$. See also Eq. (1) of [40]; In Eq. (2a), G' should be G'' , and in Eq. (2b), G'' should be G' . See Eqs. (117a) and (117b) of [49].

- ⁴² R.J. Plock, "I. Non-Newtonian Viscoelastic Properties of Rod-Like Macromolecules in Solution. II. The Debye-Hückel, Fermi-Thomas Theory of Plasmas and Liquid Metals," PhD Thesis, Yale University, New Haven, CT (June, 1957). Errata: In Eqs. (2.4a), G' should be G'' , and in Eq. (2.4b), G'' should be G' . See Eqs. (117a) and (117b) of [49].
- ⁴³ T.W. Spriggs, "Constitutive equations for viscoelastic fluids," Ph.D. Thesis, Chemical Engineering Department, University of Wisconsin, Madison, WI (1966).
- ⁴⁴ M.C. Williams and R.B. Bird, "Three-constant Oldroyd model for viscoelastic fluids," *Physics of Fluids*, **5**, 1126-1127 (September, 1962).
- ⁴⁵ M.C. Williams and R.B. Bird, "Oscillatory behavior of normal stresses in viscoelastic fluids," *Ind. Eng. Chem. Fundam.*, **3**, 42-49 (1964).
- ⁴⁶ T.W. Spriggs, "A four-constant model for viscoelastic fluids," *Chemical Engineering Science*, **20**, 931-940 (1965).
- ⁴⁷ L.C. Akers and M.C. Williams, "Oscillatory Normal Stresses in Dilute Polymer Solutions," *The Journal of Chemical Physics*, **51**(9), 3834-3841 (1969).
- ⁴⁸ E. Paul, "Non-Newtonian viscoelastic properties of rodlike molecules in solution: comment on a paper by Kirkwood and Plock," *J. Chem. Phys.*, **51**, 1271-1290 (1969).
- ⁴⁹ E.W. Paul, "Some Non-Equilibrium Problems for Dilute Solutions of Macromolecules; Part I: The Plane Polyagonal Polymer," PhD Thesis, Dept. of Chemistry, University of Oregon, Eugene, OR (September, 1970).
- ⁵⁰ N.A.K. Bharadwaj, "Low Dimensional Intrinsic Material Functions Uniquely Identify Rheological Constitutive Models And Infer Material Microstructure," Masters Thesis, Mechanical Engineering, University of Illinois at Urbana-Champaign, IL (2012).
- ⁵¹ E.W. Paul and R.M. Mazo, "Hydrodynamic Properties of a Plane-Polygonal Polymer, According to Kirkwood-Riseman Theory," *J. Chem. Phys.*, **51**, 1102 (1969).
- ⁵² I.F. MacDonald, B.D. Marsh and E. Ashare, "Rheological behavior for large amplitude oscillatory motion," *Chem. Eng. Sci.*, **24**, 1615-1625 (1969).
- ⁵³ R.B. Bird, H.R. Warner, Jr., and D.C. Evans, "Kinetic theory and rheology of dumbbell suspensions with Brownian motion," *Adv. Poly. Sci. (or Fortschr. Hochpolymeren-Forschung.)*, **8**, 1-89 (1971).

- ⁵⁴ S.I. Abdel-Khalik, O. Hassager and R.B. Bird, "The Goddard expansion and the kinetic theory for solutions of rodlike macromolecules," *J. Chem. Phys.*, **61**, 4312-4316 (1974).
- ⁵⁵ R.B. Bird, O. Hassager and S.I. Abdel-Khalik, "Co-rotational rheological models and the Goddard expansion," *AIChE J.*, **20**, 1041-1066 (1974).
- ⁵⁶ R.B. Bird, O. Hassager, R.C. Armstrong, and C.F. Curtiss, *Dynamics of polymeric liquids*, vol 2, 1st edn., John Wiley & Sons, Inc., New York (1977); Erratum: In Problem 11.C.1 d., "and ϕ_2 " should be "through ϕ_4 ".
- ⁵⁷ C.Y. Mou and R.M. Mazo, "Normal stress in a solution of a plane-polygonal polymer under oscillating shearing flow," *J. Chem. Phys.*, **67**, 5972 (1977).
- ⁵⁸ N. Phan-Thien, M. Newberry and R.I. Tanner, "Non-linear oscillatory flow of a soft solid-like viscoelastic material," *J. Non-Newtonian Fluid Mech.*, **92**, 67-80 (2000).
- ⁵⁹ W. Yu, M. Bousmina, M. Grmela and C. Zhou, "Modeling of oscillatory shear flow of emulsions under small and large deformation fields," *J. Rheol.*, **46**, 1401-1418 (2002).
- ⁶⁰ 周持兴, 聚合物加工理论, 科学出版社, 北京市 (2004).
- ⁶¹ K.S. Cho, K.-W. Song and G.-S. Chang, "Scaling relations in nonlinear viscoelastic behavior of aqueous PEO solutions under large amplitude oscillatory shear flow," *J. Rheol.*, **54**, 27-63 (2010).
- ⁶² D.M. Hoyle, "Constitutive Modelling of Branched Polymer Melts in Non-linear Response," Chapter 4: "Large Amplitude Oscillatory Shear Flow," PhD Thesis, Dept. of Applied Mathematics, University of Leeds, Leeds, England (2010).
- ⁶³ M.H. Wagner, V.H. Rolón-Garrido, K. Hyun, and M. Wilhelm, "Analysis of medium amplitude oscillatory shear data of entangled linear and model comb polymers," *J. Rheol.*, **55**, 495 (2011).
- ⁶⁴ A.K. Gurnon and N.J. Wagner, "Large amplitude oscillatory shear (LAOS) measurements to obtain constitutive equation model parameters: Giesekus model of banding and nonbanding wormlike micelles," *J. Rheol.*, **56**, 333 (2012).
- ⁶⁵ A.J. Giacomin, R.B. Bird, L.M. Johnson and A.W. Mix, 'Corrigenda: "Large-Amplitude Oscillatory Shear Flow from the Corotational Maxwell Model," [Journal of Non-Newtonian Fluid Mechanics, **166**, 1081-1099 (2011)],' *Journal of Non-Newtonian Fluid Mechanics*, **187-188**, 48-48 (2012); see also (5) above].

⁶⁶ R.B. Bird, A.J. Giacomin, A.M. Schmalzer and C. Aumtate, "Dilute Rigid Dumbbell Suspensions in Large-Amplitude Oscillatory Shear Flow: Shear Stress Response," *The Journal of Chemical Physics*, **140**, 074904 (2014); Corrigenda: In Eq. (91), η' should be η'' ; In caption to Fig. 3, " $\psi_1[P_2^2 s_2]$ " should be " $\cos 3\omega t$ " and " $\psi_2[P_2^0 c_0, P_2^2 c_2, \dots]$ " should be " $\sin 3\omega t$ ".

⁶⁷ A.M. Schmalzer, R.B. Bird and A.J. Giacomin, "Normal Stress Differences in Large-Amplitude Oscillatory Shear Flow for Dilute Rigid Dumbbell Suspensions," PRG Report No. 002, QU-CHEE-PRG-TR--2014-2, Polymers Research Group, Chemical Engineering Dept., Queen's University, Kingston, CANADA (April, 2014).

⁶⁸ A.M. Schmalzer, R.B. Bird and A.J. Giacomin, "Normal Stress Differences in Large-Amplitude Oscillatory Shear Flow for Dilute Rigid Dumbbell Suspensions," *Journal of Non-Newtonian Fluid Mechanics*, <http://dx.doi.org/10.1016/j.jnnfm.2014.09.001> (2014); Erratum: Above Eqs. (14) and (25), "significant figures" should be "16 significant figures".

⁶⁹ A.M. Schmalzer and A.J. Giacomin, "Orientation in Large-Amplitude Oscillatory Shear," *Macromolecular Theory and Simulations*, accepted (September 22, 2014).

⁷⁰ R.B. Bird, W.E. Stewart and E.N. Lightfoot, *Transport Phenomena*, Revised 2nd ed., Wiley & Sons, New York (2007).